SUVI HAIMI

Allograft Bone and Osteogenic Scaffolds Seeded with Human Adipose Stem Cells in Bone Tissue Engineering

In vitro study

■

ACADEMIC DISSERTATION
To be presented, with the permission of
the Faculty of Medicine of the University of Tampere,
for public discussion in the Lecture Room of Finn-Medi 5,
Biokatu 12, Tampere, on December 29th, 2008, at 12 o'clock.

UNIVERSITY OF TAMPERE

ACADEMIC DISSERTATION
University of Tampere, REGEA Institute for Regenerative Medicine
Tampere University of Technology, Department of Biomedical Engineering
Tampere Graduate School in Biomedicine and Biotechnology (TGSBB)
Finland

Supervised by
Professor Riitta Suuronen
University of Tampere
Finland
Professor Minna Kellomäki
Tampere University of Technology
Finland

Reviewed by
Professor emer. Risto Penttinen
University of Turku
Finland
Docent Heimo Ylänen
University of Turku
Finland

Distribution
Bookshop TAJU
P.O. Box 617
33014 University of Tampere
Finland

Tel. +358 3 3551 6055
Fax +358 3 3551 7685
taju@uta.fi
www.uta.fi/taju
http://granum.uta.fi

Cover design by
Juha Siro

Acta Universitatis Tamperensis 1371
ISBN 978-951-44-7540-5 (print)
ISSN 1455-1616

Acta Electronica Universitatis Tamperensis 793
ISBN 978-951-44-7541-2 (pdf)
ISSN 1456-954X
http://acta.uta.fi

Tampereen Yliopistopaino Oy – Juvenes Print
Tampere 2008

To Tuomas

Abstract

The use of bone substitutes in orthopedic surgery has increased tremendously over the last few years. Allograft bone is used to replace bone lost due to tumor removal or injury and for reconstruction of large skeletal defects, whereas autograft bone is only suitable for small defects. There are inherent problems with allograft tissues, however, such as the risk of disease transmission and immunologic incompatibility. Strategies to reduce these risks include improving allograft sterilization methods and developing bone tissue substitutes were evaluated in the presented studies.

Tissue engineering offers a potential avenue to overcome the limitations related to auto- and allograft tissues. To enhance the body's own repair system, i.e., tissue regeneration, biomaterial research focuses primarily on developing scaffolds for tissue engineering applications. Bioactive glass and composites of bioactive ceramics and biodegradable polymers, such as polylactides (PLA), are promising delivery vehicles for osteoprogenitor cells because they induce new bone formation *in vivo*. Among adult stem cells, multipotent adipose stem cells (ASCs) can differentiate into osteoblastic cells and other mesenchymal lineages *in vitro* when treated with appropriate factors, and are therefore a promising cell source for bone tissue engineering applications.

This work comprises two parts. First, peracetic acid-ethanol sterilization (PES) with a preceding chemical cleansing step and subsequent freeze-drying step was studied as a potential allograft processing method. Second, *in vitro* proliferation and osteogenic differentiation studies of different types of bioactive glass and PLA/bioceramic scaffolds seeded with ASCs were evaluated as enhanced constructs for bone tissue engineering applications.

The different processing methods combined with PES had only minor effects on the biomechanical properties of cortical allograft bone, suggesting that this processing method is suitable for allograft bone sterilization. Evaluation of bioactive glass scaffolds indicated that additional surface treatment with calcium phosphate or zinc inhibited the dissolution kinetics of the bioactive glass scaffolds. Surface treatment with calcium phosphate delayed early osteogenic differentiation of ASCs, whereas treatment with zinc stimulated proliferation and osteogenic differentiation of ASCs when used with a faster degrading composition of bioactive glass. PLA/β-tricalcium phosphate (β-TCP) composite scaffolds significantly enhanced ASC proliferation and osteogenic differentiation compared to PLA alone or composite forms of PLA/bioactive glass scaffolds.

In conclusion, ASCs combined with a controlled composition of bioactive glass scaffolds or PLA/β-TCP composite scaffolds are potentially useful for clinical applications regarding scaffolds with both osteoconductive and osteostimulative

properties. Further studies utilizing *in vivo* models are needed, as well as *in vivo* confirmation of the suitability of the allograft bone processing and sterilization method.

Tiivistelmä

Allograftiluun ja muiden luunkorvikkeiden käyttö ortopedisessä kirurgiassa on kasvanut huomattavasti viimeisten vuosien aikana. Autologista luuta voidaan käyttää vain pienten luuvaurioiden hoitoon ja sen vuoksi allograftiluuta käytetään korvaamaan suuria luupuutoksia, jotka ovat aiheutuneet esimerkiksi kasvaimen poiston tai vamman seurauksena. Allograftiluun käyttöä kuitenkin hankaloittaa riski tarttuvien tautien siirtymisestä kudoksen luovuttajasta siirteen vastaanottajaan ja lisäksi riski vastaanottajan immunologisesta vasteesta luusiirteelle. Näitä riskejä voidaan vähentää parantamalla allograftiluiden sterilointimenetelmiä tai kehittämällä uudenlaisia luunkorvikkeita autologisen ja allogeenisten luusiirteiden tilalle.

Kudosteknologiset keinot tarjoavat mahdollisuuden kehittää täysin uudenlaisia luunkorvikkeita. Biomateriaalialan tutkimus on keskittymässä kudosteknologisiin sovelluksiin sopiviin tukirakenteisiin, joiden tarkoituksena on edesauttaa elimistön omaa kykyä korjata kudoksia. Bioaktiiviset lasit yhdessä bioaktiivisesta keraamista ja biohajoavasta polymeeristä, kuten polylaktidista, koostuvien komposiittien kanssa ovat lupaavia materiaaleja toimimaan esiluusolujen kuljettimina elimistöön, sillä niiden on osoitettu lisäävän uuden luun muodostumista *in vivo*. Aikuisten kantasoluihin kuuluvat monikykyiset rasvakudoksen kantasolut voivat erilaistua luusolujen suuntaan, kun niitä käsitellään sopivilla kasvutekijöillä. Nämä solut ovatkin lupaava solulähde luun kudosteknologisiin sovelluksiin.

Tämä työ koostuu kahdesta erillisestä osasta. Ensimmäisessä osiossa tutkittiin soveltuuko peretikkahappoetanolisterilointi yhdistettynä kemialliseen puhdistukseen ja kylmäkuivaukseen allograftiluun prosessointimenetelmäksi. Toisessa osiossa tutkittiin erilaisten bioaktiivinen lasi- ja polylaktidi/biokeraamitukirakenteiden *in vitro* vaikutuksia rasvakudoksen kantasolujen lisääntymiseen ja erilaistumiseen luusolujen suuntaan. Tarkoituksena oli löytää uusia tehokkaita materiaaliyhdistelmiä luun muodostumiselle kudosteknologisissa sovelluksissa.

Erilaiset prosessointimenetelmät yhdistettynä peretikkahappoetanolisterilointiin eivät vaikuttaneet heikentävästi kortikaaliluun mekaanisiin ominaisuuksiin. Näiden tulosten perusteella tutkittua prosessointimenetelmää voidaan pitää potentiaalisena sterilointimenetelmänä allograftiluulle. Bioaktiivisen lasin kalsiumfosfaattipinnoite tai sinkin lisäys sen koostumukseen näytti vaikuttavan sen hajoamisominaisuuksiin hidastavasti. Kalsiumfosfaattikäsittely viivästytti rasvakudoksen kantasolujen luuerilaistusta. Tulosten perusteella voidaan olettaa, että valitsemalla koostumukseltaan nopeammin hajoava bioaktiivinen lasi sinkin stimuloiva vaikutus rasvakudoksen kantasolujen erilaistumiseen luusolujen suuntaan olisi voitu havaita. Polylaktidi/trikalsiumfosfaatti komposiitti-tukirakenteet tehostivat merkittävästi rasvakudoksen kantasolujen lisääntymisnopeutta ja lisäsivät niiden luuerilaistusta

verrattuna pelkkään polylaktidi- tai polylaktidi/bioaktiivinen lasi komposiitti-tukirakenteisiin.

Johtopäätöksenä voidaan todeta, että rasvakudoksen kantasoluilla yhdistettynä muokkaamattomaan bioaktiiviseen lasi-tukirakenteeseen tai polylaktidi/-trikalsiumfosfaatti komposiitti-tukirakenteeseen, voitaisiin soveltaa kliiniseen käyttöön, kun materiaalilta vaaditaan sekä osteokonduktiivisia että osteostimulatiivisia ominaisuuksia. Rasvakudoksen kantasolujen ja biomateriaalien yhdistelmän kykyä muodostaa luuta pitäisi tutkia myös eläinmalleissa. Lisätutkimuksia tarvitaan myös käytetystä prosessointi- ja sterilointimenetelmästä, jonka soveltuvuus allograftiluulle tulisi vielä varmistaa eläinkokein.

Content

List of abbreviations

3D	Three dimensional
ALP	Alkaline phosphatase
APC	Allophycocyanin
ASC	Adipose stem cell
AAS	Atomic absorption spectroscopy
BMP	Bone morphogenetic protein
BTB	Bone-patellar tendon-bone grafts
Ca-P	Calcium phosphate
CC	Control composition
CD	Cluster of differentiation
CMFDA	5-Chloromethylfluorescein diacetate
DMEM/F-12	Dulbecco's modified Eagle's medium: nutrient mixture F-12
DNA	Deoxyribonucleic acid
EH-1	Ethidium homodimer-1
ESC	Embryonic stem cell
E-SEM	Environmental scanning electron microscope
FACS	Fluorescence activated cell sorter
FBS	Fetal bovine serum
FGF	Fibroblast growth factor
FITC	Fluorescein iso-thiocyanate-isomer 1
HA	Hydroxyapatite
hFSP	Human Fibroblast Surface Protein
HIV	Human immunodeficiency virus
HLA-ABC	Human leukocyte antigen class I
HLA-DR	Human leukocyte antigen class II
IGF	Insulin-like growth factor
MSC	Mesenchymal stem cell
PBS	Phosphate buffered saline
PDGF	Platelet-derived growth factor
PE	Phycoerythrin
PES	Peracetic acid-ethanol sterilization
PGA	Polyglycolide
PLA	Polylactide
PLGA	Poly(lactide-*co*-glycolide)
SA/V	Surface area-to-volume ratio
SBF	Simulated body fluid
SEM	Scanning electron microscopy
STRO-1	Stromal precursor cell marker

TCP	Tricalcium phosphate
TGF-β	Transforming growth factor-β

List of original articles

The present study is base on the following original publications, which are referred to by their Roman numerals (**I-IV**).

I. **Haimi S,** Vienonen A, Hirn MY, Pelto M, Suuronen R. The effect of chemical cleansing procedures combined with peracetic acid-ethanol sterilization on biomechanical properties of cortical bone. Biologicals 36:99-104, 2008.

II. **Haimi S,** Pirhonen E, Moimas L, Lindroos B, Huhtala H, Räty S, Kuokkanen H, Sándor GK, Miettinen S, Suuronen R. Calcium phosphate surface treatment of bioactive glass causes a delay in early osteogenic differentiation of adipose stem cells. Journal of Biomedical Materials Research Part A, *in press.*

III. **Haimi S,** Gorianc G, Moimas L, Lindroos B, Huhtala H, Räty S, Kuokkanen H, Sándor GK, Schmid C, Miettinen S, Suuronen R. Characterization of zinc-releasing three dimensional bioactive glass scaffolds and their effect on adipose stem cell proliferation and osteogenic differentiation. Submitted to Acta Biomaterialia.

IV. **Haimi S**, Suuriniemi N, Haaparanta AM, Ellä V, Lindroos B, Huhtala H, Räty S, Kuokkanen H, Sándor GK, Kellomäki M, Miettinen S, Suuronen R. Growth and osteogenic differentiation of adipose stem cells on PLA/bioactive glass and PLA/ β-TCP scaffolds. Tissue Engineering Part A, *in press*.

The original publications are reproduced with the permission of the copyright holders.

1. Introduction

Bone defects have several different causes; tumor surgery, trauma, infections, and congenital abnormalities. Skeletal reconstruction by bone grafting is commonly used in orthopedic surgery (Aro and Aho 1993, Virolainen et al. 2003). For small bone defects, autologous bone remains the most suitable bone grafting material because the transfer of osteoprogenitor cells provides the graft with excellent osteoconductive and osteoinductive characteristics. For the reconstruction of large cortical and cancellous bone defects, allograft bone is established effective and reliable for the reconstructing of large cortical and cancellous bone defects, despite the risk of an immunologic response in the host and the risk of viral and bacterial contamination (Aro and Aho 1993, Eppley et al. 2005). Although donor screening and tissue testing remain the gold standard in allograft bone preparation, these methods sometimes fail. To maximize safety when using allograft bone, the bone must be cleansed and sterilized. All of the currently used methods, however, such as gamma sterilization, compromise either the safety or the biologic and biomechanical properties of the allograft.

Biomaterials used for implants have a limited lifespan, whereas tissue regeneration affords more desirable long-term repair. Tissue engineering is a new approach for regenerating bone tissue, offering the potential to overcome the many limitations of existing therapies. The optimal strategy for bone formation is to combine bioactive scaffolds with stem cells and signaling molecules.

Bioactive glass is a synthetic, silica-based surface-active bone substitute material that strongly bonds to bone (Heikkilä et al. 1995). Certain compositions of bioactive glass induce the proliferation and osteogenic differentiation of human osteoblasts and mesenchymal stem cells (MSCs) *in vitro* (Xynos et al. 2000b, Bosetti and Cannas 2005). The mechanical properties of bioactive glass and other bioceramics, however, are not optimal for clinical use. Composite materials in which the bioceramic phase is incorporated into a polymer matrix have emerged as a possible strategy to overcome this insufficiency.

Adipose stem cells (ASCs), which are abundant and can be efficiently harvested, hold great promise for reconstructive therapy applications because they can be incorporated as-is or after being manipulated *in vitro* manipulations.

The present studies were initiated to evaluate the potential of peracetic acid-ethanol sterilization (PES) preceded by a chemical cleansing and subsequent freeze-drying step as an allograft processing method. This was followed by *in vitro* studies on different bioactive materials that were used as scaffolding for ASCs to enhance the constructs for bone tissue engineering applications.

2. Review of the literature

2.1 Bone

2.1.1 Components of bone and mineralization

Bone is a highly heterogeneous tissue and its composition varies with the skeletal site, physiologic function, age, sex, and presence of bone diseases. Calcified bone is composed of a mineral phase, an organic matrix, and cells. The mineral phase, or the inorganic matrix, of bone is composed of calcium phosphate (Ca-P) or hydroxyapatite (HA), which is responsible for the stiffness and strength of bone. Over 90% of the organic matrix is composed of collagenous extracellular matrix, predominantly type I collagen, along with small amounts of types V and XII collagen. Type I collagen has a unique amino-acid content compared with other collagens and consists of relatively thick fibrils (mean diameter 78 nm), thus giving the bone its tensile properties. The remaining 10% of the organic matrix corresponds to noncollagenous proteins, including osteopontin, osteocalcin, osteonectin, bone sialoprotein, bone phosphoproteins, and small proteoglycans and phospholipids. In addition, the calcified matrix contains growth factors, such as bone morphogenetic proteins (BMPs), and enzymes, such as alkaline phosphatase (ALP) (Buckwalter et al. 1996, Bonucci 2000).

ALP is a glycosylated membrane-bound enzyme produced by osteoblasts that provides adequate local concentrations of inorganic phosphate or inorganic pyrophosphate for bone mineralization. ALP expression is present in early osteoblasts, peaks in mature osteoblasts, and possibly fades in late osteoblast cells and osteocytes, which makes it an important indicator of osteoblast function (Beck et al. 1998, Park et al. 2007). Osteopontin is proposed to be involved in processes related to cell adhesion and cell matrix attachment. It is maximally expressed at the initiation phase of mineralization and is associated with the mineralization front. Maturation of the collagenous matrix, a prerequisite for bone mineralization, may involve an association with noncollagenous proteins such as osteopontin (Robey 1996). Osteopontin induction may be linked with the generation of ALP hydrolysis products (Beck et al. 1998).

Seven cell types, all originating from two cell lines, are found in bone. Undifferentiated osteoblasts or preosteoblasts, osteoblasts, bone-lining cells, and osteocytes are derived from the primitive mesenchymal cells, osteoprogenitor cells. Monocytes, preosteoclasts, and osteoclasts are derived from hematopoetic stem cells. The main function of osteoblasts is to synthesize osteoid, *i.e.,* organic bone matrix, and influence its mineralization through the generation of organic matrix

components and the synthesis of matrix vesicles. Osteocytes are mature osteoblasts trapped within formed bone, whereas osteoclasts are phagocytic cells that are capable of bone resorption. Bone-lining cells lie directly against the bone matrix and, similar to osteocytes, they have less cytoplasm and fewer organelles than active osteoblasts. Osteoblasts and osteoclasts together are responsible for constant bone turnover and remodeling (Buckwalter et al. 1996, Heath and Young 2000).

In the bone mineralization stage, the essential phase transformation reaction is the formation of solid Ca-P from soluble Ca-P. When mineralization proceeds, the amount of water and probably also the amount of non-collagenous protein decrease simultaneously with the increase in the mineral concentration, but the collagen concentration and organization remain relatively unchanged (Buckwalter et al. 1996).

2.1.2 Structure of bone

Bone exists in two main histologic forms, woven bone and lamellar bone. Woven bone is synthesized when osteoblasts produce osteoids rapidly, as in skeletal embryogenesis, and in pathologic conditions, such as callus formation, bone tumors, and ectopic ossification. The collagen fibers in the osteoid of woven bone are randomly arranged. Lamellar bone is stronger and more resilient than woven bone and is characterized by regular parallel bands of collagen arranged in sheets. Immature woven bone is eventually remodeled to form lamellar bone. Lamellar bone in the mature skeleton can be further classified into two distinct macroscopic structures: cortical, *i.e.,* compact bone; and cancellous, *i.e.,* trabecular bone (Bonucci 2000, Heath and Young 2000).

Cortical bone forms the outer bone layer and the thick dense walls of the diaphysis. The basic structure of cortical bone is composed of concentric bony layers or lamellae. These lamellae form cylindrical structures, called osteons. The major axis of an osteon comprises neurovascular canal or Haversian canal. The osteons are arranged parallel to the axis of bone. Between the lamellae are spaces called lacunae where osteoblasts are trapped as osteocytes. The osteons are thus oriented in concentric rings within the lamellae. Cancellous bone is found in the medulla of flat, short bones, and in the epiphysis and metaphysis of long bones.

Cancellous bone consists of trabecular networks separated by interconnecting spaces containing bone marrow. Cancellous bone does not usually contain osteons but if the trabeculae are thick enough, osteons can be found. The porosity of cancellous bone varies from 30% to more than 90%, whereas the porosity of cortical bone ranges from 5% to 30%. Although cancellous and cortical bone can be easily distinguished by their porosity or density, the actual differences arise from the microstructure of bone tissue observed histologically (Rho et al. 1998, Bonucci 2000, Heath and Young 2000).

The external bone surface is covered by a dense fibrous layer known as the periosteum, which contains undifferentiated osteogenic cells capable of continuous remodeling and repair of bone fractures. The inner bone surface is covered with

endosteum, which has properties and function similar to periosteum (Bonucci 2000, Heath and Young 2000).

2.1.3 Bone fracture healing

In bone fracture healing, the properties of pre-existing tissue are largely restored and eventually new bone is regenerated. Thus, bone is unique because it can completely reconstitute itself without the formation of scar tissue, by a process that normally occurs during embryogenesis (Rosenberg 2005). Histologically, bone fracture healing can be divided into primary fracture healing, or primary cortical healing, and secondary fracture healing. In primary healing, the bone cortex heals directly without forming a callus. This healing pattern occurs only when there is possible anatomic restoration of the fracture fragments and stability of the fracture reduction is ensured. Secondary healing involves activation of the periosteum, followed by callus formation. The initial response to a fracture is similar to the response of any tissue to a traumatic force sufficient to cause tissue damage and hemorrhage (Einhorn 1998).

In the initiation phase of bone fracture healing, blood vessel rupture results in a hematoma. The blood clot that forms provides a fibrin mesh, which is replaced later by highly vascular granulation tissue. The granulation tissue gradually becomes more fibrous. At the same time, degranulated platelets and migrating inflammatory cells release platelet-derived growth factor (PDGF), transforming growth factor-β (TGF-β), fibroblast growth factor (FGF), and other cytokines, which activate the MSCs and enhance of osteoclastic and osteoblastic activity. In this phase, MSCs differentiate into chondroblasts and a provisional callus is formed. The callus forms via intramembranous ossification whether or not the fractured parts of the bone are in close proximity. The function of the callus is to stabilize and bind the fractured bone together. Even while the callus is forming, osteoprogenitor cells in the periosteum and endosteum are activated and progressively transform the provisional callus into a bony callus. The cartilage in the provisional callus calcifies and is replaced by lamellar bone by a process that resembles endochondral ossification, such as normally occurs at the growth plate. At this stage a network of bone that connects to the reactive trabeculae deposits in the medullary cavity and beneath the periosteum. Finally the bony callus is remodeled gradually by osteoclasts, and increased mechanical loading restores the bone near to its original shape and mechanical properties (Heath and Young 2000, Ross et al. 2003, Rosenberg 2005).

2.1.4 Mechanical properties of bone

Because bone is an anisotropic material its mechanical properties depend on the loading direction of the testing method. Furthermore, biologic variables, such as race, sex, age, function, and level of activity, together with pathologic diseases affect the mechanical properties of the bone (Natali and Meroi 1989, Zioupos et al.

2000). In addition, the dense nature of cortical bone makes it strong and stiff thus differing significantly from cancellous bone. For example, the average values of Young's modulus of cancellous bone are measured in megapascals (MPa) whereas 1000-fold higher gigapascals (GPa) are used to measure the same average values of cortical bone. Also, the mechanical properties of cancellous bone vary more than those in cortical bone. This may be explained by the fact that the density of cancellous bone varies more than that of cortical bones depending on the anatomic location and donor. The lower heterogeneity of cortical bone may be due to its lower turnover rate (Rho et al. 1998, An 2000). The mechanical properties of cancellous bone are not discussed in more detail because only cortical bone was assessed in study **I**.

2.1.4.1 Mechanical properties of cortical bone

As cortical bone is anisotropic, it is also heterogenic, thus its mechanical properties vary along the longitudinal axis of bone and transversely in different anatomic quadrants. Evans *et al*. showed in the early 1950s that the lateral quadrant of the femur has the highest ultimate tensile strength and the anterior quadrant has the lowest. The middle third of the femoral shaft has the highest ultimate strength and Young's modulus whereas the lower third has the lowest average strength and elastic modulus (Evans and Lebow 1951). The mechanical properties of bone are thought to be more heterogeneous transversally in the anatomic quadrants than along the length. The variations in the properties around the circumference of cortical bone are minor, however, less than 10% (An 2000).

The mechanical properties of cortical bone are positively correlated with its apparent density, which is determined by the porosity and bone mineralization. The average apparent density of cortical bone is approximately 1.9 g/cm^3 (An 2000). Minor changes in the mineral density of cortical bone have a more pronounced effect on its elastic properties than similar changes in cancellous bone (Currey 1969a, Currey 1969b). The porosity and degree of mineralization together account for 84% of the stiffness variation of cortical bone (Currey 1988).

Three-point bending is a common method for mechanically testing cortical bone. One reason for this is that it produces information regarding three different mechanical properties in a single test; bending strength, Young's modulus and energy absorbed by the sample (Currey et al. 1997, An 2000). Previous studies demonstrated that the strength and elastic modulus of human cortical bone samples determined by bending tests range from 103 to 283 MPa and from 9.1 to 15.7 GPa, respectively (An 2000).

2.2 Allograft bone

Allograft bone is currently the graft of choice in the treatment of large bone defects, regardless of the fact that bone tissue engineering has developed enormously during

the past decade. Cortical bone allografts are used clinically to repair fractures and defects caused by illness, trauma, or radical tumor surgery (Virolainen et al. 2003, Akkus and Belaney 2005). Cortical allografts are required for the induction of osteogenesis and to provide sufficient structural support to the defect area until the formed new bone can restore adequate strength (Currey et al. 1997, Virolainen et al. 2003). Finite-element modeling study has demonstrated that stresses are transferred to allograft bone (Mihalko et al. 1992), therefore the main characteristic of structural cortical allograft is its ability to support mechanical loads and to resist breakage (Boyce et al. 1999). Failure of the cortical allograft before healing and initial integration to the host tissue can be clinically crucial and easily lead to reoperation.

Allograft bone has several advantages over autograft bone. Allograft bone can be manufactured in several configurations (powder, cortical chips and struts, cancellous cubes etc.) and harvested in an unlimited manner. In addition, the use of autograft bone results in donor site morbidity (Boyce et al. 1999, Barbour and King 2003, Eppley et al. 2005). Allograft bone has greater incorporation times than autograft bone, however, and does not can not elicit the same osteogenic response as autograft bone due to the lack of cells in processed allograft bone (Eppley et al. 2005). Processing of allograft bone is necessary to minimize the risk of an immunologic response of the recipient (Galea and Kearney 2005). The major concern in the use of allograft bone is the risk of viral transmission and bacterial contamination (Barbour and King 2003, Eppley et al. 2005, Eastlund 2006).

Allograft bone can transmit a variety of pathogens such as human immunodeficiency virus (HIV), *Myobacterium tuberculosis*, hepatitis, human T-cell lymphotropic virus, rabies, *Herpes simplex virus*, cytomegalovirus, fungus, and transmissible spongiform encephalopathies (Tomford 1995, Aspenberg 1998, Eastlund 2006). At present, the risk of viral transmission through allograft tissue is extremely low because serologic donor screening and tissue sterilization methods are effective (Boyce et al. 1999, Lomas et al. 2000, Barbour and King 2003).

The success rate after the implantation of massive osseous allografts varies from 60% to 90% when assessed through clinical, radiographic, and biologic methods. This illustrates the advantage of using allograft bone, although there is also justification for the development of new technologies that are emerging from bone tissue engineering studies (Boyce et al. 1999, Eppley et al. 2005).

2.2.1 Methods for cleansing allograft bone

After donor screening and tissue testing, the safety level of allograft bone can be further improved by cleansing the bone to minimize the risk of infection, which is directly related to the amount of blood and cellular tissue remaining in the bone graft (Tomford 1995). In addition, the incorporation of chloroform methanol defatted bone is enhanced compared to that of a graft that has not been lipid-extracted (Thoren et al. 1995, van der Donk et al. 2003). Fat removal from the bone also facilitates the penetration of sterilization solution into the tissue (Pruss et al. 1999).

A number of procedures have been proposed to remove necrotic and cellular tissue such as adipose tissue from allograft bone, including pulse lavage washing, chemical cleansing, and centrifugation (Lomas et al. 2000, DePaula et al. 2005, Haimi et al. 2008). The chemical and physical cleansing of allograft bone reduces the bioburden and cellular antigens in the graft. Commonly used chemical cleansing methods include aqueous solutions of detergents, hydrogen peroxide, organic solvents, acids, and alcohol. Chemical methods can also be used in combination with mechanical methods, such as ultrasonic baths, vacuum, centrifugation, and agitation, which may intensify the chemical cleansing (DePaula et al. 2005, Galea and Kearney 2005). Although the cleansing step preceding sterilization is necessary, it is likely that this affects the mechanical and biologic properties of the bone.

2.2.2 Methods for sterilizing allograft bone

Bone sterilization methods are either used alone or in combination with cleansing methods. Currently, commonly used sterilization methods of allograft bone are irradiation procedures, mainly gamma irradiation (Currey et al. 1997), and chemical sterilizations, such as PES (Pruss et al. 2003). An effective allograft bone sterilization method should penetrate through the bone structure into the cavities, to the blood and adipose tissue. There it should inactivate existing viruses and bacteria. At the same time, the sterilization method should not have adverse effects on the mechanical and biologic properties of the allograft bone.

Gamma sterilization is one of the most widely employed methods for musculoskeletal allograft tissue sterilization because it is an effective sterilization procedure with high tissue penetration properties. Pathogens are inactivated via disruption of their genetic material by direct and indirect damage. A dose of 25 to 35 kiloGrays (kGy) is reported to be sufficient to inactivate bacteria (Currey et al. 1997, Akkus and Rimnac 2001, Butler et al. 2005, Grieb et al. 2005). This is the standard radiation dose used in tissue banks for allograft bone. Regardless of the irradiation dose needed to achieve bacterial safety, the level required to assure viral inactivation is 90 kGy (Currey et al. 1997, Boyce et al. 1999). Doses over 25 kGy, however, significantly reduce the mechanical integrity of the bone (Cornu et al. 2000). The high doses of gamma irradiation especially affect the absorbed energy of cortical bone making the bone more brittle (Currey et al. 1997, Boyce et al. 1999). Gamma irradiation promotes the formation of toxic radicals, which are responsible for the majority of the damage that occurs to tissues during the irradiation procedure (Grieb et al. 2005).

Radioprotectants may minimize the changes in mechanical properties after high dose of irradiation. The purpose of radioprotectants is to minimize the formation of free radicals and reactive oxygen species generated during the irradiation procedure. Tissue grafts pre-treated with radioprotectants can be sterilized even with 50 kGy without reducing of the mechanical integrity of bone (Grieb et al. 2005). The effects of radioprotectants on osteoconductive properties of bone, however, have not yet been determined.

2.2.2.1 Peracetic acid-ethanol sterilization

Peracetic acid [$CH_3C(O)OOH$] is colorless and water soluble liquid, which is not carcinogenic and has low acute toxicity. The dose at which 50% of animals die (LD 50) is 1410 mg/kg when applied to the skin of a rabbit and 1540 mg/kg when orally dosed in the rat (Pruss et al. 2003). Peracetic acid is used as a disinfectant for heat-sensitive medical equipment and in the food industry because of its ability to rapidly inactivate broad-spectrum bacteria, fungi, spores, and viruses (Kline and Hull 1960, Werner and Wewalka 1973, Pruss et al. 2003). It is a strong oxidizing agent, produced by the reaction of acetic acid and hydrogen peroxide. The sterilization efficiency of peracetic acid relates to its rapid penetration into micro-organisms and the production of free radicals, which is crucial for the oxidation and destruction of microbial enzymes. Furthermore, treatment with peracetic acid does not destroy the bone morphology or bone structure (Pruss et al. 2002, Pruss et al. 2003).

The addition of ethanol to peracetic acid solution reduces the surface tension and enhances the tissue penetration of the sterilization medium. Furthermore, application of a vacuum system removes gas vesicles that prevent complete tissue penetration of the sterilization medium. The tissue penetration ability of the sterilization medium can be further enhanced by constant agitation of the sterilized tissues (Pruss et al. 2003). The PES treatment for allogenic bone is considered reliable and its use has been growing since the 1980s. Pruss *et al.* showed that 1% PES solution efficiently sterilizes contaminated bone tissue transplants, if the thickness of bone tissue does not exceed 15 mm (Pruss et al. 2003). PES does not cause any significant reductions in the osteoinductive properties of allograft bone (Pruss et al. 2002) and several growth factors necessary for bone formation *in vivo* remain after PES sterilization of the bone allografts (Wildemann et al. 2007). The effects of PES on cortical bone mechanical properties, however, have not yet been studied.

2.2.3 Freeze-drying of allograft bone

Allograft bone can be stored by deep freezing the bone at a temperature –70 ºC to –80 ºC or freeze-drying. The purpose of deep freezing is to reduce the free water amount to critical levels, where no degradation reactions can occur. The freeze-drying process consists of separating liquid water from a wet product of a given concentration in the form of ice followed by its removal by negative pressure sublimation, leaving the product almost totally anhydrous. Freeze-drying of bone enhances its chemical stability and prevents degradative changes such as protein denaturation (Franks 1998, Galea and Kearney 2005). Freeze-dried tissue that has a residual moisture content of less than 6% can be stored at room temperature for 5 years after processing (Conrad et al. 1993, Boyce et al. 1999).

The negative effects of freeze-drying on the biomechanical integrity of bone are well recognized (Conrad et al. 1993, Cornu et al. 2000, Nather et al. 2004). Cornu *et al*. demonstrated that freeze-drying cancellous bone with a less than 1% residual moisture content significantly reduces ultimate stress and stiffness, or Young's modulus (Cornu et al. 2000). In addition, Nather *et al*. demonstrated that cortical

allografts freeze-dried to 5% to 8% residual moisture content and sterilized with 25 kGy radiation are significantly weaker mechanically than deep-frozen allografts (Nather et al. 2004). Weakening of the mechanical properties is thought to be associated with micro-cracks along the collagen fibers in the bone matrix (Boyce et al. 1999). Freeze-drying of allograft bone makes it more brittle, but the original mechanical properties can be at least partially regained by rehydration (Conrad et al. 1993).

2.3 Stem cells

Stem cells are desirable candidates for tissue engineering applications due to their ability to commit to multiple cell lineages. By definition, a stem cell can replicate itself and provide additional undifferentiated stem cells or differentiate into more specialized directions (Fuchs and Segre 2000). Stem cells can be classified according to their origin, *i.e.*, embryonic, germinal, fetal, or adult, and their capacity to differentiate into other cell types is classified as totipotent, pluripotent, multipotent, and unipotent. Totipotent cells such as embryonic stem cells (ESC) derived from 1 to 3-d old embryos can differentiate into and renew any cell type that comprises the organism, whereas pluripotent cells such as the inner cell mass-derived ESCs and multipotent cells such as adult stem cells have a limited differentiation capacity. Unipotent cells give rise to only one type of differentiated cell. One of the unique characteristics of ESCs derived from the inner cell mass of a blastocyst is their ability to proliferate in long-term cultures while maintaining their pluripotent nature. Another important feature of ESCs is their capacity to differentiate into the three primary germ layers: ectoderm, mesoderm, and endoderm. Multipotent stem cells can be derived from a myriad of fetal and adult sources. These cells have limited self-renewal and differentiation capability, restricted to cell types of their germ layer of origin (Shamblott et al. 2000, Rao and Mattson 2001, Choumerianou et al. 2008).

The main potential of the possible use of ESCs is their ability to differentiate into any cell type, which will make available a ready-to-use source of cells for application to regenerative medicine. Furthermore, ESCs can be provided in adequate quantities and it is possible to reprogram these cells, which would allow for the treatment of different genetic diseases. Human ESCs may also be advantageous for disease modeling. The limitations of ESCs for regenerative medicine, however, include the possibility of immune rejection leading to the need for lifelong immunosuppression. There are also major political and ethical considerations regarding the use of human embryos, which present great challenges for the use of ESCs in patients (Lensch et al. 2006, Choumerianou et al. 2008).

2.3.1 Mesenchymal stem cells

Among adult stem cells, MSCs have been the subject of considerable research over the past few decades. In contrast to ESCs, there are no ethical issues related to the use of MSCs and they can also be used autologously and are therefore immunocompatible. Friedenstein was the first to isolate multipotent cells from bone marrow and showed that these stromal cells are able to differentiate towards a number of specific mesenchymal tissues under suitable conditions *in vivo* and *in vitro* (Friedenstein et al. 1966, Friedenstein et al. 1968, Friedenstein et al. 1987). MSCs can also be isolated from many other tissues than from bone marrow, such as adipose tissue, synovium, cartilage, periosteum, placenta, and cord blood (Barry and Murphy 2004). These multipotent stem cells can give rise to bone, cartilage, muscle, marrow stroma, tendon, ligament, adipose tissue, and a variety of other connective tissues (Caplan 1994, Pittenger et al. 1999). The International Society for Cellular Therapy recently suggested that MSC be defined by three criteria: 1) properties of adherence to culture dishes, 2) surface antigen expression or absence of expression: cluster of differentiation (CD)73^+, $CD90^+$, $CD105^+$, $CD14^-$ or $CD11b^-$, $CD19^-$ or $CD79\alpha^-$, $CD34^-$, $CD45^-$, human leukocyte antigen class II $(HLA\text{-}DR)^-$, and 3) ability to differentiate into chondrogenic, osteogenic, and adipogenic lineages (Dominici et al. 2006). Although MSCs can be identified by the presence or absence of many surface markers, no specific single marker of MSCs has yet been identified.

Because MSCs were originally demonstrated in bone marrow, bone marrow-derived MSCs are the most extensively studied. Their multipotency *in vitro* and *in vivo* is well known and therefore the use of bone marrow-derived MSCs in treating a variety of disorders has considerable potential. These stem cells have been successfully used to reconstruct skeletal defects in a number of animal models (Bruder et al. 1998, Schantz et al. 2003), which has led to their clinical use in a pilot study of their use in the treatment of osteogenesis imperfecta with encouraging results (Horwitz et al. 2002). Although bone marrow-derived MSCs are attractive candidates for tissue engineering applications, there are many disadvantages to their use. In particular, a low number of MSCs can be harvested in bone marrow aspirate, generally 1 in 25 000 to 1 in 100 000, and considerable pain is related to the bone marrow harvesting procedure. The MSC yield from the bone marrow is also critically dependent on donor age and sex (D'Ippolito et al. 1999, Banfi et al. 2000, Muschler et al. 2001). Furthermore, it has been proposed that MSCs express a limited capacity for self-renewal and their ability to differentiate diminishes with increasing age (D'Ippolito et al. 1999, Banfi et al. 2000). The low cell numbers of bone marrow-derived MSCs require an additional *in vitro* expansion step to obtain enough cells for clinical use. This process is both time-consuming and expensive.

2.3.2 Adipose stem cells

Recently, adipose tissue, a mesodermally derived organ, has emerged as a promising source of MSCs. Adipose tissue has been reported to consist of a stromal population

containing low levels of endothelial cells, smooth muscle cells, pericytes and stem cells (Zuk et al. 2001). The pioneering work of Zuk *et al*. showed that multipotent cells isolated from the stromal vascular compartment of adipose tissue have the ability to differentiate toward osteogenic, adipogenic, myogenic, and chondrogenic lineages *in vitro* when cultured with suitable inducing factors (Figure 1) (Zuk et al. 2001).

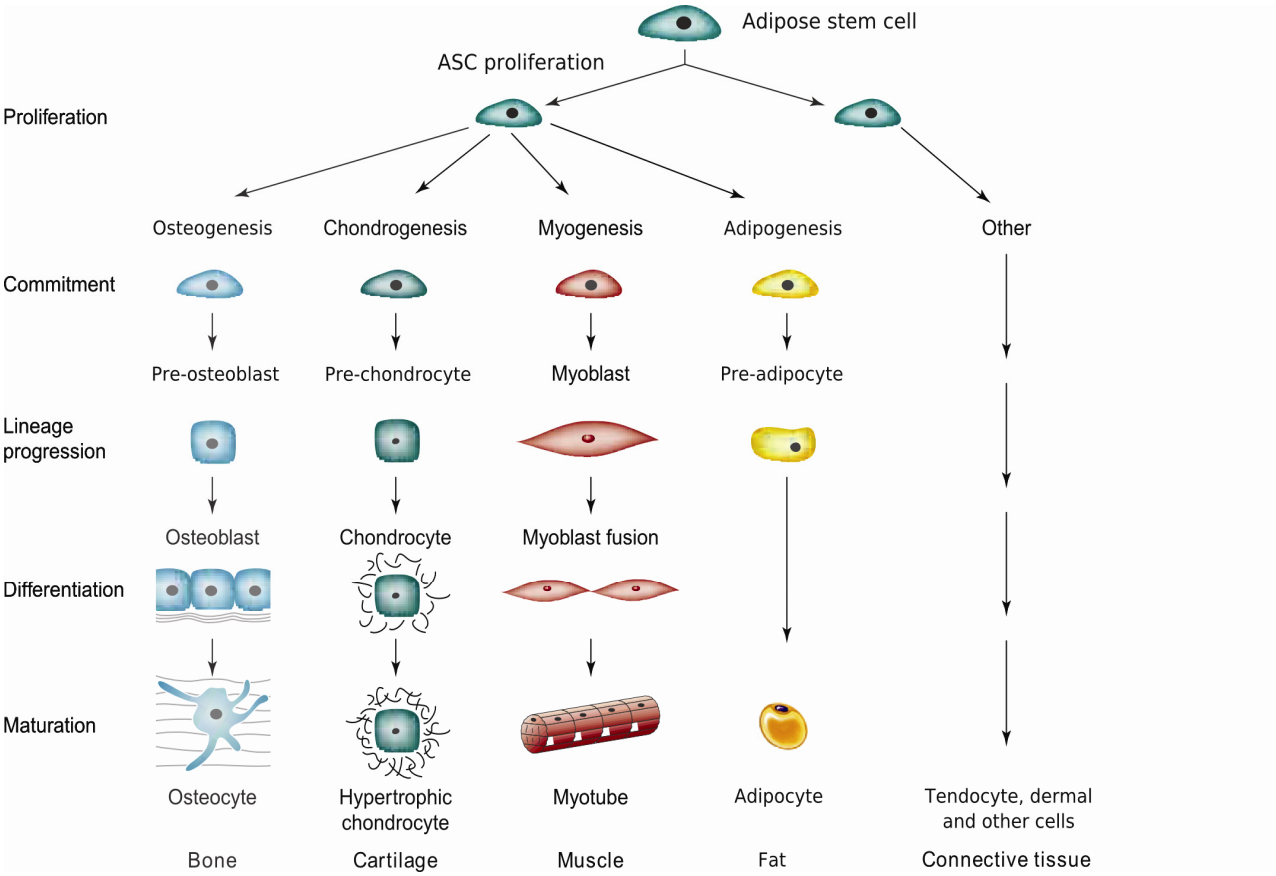

Figure 1. *The stepwise cellular transition from ASCs to highly differentiated phenotypes is depicted schematically. Modified from the original image (Caplan and Bruder 2001).*

The cell surface marker phenotype of human ASCs is similar to that of bone marrow-derived MSCs. For example, both cell populations express CD29, CD44, CD71, CD90, CD105, and CD73 (Zuk et al. 2002). In addition, CD105, stromal precursor cell marker STRO-1, and CD166 are commonly used to identify multipotent cells and are consistently expressed on ASCs and bone marrow-derived MSCs (Strem et al. 2005).

The first isolation method for mature adipocytes and progenitors from rat adipose tissue was introduced by Rodbell, in which the tissue was first digested with collagenase type I at 37 °C and then the cellular components were sorted out by differential centrifugation. After centrifugation, supernatant containing the mature adipocytes was separated from the pellet that consisted of the adipocyte progenitor cells and hematopoietic cells (Rodbell 1964). The isolation method remains the same, but with minor modifications to more efficiently isolate the ASCs. A typical

harvest of adipose tissue is 200 ml or more, yielding approximately one million stem cells per 100 ml of liposuction aspirate (Muschler et al. 2001, Aust et al. 2004), whereas the volume of bone marrow aspirate is generally no more than 40 ml (Bacigalupo et al. 1992), containing approximately 2.4 x 10^4 MSCs (D'Ippolito et al. 1999, Muschler et al. 2001). Adipose tissue is easy to obtain and cell number yields are sufficient to obviate extensive expansion in culture; therefore this tissue may be an ideal candidate for tissue engineering applications.

2.3.3 The use of adipose stem cells in treating bone defects

The osteogenic capacity of ASCs is well established (Halvorsen et al. 2001, Lee et al. 2003, Hattori et al. 2004, Hicok et al. 2004, Hattori et al. 2006, Elabd et al. 2007). ASCs give rise to osteoblasts in the presence of ascorbate-2-phosphate, ß-glycerophosphate, dexamethasone, and 1,25 vitamin D_3 (Halvorsen et al. 2001, Zuk et al. 2002, Bunnell et al. 2008). Under these osteogenic conditions, *in vitro* ASCs deposit Ca-P in their extracellular matrix; and express genes and proteins associated with an osteoblastic phenotype, including ALP, BMPs and their receptors, osteocalcin, osteonectin, and osteopontin (Halvorsen et al. 2000, Halvorsen et al. 2001, Zuk et al. 2001, Zuk et al. 2002). In addition, human ASCs show spontaneous osteogenic differentiation ability when seeded on osteoconductive scaffolds such as HA (De Girolamo et al. 2008). During osteogenesis of ASCs, the organization of cytoskeletal elements leads to changes in morphology. These changes in the assembly and disassembly kinetics of actin microfilaments may be crucial for supporting the osteogenic commitment of ASCs (Rodriguez et al. 2004).

In vivo, ASCs combined with various types of biomaterial scaffolds form bone in rodent ectopic bone models (Lee et al. 2003, Hattori et al. 2004, Hicok et al. 2004, Elabd et al. 2007). Lee *et al.* subcutaneously transplanted *in vitro* osteogenicly-induced ASCs seeded onto polyglycolide (PGA) scaffolds into rats (Lee et al. 2003). Histologic and immunohistochemical analysis of these implants revealed bone formation. Hicock *et al*. showed new osteoid, derived from human ASCs seeded on HA/tricalcium phosphate (TCP) cubes in immunodeficient mice 6 wk after implantation (Hicok et al. 2004). In a murine critical-size calvarian defect model, Cowan *et al*. demonstrated that ASCs seeded onto apatite-coated scaffolds regenerate cranial bone in a critical-size bone defect. The cranial bone formed through intramembraneous ossification, which is the normal development mechanism of calvarium. That study was the first to demonstrate the healing capability of ASCs for critical-size bone defects without genetic manipulation or the addition of exogenous growth factors (Cowan et al. 2004). Furthermore, the bone formation ability of ASCs is comparable to that of bone marrow-derived MSCs (Cowan et al. 2004, Hattori et al. 2006).

Adult stem cell-based applications are also increasing in the clinical practice. In the early 1990s bone marrow-derived MSCs have been successfully used to treat skeletal defects in clinical cases (Wakitani et al. 1994, Kitoh et al. 2004). ASCs have also been used clinically to treat a large, bilateral calvarial defect in a 7-year-

old girl; ASCs were seeded in fibrin glue to the calvarial defect and almost complete healing was detected 3 months after implantation (Lendeckel et al. 2004).

2.4 Biomaterials in bone tissue engineering

A biomaterial can be defined as a nonviable material used in a medical device intended to interact with biologic systems to evaluate, treat, augment, or replace any tissue, organ, or function of the body (Williams 1986). Biomaterials can be divided into four major classes of materials according to their chemical composition: polymers, metals, ceramics, and composites. A composite material is defined by a combination of two different classes of materials such as TCP particle-reinforced polylactide (PLA) (Hoffman 2004). Biocompatible ceramic biomaterials can be further classified as bioinert, resorbable, and bioactive. Resorption or biodegradation can be defined by the chemical breakdown of materials by action of living organisms that leads to changes in physical properties (Coury 2004). Encapsulation of the implant by fibrous tissue consistently occurs as a response to the implantation of bioinert materials. Therefore, no material can be classified or assumed to be completely inert after implantation. Resorbable materials gradually dissolve when they come in contact with body fluids and are replaced by the host tissue, and then the dissolution products are secreted in the urine. Bioactive materials are those that elicit a biologic response from the body such as bonding osteogenesis. This means that the biomaterial allows the formation of new bone onto its surface. There are two distinct types of bioactive materials according to their biologic behavior: osteoconductive and osteoproductive. Osteoconductive materials such as TCP allow for bone growth along their surface and therefore bond to bone tissue tightly. Osteoproductive materials, such as bioactive glass, react at a cellular level in the body to stimulate new bone growth on the material away from the bone/implant interface. The bone bonding mechanism behind the bioactive materials is suggested to relate to the formation of HA on the surface of the materials, which provides the bonding interface with tissues. The HA layer is similar to the apatite layer in bone and therefore a strong bond can be formed (Hench and Best 2004, Jones 2005). This review will concentrate on synthetic resorbable bioactive ceramics and resorbable bioactive composites of PLA and bioceramic.

Tissue engineering is a broad term that can best be defined by its aim: to create a medical device comprising functional and living components that is used to regenerate damaged or malfunctional tissue. Tissue engineering is a multidisciplinary field involving biology, medicine, and engineering and involves three basic components: cells, three dimensional (3D) scaffold and signals such as growth factors. The design of tissue-engineered bone constructs, as depicted in Figure 2, typically involves cell seeding on a highly porous biodegradable matrix, in the shape of the desired bone, then culturing the cell-construct with signaling molecules *in vitro* and transplanting the cell-biomaterial construct into the defect to induce and direct bone formation. The signaling molecules can be added during the

culture period or incorporated directly into the scaffold material (Schoen 2004, Buttery and Bishop 2005).

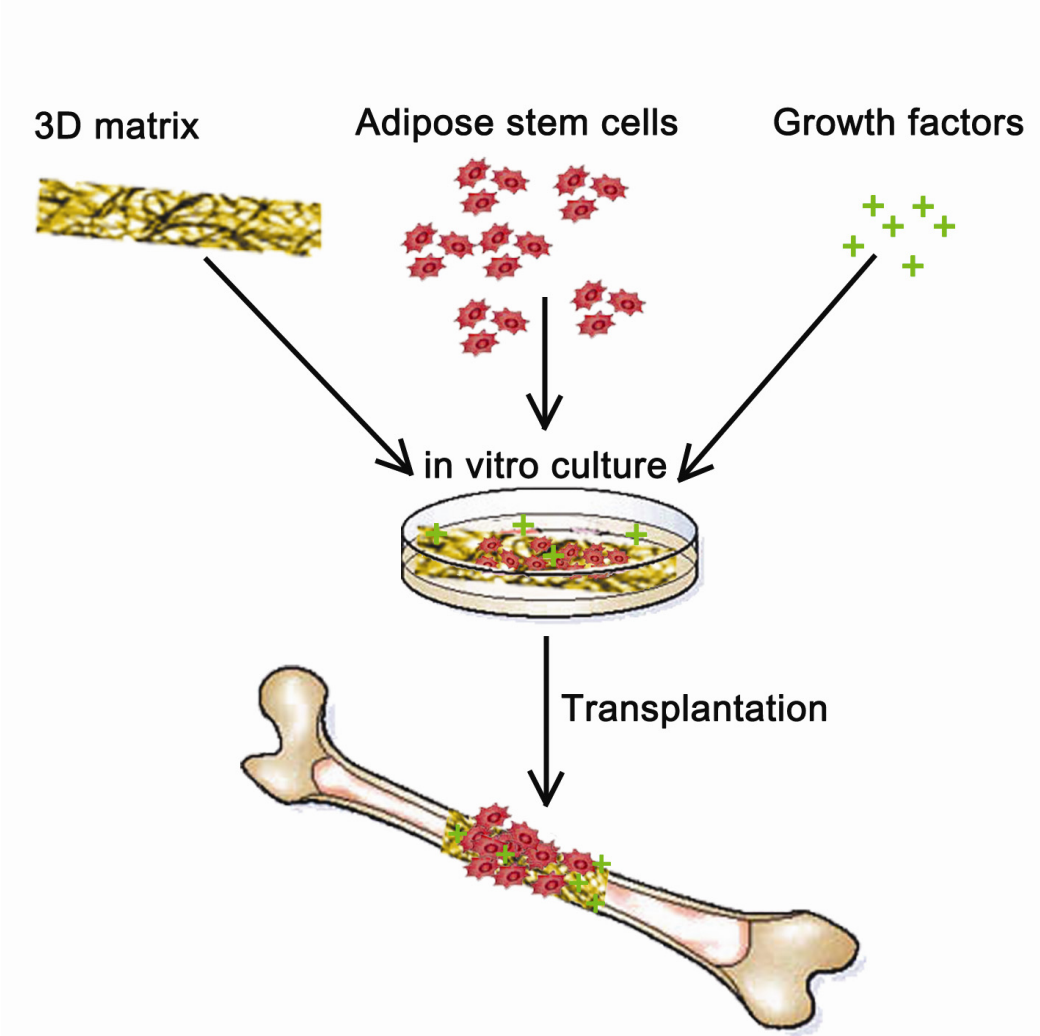

Figure 2. *Schematic illustration of tissue engineering of bone.*

The first challenge for bone tissue engineering is to optimize the isolation, proliferation, and differentiation of cells using specific signaling cues. The second challenge for bone tissue engineering is to solve the problems involved in all present-day orthopedic implants, the lack of three critical features of bone tissue: 1) the ability to self-repair, 2) the ability to maintain blood supply, and 3) the ability to modify their structure and properties in response mechanical load. To achieve the goal of tissue engineering, ideal scaffolds that fulfill several criteria are needed (Peter et al. 1998, Mathineu et al. 2006). The primary function of a scaffold is to provide a temporary substrate to which transplanted cells can adhere (Jones 2005). The scaffolds should be biocompatible and act as a 3D template for *in vivo* bone growth. To allow for cell migration and bone tissue growth in 3D, the template should ideally consist of interconnected macroporous networks. Some studies have concluded that the interconnecting pore diameter should be at least 100 µm to allow for cell migration and regeneration of mineralized bone (Hulbert et al. 1970,

Freyman et al. 2001, Hench and Polak 2002). The average size of human osteon is approximately 223 μm, thus the optimal range of a bone-filling scaffold should be near this value (Holmes 1979). Itälä *et al.*, however, reported that with an interconnected pore diameter ranging from 50 to 125 μm, the bone ingrowth ability into the implant remains at the same level despite the change in the pore diameter (Itälä et al. 2001b). Although the macropore morphology is important, the surface topography also needs to be optimized. For example, osteogenic cells must attach to a substrate before they can lay down their extracellular matrix. Importantly, the tissue-engineered construct should also have a degradation rate tailored to match the rate of tissue growth once it has been implanted (Freyman et al. 2001, Okii et al. 2001, Mikos et al. 2004, Jones 2005). Furthermore, the mechanical properties of the scaffold should match that of the host tissue. An ideal scaffold material should promote cell adhesion and stimulate osteogenesis. The scaffold should also act as a delivery system for the controlled release of signaling molecules that activate the cell self-regeneration ability (Hench and Polak 2002). The scaffolds should be efficiently produced with a processing technique that can be scaled-up for mass production, so that surgeons can apply them clinically. Finally, the scaffold material should pass international safety standards, such as those of Food and Drug Administration, to be able to be utilized clinically. The development of such biomaterial scaffolds and the understanding of biomaterial-cell interactions continue to present a great scientific challenge (Jones 2005).

2.4.1 Bioactive glass

2.4.1.1 Chemistry of bioactive glass and manufacturing processes

The concept of bioactivity via good bone bonding has been well documented for bioactive glass and glass ceramics since the 1970s (Hench et al. 1971). Bioactive glass bonds well to both hard and soft tissues. The bone bonding was first demonstrated for synthetic bioactive glass that contained SiO_2, Na_2O, CaO, and P_2O_5 in specific proportions. For example, Andersson *et al*. developed the famous bioactive glass S53P4 based on these four components (Andersson et al. 1990). The problem with the first generation bioactive glass was that the material had a tendency to crystallize during repeated hot processing. Brink *et al*. overcame this problem by developing novel bioactive glass comprising SiO_2-Na_2O-CaO-P_2O_5-B_2O_3-MgO-K_2O (Brink et al. 1997). This bioactive glass exhibits a wide melt-processing range with a diminished risk of crystallization. Thus, it can be manufactured in the form of microspheres, fibers, and sintered porous structures (Brink 1997, Ylänen et al. 1999, Ylänen et al. 2000, Arstila et al. 2005). Further studies on bioactive glasses based on the SiO_2-Na_2O-CaO-P_2O_5-B_2O_3-MgO-K_2O system have demonstrated that glasses showing wollastonite type crystallization should be used instead of glasses showing sodium-calcium-silicate crystallization for demanding glass-forming processes, such as sintering or fiber drawing (Arstila et al. 2007, Arstila et al. 2008). Recently, sol-gel based bioactive glasses have been

successfully electrospun to nanofibers with diameters that can be tailored from tens to hundreds of nanometers (Kim et al. 2006a, Kim et al. 2008). The rate of bioactivity is dependant on the chemical composition of the bioactive glass. The critical characteristic of bioactivity is the SiO_2 content. When the SiO_2 content is less than 60 mol%, bioactive glass can be distinguished from traditional soda-lime-silica glasses. The most rapid bone bonding to bone is achieved with bioactive glass that contains 45% to 52% SiO_2, a high Na_2O and CaO content, and a high CaO/P_2O_5 ratio (Hench and West 1996, Hench and Best 2004).

Bioactive glass can be manufactured by two methods: melt-processing (Kaufmann et al. 2000) and the sol-gel process (Balamurugan et al. 2007). Dissolution is more rapid in sol-gel-derived bioactive glasses than in melt-derived bioactive glasses of a similar composition. The surface of sol-gel-derived bioactive glass consists of many silanol groups that act as a nucleation sites for Ca-P formation, therefore making sol-gel-derived glass more bioactive (Jones 2005).

2.4.1.2 The mechanism of bioactive bone bonding

The bone-bonding ability of bioactive glass arises from the high rate of Ca-P layer formation at the surface of the material when exposed to body fluids. This reaction can also be produced *in vitro* by immersing the bioactive glass in simulated body fluid (SBF) or other acellular solutions containing all of the essential inorganic components of human body fluid (Kokubo et al. 1990b).

The chemical mechanism of bone bonding is initiated on the surface of the bioactive glass after contact with body fluids. At stage 1, rapid ion exchange of Na^+ and K^+ from the bioactive glass occurs with H^+ and H_3O^+ from the extracellular fluids, which causes subsequent leaching of Na^+, Ca^{2+}, Mg^{2+}, P^{5+}, and Si^{4+} and the formation of silanols (SiOH). At the next stages, the formation of a Si-rich layer through polycondensation of the hydrated silica groups starts after the loss of soluble silica. At stage 4, the formation of an amorphous Ca-P layer follows the adsorption of Ca^{2+}, PO^{4+}, and CO_3. Finally, crystallization of the hydroxycarbonate apatite layer occurs (Kokubo et al. 1990a, Hench and West 1996, Hench and Best 2004).

Formation of the Ca-P layer, which directs new bone formation together with absorbing proteins, is the first stage of cellular mechanism that underlies bonding of bone to bioactive glass. In the next stages, the extracellular proteins attract macrophages, and enhance MSC and osteoprogenitor cell attachment (Ducheyne and Qiu 1999, Hench and Best 2004). At the final stages, MSCs and osteoprogenitor cells proliferate and differentiate into osteoblasts. Particle size and material porosity are also important factors along with protein absorption that affect the osteoblasts function for bone ingrowth to bioactive glass (Itälä et al. 2001b, Hench and Best 2004).

2.4.1.3 Surface and compositional modifications of bioactive glass

The mechanism of the Ca-P layer formation on top of different surfaces and the stimulatory effect of Ca-P on cell activity has attracted the attention of several research groups (Radin et al. 1997, Bigi et al. 2005, Vaahtio et al. 2006). The composition and structure of the Ca-P layer on bioactive ceramics and the dissolution kinetics of the ceramic can be easily modified by controlling the immersion time and by changing the SBF solution (Vaahtio et al. 2006). Surface reaction studies performed with bioactive glass 45S5 indicated that compared to Tris buffer, Ca^{2+} and P^{5+} ions in SBF solutions accelerate the repolymerization of the Si-rich layer and formation of an amorphous Ca-P layer and eventually crystallization of the Ca-P layer (Filgueiras et al. 1993). Radin *et al*. documented that solution-mediated reactions of bioactive glass leading to the formation of silica gel in solutions with plasma and/or serum occur in parallel with serum protein adsorption. Reaction surfaces of bioactive glass formed in these solutions consisted of two layers: one composed of silica-gel and the other consisting of silica mixed with amorphous Ca-P phases (Radin et al. 1997).

The Ca-P rich layer on the surface of modified bioactive glass stimulates the adsorption of fibronectin and fibronectin-mediated cell attachment (Garcia et al. 1998, El-Ghannam et al. 1999). Also, the nanotopography of the Ca-P layer and dissolution rate of calcium and silica affects osteoblast growth and osteoclast survival (Vaahtio et al. 2006). Surface modifications involving the formation of fine precipitates of poorly crystallized carbonated apatite are also favorable for the adsorption of BMPs and other growth factors. The enhanced BMP-2 adsorption has a stimulatory effect on rat bone marrow-derived MSC osteogenic differentiation (Santos et al. 1998).

As stated in section 2.4.1.1, the composition of bioactive glass affects its bone bonding ability. Several ions such as zinc have been added to bioactive glass compositions to further enhance bone formation (Yamaguchi et al. 1987, Ito et al. 2000, Ikeuchi et al. 2003). The addition of zinc also improves the mechanical properties of bioactive glass, and extends its chemical durability by slowing down its dissolution and reaction in aqueous solutions (Lusvardi et al. 2002). The increased chemical durability of zinc containing bioactive glass has shown to be associated with a decreased formation rate of Ca-P layer (Kamitakahara et al. 2006, Jaroch and Clupper 2007). Zinc is an essential trace element that acts as a cofactor for many enzymes, stimulates protein synthesis, and is necessary for deoxyribonucleic acid (DNA) synthesis (Tang et al. 2001). Zinc is tightly involved in bone metabolism and its addition to bioceramic materials stimulates osteoblastic differentiation of osteoprogenitor cells *in vitro* (Ikeuchi et al. 2003, Storrie and Stupp 2005). The stimulatory effect of zinc on bone metabolism may be mediated by growth hormone or insulin-like growth factor (IGF) (Ovesen et al. 2001). The importance of the dosage and the possible cytotoxic effect of the zinc ions, however, have also been reported for certain bioactive glass and glass-ceramic compositions (Ito et al. 2000, Aina et al. 2007).

2.4.1.4 Applications of bioactive glass in bone tissue engineering and clinical use

The cellular basis by which bioactive glass influences ostoblastic cells has been widely investigated. Numerous studies of the molecular mechanisms of bioactive glass have mainly focused on osteoblasts and their gene expression *in vitro* (Xynos et al. 2000a, Xynos et al. 2000b, Gao et al. 2001, Xynos et al. 2001, Bosetti et al. 2003, Radin et al. 2005). These studies have uniformly demonstrated that bioactive glass stimulates the growth and maturation of osteoblasts, and promotes the expression and maintenance of the osteoblastic phenotype. Jones *et al.* showed that 70S30C bioactive glass composition without phosphate stimulated the formation of mineralized bone nodules of human osteoblasts, without the addition of ascorbic acid, β-glycerophosphate and dexamethasone (Jones et al. 2007b). In addition, ionic products of 45S5 bioactive glass dissolution alone can increase osteoblast proliferation. The increased proliferation may be due to increased availability of unbound IGF-II in osteoblasts (Xynos et al. 2000a). Alternatively, Christodoulou *et al*. demonstrated that ionic products of 58S bioactive gel-glass did not have a significant effect on the osteoblast phenotypic marker expression of human fetal osteoblastic cells (Christodoulou et al. 2005). Besides these studies, bioactive glass enhances rat bone marrow-derived MSC osteogenic differentiation, both surface-mediated and solution-mediated mechanism (Bosetti and Cannas 2005, Radin et al. 2005).

Various *in vivo* studies have demonstrated an osteopromotive effect of bioactive glass (Itälä et al. 2001b, Itälä et al. 2003, Välimäki et al. 2005a, Välimäki et al. 2005b). Furthermore, bioactive glass induces a high but balanced local bone turnover in rat models (Välimäki et al. 2005b, Välimäki et al. 2006).

The first clinical use of bioactive glass in patients was as a middle ear prosthesis in the early 1980s (Reck 1981), however, the first clinical case in which glass/tissue bonding was detected was reported in 1986 (Merwin 1986). Since then, bioactive glass has been successfully used clinically in dental, craniomaxillofacial, and spine surgery applications in a variety of different forms, such as plates, granules, and powder (Lovelace et al. 1998, Anderegg et al. 1999, Aho et al. 2003, Elshahat et al. 2004, Turunen et al. 2004, Peltola et al. 2008).

2.4.2 Calcium phosphate ceramics

Sixty percent of bone consists of a mineral phase, which is primarily calcium and phosphate. Therefore Ca-P ceramics have been studied intensively. Ca-P ceramics are crystalline materials that include various ceramic analogs of bone mineral phase, but only certain compounds are useful for implantation in the body, due to the fact that both the solubility and speed of hydrolysis increase with a decreasing Ca/P ratio. Compounds with a Ca/P ratio of less than 1/1 are not suitable for biologic implantation (Hench and Best 2004). Among these ceramics, HA is highly osteoconductive, allowing for significant bone ingrowth into cavities and pores of a biomaterial coated with HA compared to non-coated biomaterials (Hing et al. 1998).

HA ($Ca_{10}(PO_4)_6(OH)_2$) and other family members of Ca-P ceramics, α-TCP (α-$Ca_3(PO_4)_2$) and β-TCP (β-$Ca_3(PO_4)_2$), have been used successfully in clinical applications (de Groot et al. 1998, Block and Thorn 2000, Bohner 2001, Dorozhkin and Epple 2002, Daculsi et al. 2003, LeGeros et al. 2003). The solubility and biodegradation rate of α-TCP are higher than those of β-TCP (Dorozhkin and Epple 2002). In addition, bioresorbable β-TCPs dissolve in the presence of acids released by osteoclasts and macrophages whereas HA is barely degradable (Bohner 2000). β-TCP is highly biocompatible, osteoconductive, and stimulates proliferation and osteogenic differentiation of MSCs in a number of *in vivo* and *in vitro* studies (Gürpinar and Onur 2005, Takahashi et al. 2005, von Doernberg et al. 2006, Kasten et al. 2008). The bone tissue engineering applications of Ca-P ceramics and other bioceramics such as bioactive glass, however, are limited, due to their brittleness and low mechanical strength (Wang 2003, Hench 2006).

2.4.3 Polylactide based polymers

Recently, PLA-based polymers have been studied as 3D biomaterial scaffolds for different tissue engineering applications due to their desirable characteristics such as biocompatibility and controllable degradation (Jagur-Grodzinski 1999, Seal et al. 2001, Navarro et al. 2004, Wang et al. 2005, Ren et al. 2007). The chemical properties of PLA-based polymers allow hydrolytic degradation via de-esterification. The degradation products, such as carbon dioxide and water, are non-toxic and can be metabolized by natural pathways. Furthermore, these polymers are transparent, thermally stable, and easily processed. They have good mechanical properties, which can be modified according to the required implant properties (Mano et al. 2004). PLA can be produced using stereoisomer lactides of L and D, and DL-lactides via polycondensation or ring-opening polymerization (Södergård et al. 1996). The *in vivo* and *in vitro* degradation rate of poly(α-hydroxy acids) is associated with the microstructural factors such as chemical composition and structure, macrostructural factors such as size and geometry of the implant, and environmental factors such as pH and ion exchange (Södergård et al. 1996, Hiltunen et al. 1997, Karjomaa et al. 1998). The mechanical properties and the degradation rates of these polymers can be tailored by copolymerization of L-lactide with varying amounts of D-lactide. If the amount of D-lactides is increased, the disorder in polymer chains increases and the polymer becomes more amorphous and fragile (Mainil-Varlet et al. 1997, Törmälä et al. 1998). A self-reinforcing technique to increase the initial strength and strength retention time of semicrystalline and amorphous PLA was introduced in 1992 by Törmälä *et al.* (Törmälä 1992).

PLA have been used clinically for two decades as internal orthopedic fixation devices such as pins, screws, tacks, and plates (Suuronen et al. 2000, Peltoniemi et al. 2002, Ashammakhi et al. 2004, Suuronen et al. 2004, Waris et al. 2004, Eppley et al. 2005, Matsumoto et al. 2005). Furthermore, these polymers have been extensively studied as potential scaffold materials for skeletal tissue engineering (Mikos et al. 1994, Lo et al. 1995, Giordano et al. 1996, Puelacher et al. 1996, Park

et al. 1998). Moreover, bone marrow-derived osteoblasts attach, grow, and express an osteoblastic phenotype *in vitro* and *in vivo* in 3D poly(lactide-*co*-glycolide) (PLGA) scaffolds (Ishaug-Riley et al. 1997, Ishaug et al. 1997, Ishaug-Riley et al. 1998). However, there are many disadvantages involved in the use of these materials, such as premature failure of the implant caused by a bulk erosion process and strong inflammatory response due to the acidic degradation products, which can lead to delayed bone healing or osteolytic reactions (Bergsma et al. 1993, Martin et al. 1996, Takizawa et al. 1998). PLA polymers also have a limited osteoconductivity (Cornell 1999), and therefore are often used in conjunction with bioactive materials.

2.4.4 Polylactide/bioceramic composites

A composite material can be defined as a material consisting of two or more chemically distinct phases such as metallic, ceramic, or polymeric which are separated by interfaces. The definition covers the fiber and particulate composite materials that consist of one or more discontinuous phases embedded within a continuous phase. The discontinuous phase is often harder and stronger than the continuous phase and is therefore referred to as a reinforcing material, whereas the continuous phase is called the matrix. The engineered composite materials can be classified into matrix materials or re-inforcement dimensions/shapes. The matrix materials include metals, ceramics, and polymers, whereas the re-inforcement dimensions/shapes consist of particulates, short fibers, and continuous fibers (Migliaresi and Alexander 2004). A composite is designed to provide a combination of properties that cannot be achieved with a single phase material (Thompson 2005). The fiber-reinforced composites with continuous fibers have been studied as synthetic biomaterials in dentistry (Vallittu 1997, Lassila et al. 2002). Furthermore, in a rabbit model, the surface porous fiber-reinforced polymethyl methacrylate composites have been shown to allow bone ingrowth to the implant while having biomechanic properties similar to native bone (Hautamäki et al. 2008). There are several factors affecting the properties of biomedical composites. These include the shape, bioactivity and the micro- and macrostructure of the reinforcement, as well as the micro- and macrostructural properties of the matrix, distribution of the reinforcement in the matrix, and the reinforcement-matrix interfacial state (Wang 2003). Niemelä *et al*. demonstrated that the addition of bioactive glass modifies the degradation kinetics and material morphology of the matrix PLA (Niemela et al. 2008). Moreover, bioactive glass affects the initial mechanical properties and bioactivity of the PLA/bioactive glass composites. Currently, the polymer/bioceramic composites most often used clinically are interference screws such as Calaxo by Smith&Nephew (www.smith-nephew.com).

Various bioactive composites have been studied for tissue replacement and tissue regeneration purposes. In particular, for bone tissue engineering, the development of composite materials comprising a biodegradable polymeric phase such as PLA and an osteoconductive or osteopromotive inorganic phase, such as TCP or bioactive glass, has emerged as a promising approach for 3D scaffold production (Niemeyer et al. 2004, Verrier et al. 2004, Takahashi et al. 2005, Kim et al. 2006b, Meretoja et

al. 2006, Yang et al. 2006). The addition of bioactive glass or TCP particles to a biodegradable polymer leads to the rapid exchange of protons in water for the alkali in the inorganic phase, which should buffer the acidic degradation products of PLA. This same reaction can be used to alter the polymer degradation behavior (Maquet et al. 2004). Moreover, the mechanical properties of the brittle bioceramics may be improved by using the traditional composite approach, such as inclusion of a particulate ceramic phase in the polymer matrix and also the osteoconductivity of the original polymer is expected to be enhanced by addition of the bioactive phase (Stamboulis et al. 2002, Boccaccini and Maquet 2003). Each of the composite materials studied have their distinctive features and may be used in specific clinical situations. Polymer/bioceramic composite scaffolds, however, are not yet used in clinical practice.

The addition of a bioactive bioceramic to a polymer matrix has a stimulatory effect on bone formation *in vitro* and *in vivo* (Kim et al. 2006b, Yang et al. 2006). The addition of increasing percentages of the bioactive phase also leads to stimulated cell adhesion and growth in a dose-dependent manner (Verrier et al. 2004, Takahashi et al. 2005, Aunoble et al. 2006). Yao *et al.* suggested that the mechanism by which polymer/bioactive glass composites promote the osteogenic differentiation of multipotent MSCs is through solution-mediated factors (Yao et al. 2005). Although there are a number of studies on different bioactive glass and β-TCP/ biodegradable polymer composites, mainly the effect of the concentration of bioactive glass or β-TCP in the composite on cell activity has been evaluated. There has been no systematic comparison between PLA/β-TCP and PLA/bioactive glass composite scaffolds.

3. Aims of the study

The aim of this study was to evaluate whether sterilized allograft bone and ASCs used in combination with different biomaterials show potential *in vitro* for the treatment of bone defects. In the first section, we aimed to determine the potential of chemical cleansing combined with PES as a sterilization method for cortical allograft bone. This was followed by the evaluation of different bioactive glass and PLA/β-TCP and PLA/bioactive glass scaffolds in combination with ASCs for bone tissue engineering applications. After observing the positive effects of bioactive glass on ASC proliferation and differentiation, we hypothesized that the application of bioactive glass or β-TCP to a PLA matrix would result in an osteostimulative composite scaffold for ASCs.

Specific aims of the study were as follows:

I. To determine whether different chemical cleansing methods combined with PES affect the residual fat content and the biomechanical properties of cortical bone and to evaluate the effect of different residual moisture contents on the biomechanical properties of cortical bone.

II. To study the effect of two different Ca-P treatments of 3D bioactive glass constructs on ASC viability, proliferation, and osteogenic differentiation.

III. To investigate the effect of zinc addition to 3D bioactive glass scaffolds on degradation and on ASC viability, proliferation, and differentiation into osteogenic lineages.

IV. To compare the effects of 3D composite scaffolds comprising different concentrations of bioactive glass or β-TCP incorporated within a PLA matrix on ASC viability, morphology, proliferation, and ALP activity.

4. Materials and methods

4.1 Allograft bone material (**I**)

Bone grafts were obtained from the Tampere University Hospital bone bank. Four pairs of proximal tibias, four pairs of distal tibias, and one pair of proximal femurs were harvested from 6 male donors (mean age=51±16 years) and from 2 female donors of 31 and 45 years of age. The donors had no medical history of diseases or traumas that could affect the biomechanical properties of the studied allografts. All of the donors were screened to be bacteria- and virus-negative according to the standards of the European Association of Tissue Banks (EAMST/EATB 1997). The bones were obtained in the operation theatre with full aseptic precautions and stored at -75ºC. The study was implemented in accordance with the Ethics Committee of the Pirkanmaa Hospital District (R05048), Tampere, Finland.

4.2 Bone sample preparation and processing (**I**)

Because the biomechanical properties of bone from different donors may vary, pairs of bones from the same donor were investigated. The unprocessed controls and the processed samples were taken in equal amounts from the contralateral sides of bone from the same donor to ensure that possible differences due to anatomical heterogeneity in the bones did not influence the results. The paired specimens were analyzed.

The cortical bone samples were cut from the diaphysial part of the bones, using a grinding machine (model 40BKS; Scantool 40, Brovst, Denmark), shaped with a band saw (model DW738; Dewalt, Monza, Italy), and trimmed to dimensions of 40 mm x 4 mm x 2 mm using a milling machine. A sliding gauge was used to measure the dimensions of the samples. Paired cortical samples (5-12; mean = 6) were obtained from each bone pair. The specimens were continuously irrigated with distilled water during sample preparation and mechanical testing. All the bone samples were stored at -75ºC until processing and/or mechanical testing. The 96 cortical samples obtained were evenly divided to serve as processed samples or as unprocessed controls.

4.2.1 Bone sample cleansing

Cleansing procedure A was based on the cleansing procedure used by the National Blood Service, Tissue Service, UK. For all cleansing steps, the cortical samples were placed in a 1-L glass container and covered with 800 ml treatment solution. After sonicating the samples with distilled water in a temperature-controlled ultrasonic bath (model DU-14; Nickel Electro Ltd, North Somerset, UK) for 15 min at 54ºC, the bone samples were washed in distilled water four times (60 min, 10 min, 10 min, 10 min) under agitation (200 rpm) on a temperature-controlled shaker (model SM 30 A/B/C; Edmund Bühler GmbH, Hechingen, Germany) at 60ºC. The samples were soaked for 10 min in 3% hydrogen peroxide, followed by a 10 min soak in 70% ethanol in an ultrasonic bath at room temperature. After the sonicating phase, the bone samples were washed five times in distilled water (10 min, 10 min, 20 h, 10 min, 10 min) under constant agitation (200 rpm) on the shaker at 60ºC.

Cleansing procedures B and C were modifications of procedure A. In cleansing procedure B, the incubation times in hydrogen peroxide and 70% ethanol were two times longer than in procedure A, and the overnight (20 h) as well as the following two 10-min water washes were omitted. In cleansing procedure C, the 20 h and the following two 10-min water washes were omitted. Twenty-four samples (3 separate batches, each with 8 samples) were processed with cleansing procedure A, 16 (2 separate batches, each with 8 samples) were processed with cleansing procedure B, and 8 samples in a single batch were processed with cleansing procedure C.

4.2.2 Sterilization of bone samples and freeze-drying

All the processed samples were sterilized with 1% PES solution according to the method previously described (Pruss et al. 2003). Briefly, the PES procedure was performed under constant agitation (on a shaker at low pressure, 200 mbar) at room temperature in a desiccator for 4 h. This was followed by the removal of the PES solution by washing the bone samples four times for 10 min in distilled water under agitation (on a shaker at low pressure 200 mbar) at room temperature in a desiccator. Finally, the absence of peracetic acid was verified using a Merckoquant® test (Merck KGaA, Darmstadt, Germany) with a sensitivity of 5 ppm.

After sterilization, all the processed cortical samples were freeze-dried (Heto Drywinner with a CT 110 Cooling Trap, Jouan Nordic, Copenhagen, Denmark). The eight samples processed using cleansing method A were freeze-dried for 27 h (condenser temperature -110°C, and working vacuum approximately 1 mbar) to 0% residual moisture content. The residual moisture was removed with hygroscopic P_2O_5 treatment in a desiccator for 9 d at low pressure (200 mbar). The removal of residual moisture was confirmed when the mass of the bone samples was stabilized. All the other cortical samples were freeze-dried for 5 h to a residual moisture content of 4.5%.

4.3 Mechanical testing of bone samples and residual lipid content determination (**I**)

Three-point bending tests were performed with a mechanical testing machine (model 4411; Instron, Bucks, UK). The data were analyzed using Instron series IX software version 8.31. The machine sensors measured travel and load throughout the procedure. All the freeze-dried cortical samples were rehydrated for 30 min in physiologic saline solution at room temperature. The frozen controls were thawed and tested wet at room temperature.

The samples were oriented so that the periosteal surface was in tension and the endosteal surface in compression. The three-point bending test was performed as described by Currey *et al.,* except that the crosshead speed was 1 mm/min (Currey et al. 1997). Young's modulus of elasticity was calculated from the linear part of the stress-strain curve. The bending strength was calculated using the following formula, $\sigma = 3FL/2bd^2$, where F is the external force influencing the sample, L is the gauge length (32 mm), b is the sample width, and d is the sample thickness. The energy absorbed by the sample at the breakpoint was calculated by measuring the area under the load deformation curve.

Following mechanical testing, the residual fat content was analyzed using an ultrasonic hexane elution assay. All processed cortical samples were ground with a grinder (model Polymix A10; Kinematica AG, Lucerne, Switzerland). All the cortical samples from each processing group were pooled to yield one sample. After the lipids from the bone powder samples were extracted in hexane, the hexane was evaporated and the resultant residual weight was expressed as a percentage of the (extracted original) dried cortical bone powder weight.

4.4 Scaffold manufacturing

4.4.1 Preparation of bioactive glass scaffolds (**II**, **III**)

Three-dimensional porous bioactive glass scaffolds (Inion BioRestore™, Inion Oy, Tampere, Finland), with a nominal composition of 11-12 wt% Na_2O, 16-17 wt% K_2O, 3-4 wt% MgO, 12-14 wt% CaO, 3-4 wt% P_2O_5, 1-2 wt% B_2O_3, 0-1 wt% TiO_2, 50-51 wt% SiO_2 were used in studies **II** and **III**. In study **III**, CaO was substituted with ZnO to produce bioactive glass with six different amounts of zinc (0, 0.25, 0.5, 1.0, 1.5, 2.0, and 5.0 mol%). In the cell culture experiments, only 0, 0.25, and 1.0 mol% zinc-containing bioactive glass scaffolds were studied. The bioactive glass scaffolds were manufactured via melt processing. After manufacturing 3-mm long and 75-µm thick bioactive glass fibers by melt spinning, the matrices were manufactured by sintering the bioactive glass fibers and characterized with respect to their total porosity by direct measurement of their volume and weight, according to the equation

$$\varepsilon = \frac{\rho_g - \rho_s}{\rho_g} \times 100\% \; \varepsilon = \frac{\rho_g - \rho_s}{\rho_g} \times 100\%$$

where ρ_g is the density of the bulk glass and ρ_s is the density of the scaffold. The porosity was also calculated in a few samples by image analysis processing of two dimensional scaffold sections obtained by molding the scaffolds in epoxy and polishing the surfaces, according to the following equation

$$\varepsilon = \frac{A_t - A_f}{A_t} \times 100\% \; \varepsilon = \frac{A_t - A_f}{A_t} \times 100\%$$

where A_t represents the total area of the scaffold section, and A_f is the area occupied by the fibers in the section. Scaffolds with a total porosity of 70% were chosen for these studies because scaffolds with the same porosity were previously studied with respect to degradation (Moimas et al. 2006b), permeability (Moimas et al. 2004), and *in vivo* behavior (Moimas et al. 2006a). Scaffolds with dimensions of 14 mm x 14 mm x 5 mm were obtained by cutting commercially available products with a rotating saw and surgical knife.

In study **II**, the samples were neither treated nor immersed in SBF to achieve the formation of a Ca-P surface layer. One group of samples was immersed in SBF following the procedure described by Kokubo *et al.* (Kokubo et al. 1990b). The samples were stored at 37ºC for 4 d, a surface area-to-volume ratio (SA/V) of 1 cm^{-1} was selected and no agitation was applied to obtain a thin homogenous Ca-P layer. Another group of samples was covered with media comprising 2-fold concentrated Kokubo's SBF, at 37ºC for 7 d, SA/V 1 cm^{-1}, and without agitation in order to produce a thick and irregular Ca-P layer. For scanning electron microscopy (SEM) analysis, the scaffold samples were sputter-coated with a gold-platinum mixture and viewed using a Leica Stereoscan 430i SEM (Leica, Solms Germany).

In study **III**, the effect of zinc on the degradation profile of the bioactive glass was studied in both deionized water and SBF. Chopped fibers (110 mg) of the different compositions were immersed in 110 ml deionized water and incubated at 37ºC for 0.5, 4, 12, 24, and 72 h. At each time-point, the fluid was filtered and the amounts of Zn^{2+}, Ca^{2+}, K^{+}, and Mg^{2+} ions were determined by atomic absorption spectroscopy (AAS) (Perkin Elmer, Waltham, MA). The scaffolds were immersed and incubated in SBF (Kokubo et al. 1990b) at 37 ºC for different time periods (1 h, 8 h, 1 d, 3 d, 1 wk, 2 wk, 3 wk) with a SA/V of 0.2 cm^{-1}. Following immersion, the scaffolds were gently washed with deionized water, flushed with ethanol, and dried under laminar flow. The degradation was evaluated by Leica Stereoscan 430i SEM. Fibers with diameters of 0.25 and 1 mm were also immersed in SBF and incubated at 37ºC for different times (1, 3, 7, and 14 d) and treated as just described. The fibers were weighed before and after the immersion. In studies **II** and **III**, the scaffolds were sterilized with ethanol before the *in vitro* cell culture.

4.4.2 Preparation of PLA, PLA/bioactive glass, and PLA/β-TCP scaffolds (**IV**)

Poly(L/D, L-lactide (PLA) 70/30 (PURAC Biochem b.v., Gronichem, Netherlands) with an inherent viscosity of ~ 3.1 dl/g was used as a matrix polymer. β-TCP ("Beta Whitlockite", Plasma Biotal Limited, Tideswell, UK) and bioactive glass with a composition of 5% Na_2O, 7.5% K_2O, 3% MgO, 25% CaO, and 59.5% SiO_2 (BaG0127, Åbo Akademi, Turku, Finland) were used as the filler materials. After being ground to a powder, the particle size distribution of the porous β-TCP granules and the bioactive glass granules was 75 to 106 μm and 75 to 125 μm, respectively.

PLA solution (2.0 wt%) was produced by dissolving PLA in 1,4-dioxane (Sigma-Aldrich, Helsinki, Finland). One of the above-mentioned fillers was added to the PLA solution. The PLA-filler ratios used are shown in Table 1. The solutions were frozen at -30ºC prior to freeze-drying in the Heto Drywinner freeze-drier. The solution was placed into custom-made Teflon moulds (Ø15 mm and height 3 mm) and frozen at -30ºC for 24 h prior to 24 h of freeze-drying. As a reference material, plain PLA scaffolds were prepared with the same procedure as composite scaffolds. After freeze-drying, all of the samples were at room temperature under vacuum for at least 48 h before sterilization with 25 kGy gamma irradiation.

Table 1. *A. PLA/β-TCP composite scaffolds, B. PLA/Bioactive glass composite scaffolds (study **IV** copyright by Tissue Engineering reproduced with permission).*

A.	**PLA [wt%]**	***β*-TCP [wt%]**	**B.**	**PLA [wt%]**	**Bioactive glass [wt%]**
PLA	**100**	**0**	PLA	**100**	**0**
PLA/10 *β*-TCP	**90**	**10**	PLA/10 Bioactive glass	**90**	**10**
PLA/20 *β*-TCP	**80**	**20**	PLA/20 Bioactive glass	**80**	**20**

4.5 Cell culture methods

4.5.1 Adipose stem cell isolation and cell culture (**II**, **III**, **IV**)

ASCs were isolated from adipose tissue samples acquired from surgical procedures (study **II**, 10 donors, mean age = 48±8 years; study **III**, 9 donors, mean age=48±9 years; and study **IV**, 6 donors, mean age = 44±7 years). The adipose tissue samples were obtained from the Department of Plastic Surgery and from the Department of Gastroenterology and Alimentary Tract Surgery, Tampere University Hospital. Studies **II**, **III**, and **IV** were implemented in accordance with the Ethics Committee

of the Pirkanmaa Hospital District (R03058), Tampere, Finland. The adipose tissue was digested with collagenase type I (1.5 mg/mL; Invitrogen, Paisley, UK). Isolated ASCs were maintained and expanded in T-75 cm^2 polystyrene flasks (Nunc, Roskilde, Denmark) in maintenance medium comprising Dulbecco's modified Eagle's medium: nutrient mixture F-12 (DMEM/F-12 1:1) (Invitrogen), 10% fetal bovine serum (FBS) (Invitrogen), 1% L-glutamine (GlutaMAX I; Invitrogen), and 1% antibiotic/antimycotic (100 U/mL penicillin, 0.1 mg/mL streptomycin, and 0.25 µg/mL amphotericin B; Invitrogen). Half of the medium was exchanged 3 times per wk. Cells from passages 3-6 were used for study **II** and **III** experiments, and cells from passages 4-7 were used for study **IV** experiments.

ASCs were harvested from T75 cm^2 flasks and analyzed by a fluorescence activated cell sorter (FACS) (FACSAria; BD Biosciences, Erembodegem, Belgium). For studies **II**, **III**, and **IV**, monoclonal antibodies against CD9-phycoerythrin (PE), CD10-PE-Cyanine7Cy7, CD13-PE, CD29-allophycocyanin (APC), CD49d-PE, CD90-APC, CD106-PE-Cyanine5Cy5, and CD166-PE (BD Biosciences); CD45-fluorescein iso thiocyanate isomer 1 (FITC;Miltenyi Biotech, Bergisch Gladbach, Germany); CD31-FITC, CD34-APC, CD44-FITC, and CD105-PE (R&D Systems Inc, MN) were used. Monoclonal antibodies against STRO-1 (R&D Systems Inc) and Human Fibroblast Surface Protein (hFSP; Sigma-Aldrich, St. Louis, MO) were conjugated with immuno globulin IgM-PE (CalTag Laboratories, Burlingame, CA). In addition, surface marker against CD59-FITC (Immunotools GmbH Friesoythe, Germany) was determined in studies **II** and **III**. Analysis was performed on 10 000 cells per sample and positive expression was defined as a level of fluorescence greater than 99% of the corresponding unstained cell sample.

Based on FACS analysis, ASCs used in studies **II**, **III**, and **IV** expressed the adhesion molecules CD9, CD29, CD34, CD49d, CD105, and CD166; receptor molecule CD44; surface enzymes CD10 and CD13; and extracellular matrix protein CD90. Furthermore, ASCs showed moderately positive expression of the putative stem cell marker STRO-1, major histocompatibility class I antigen human leukocyte antigen class I (HLA-ABC), and fibroblast marker hFSP. ASCs used in studies **II**, **III**, and **IV** did not express the hematopoietic surface markers CD31, CD45, and CD106. Complement regulatory protein CD59 was expressed in the cell lines used in studies **II** and **III**.

For all the ASC experiments in studies **II**, **III**, and **IV**, samples from 2 to 4 patients were pooled to yield enough cells for one experiment. The scaffolds were pretreated with maintenance medium for 48 h at 37ºC, following cell seeding with 500 000 cells in a 0.25 ml medium volume (**II**, **III**), or 350 000 cells in a 0.175 ml medium volume (**IV**). The pretreatment with maintenance medium was done to allow serum proteins to adsorb to the biomaterials, a process which was demonstrated to stimulate osteoblast-like cell attachment and osteogenic differentiation (El-Ghannam et al. 1999). To optimize ASC attachment, the cell-seeded constructs were incubated for 3 h at 37ºC in 5% CO_2 before additional media was added. The cell-seeded scaffolds were cultured in maintenance medium until analyses.

4.5.2 Adipose stem cell viability and proliferation (**II**, **III**, **IV**)

ASC viability and attachment was examined using live/dead staining. ASC-biomaterial constructs were incubated for 45 min at room temperature with a mixture of 5 μM CellTracker™ green (5-chloromethylfluorescein diacetate [CMFDA]; Molecular Probes, Invitrogen) and 2.5 μM ethidium homodimer-1 (EH-1; Molecular Probes). The probe solution was replaced with pre-warmed maintenance medium and incubated for 30 min at 37ºC. The viable cells (green fluorescence) and dead cells (red fluorescence) were investigated using a fluorescence microscope. In the ASC studies **II**, **III**, and **IV** cell viability was assessed at 3 h and 2 wk.

The DNA content of the ASCs seeded on biomaterials was determined using a CyQUANT® Cell proliferation assay kit (Molecular Probes, Invitrogen). Prior to sample collection, the cell-seeded scaffolds were rinsed once with phosphate buffered saline (PBS), transferred to clean plates, and lysed with 0.1% Triton X-100 buffer (Sigma-Aldrich), and then stored at -70ºC until analyzed. Constructs were freeze-thawed three times before measurement to complete the cell lysis. The CyQUANT® GR dye was mixed with 10 μl of the Triton X-100 sample in cell-lysis buffer, and fluorescence was measured in a microplate reader (Victor 1420 Multilabel Counter; Wallac, Turku, Finland) at 480/520 nm. DNA content was analyzed in all the studies (**II**, **III**, and **IV**), at 1 and 2 wk on cell-scaffold constructs.

4.5.3 Evaluation of cell morphology using scanning electron microscopy (**II**, **III**, **IV**) and environmental scanning electron microscopy (**IV**)

Two weeks post-seeding, the scaffolds were fixed in 5% glutaraldehyde (Sigma-Aldrich) in 0.1 M phosphate buffer, pH 7.4, for 48 h. After rinsing in PBS, the samples were dehydrated through increasing concentrations of ethanol and then the samples were transferred to liquid carbon dioxide and dried in a critical point dryer. Samples were sputter-coated with gold–palladium for SEM observations. Four parallel scaffolds (**II**, **III**) or two parallel (**IV**) scaffolds from each group were observed by SEM (Jeol JSM-5500, Sundbyberg, Sweden).

Additionally, a Philips XL30 E-SEM-TMP environmental scanning electron microscope (E-SEM) (BioMater Centre, University of Kuopio, Kuopio, Finland) was used to evaluate the microstructure and morphology of the ASC-biomaterial constructs (**IV**). The E-SEM images were taken with a beam intensity of 8.0 to 12.0 kV and the gaseous secondary electron detectors at 1.0 to 4.0 Torr.

4.5.4 Osteogenic differentiation evaluation methods (**II**, **III**, **IV**)

ALP activity, ALP staining, and osteopontin concentration were determined to detect early osteogenic differentiation of ASCs. After 1 and 2 wk in culture, scaffolds were transferred to clean wells and 0.1% Triton X-100 was added to each scaffold. The cell-seeded scaffolds were freeze-thawed twice, and then p-nitrophenol phosphate and 2-amino-2-methyl-1-propanol (Sigma-Aldrich) were added to the Triton solution and incubated at 37ºC for 15 min. The amount of p-nitrophenol was measured at 405 nm in a microplate enzyme-linked immunosorbent assay reader (Multiscan MS, Labsystems, Helsinki, Finland). The ALP activity was determined from a standard curve produced with NaOH and a p-nitrophenol standard solution (Sigma-Aldrich) (**II**, **III**, **IV**). Additionally, at 2 wk, the ASC-biomaterial constructs were stained with a leukocyte ALP kit (Sigma-Aldrich) according to the manufacturer's protocol (**II**, **III**).

Osteopontin was measured using the Quantikine® Human Osteopontin Immunoassay (RD Systems Europe Ltd, Abingdon, UK) according to the manufacturer's protocol (**II**, **III**). Fluorescence was measured with a microplate reader (Victor 1420).

4.6 Statistics

Statistical analysis of the results in all studies (**I**-**IV**) was performed with SPSS version 13 (SPSS Inc, Chicago, IL). Data was reported in all studies as the mean ± standard deviation and an alpha value (p) of less than 0.05 was considered significant. In study **I,** the mechanical results of processed samples and unprocessed controls were compared using a paired Student's t-test. The effects of different cleansing processes combined with PES on the biomechanical properties of cortical samples were compared using one-way analysis of variance (ANOVA). According to the test of homogeneity of variances, ANOVA was not an appropriate test for comparison of the Young's modulus values of cortical samples, therefore the Mann-Whitney U test was used instead for these measured values. Power calculations were performed using PS-Power and Sample Size Calculations version 2.1.30.

In studies **II**, **III**, and **IV**, the effect of culture duration (1 wk *vs* 2 wk) was analyzed using a paired Student's t-test. The effects of different scaffold materials on the DNA content (**II**, **III**, **IV**), ALP activity (**II**, **III**, **IV**), and osteopontin concentration (**II**, **III**) were compared using a one-way ANOVA, after verifying a normal distribution and homogeneity of variance. Post hoc tests were performed to detect significant differences between groups. The experiments were repeated three to four times in studies **II** and **III**, and three times in study **IV**.

5. Results

5.5 Mechanical testing of bone samples and lipid content determination (**I**)

The results of the mechanical testing are presented in Table 2. The different processing methods had no significantly different effects on the biomechanical properties of the cortical samples. Each of the processing methods significantly reduced the Young's modulus of the cortical samples (freeze-dried to <5% residual moisture content) compared to the unprocessed samples. The processing improved the bending strength and the absorbed energy of the cortical samples compared to unprocessed controls.

***Table 2**. Mechanical testing of cortical bone. The mean values of the cortical controls and processed specimens (methods A, B, and C) are given. n = number of pairs of specimens, % = mean value of the processed samples expressed as a percentage of the mean value of the controls, p = probability resulting from a paired t-test on the differences between the paired specimens (not significant values p > 0.05 in bold face) (study **I** copyright by Biologicals, reproduced with permission).*

	n	Method	Residual moisture %	Controls Mean	Controls SD	Sample Mean	Sample SD	%	p
Young's	8	A1	0	**15.3**	1.5	**14.1**	1.1	**92.7**	0.026
modulus (GPa)	16	A2	<5	**16.9**	1.1	**14.3**	1.2	**84.3**	<0.001
	16	B	<5	**15.4**	1.4	**13.4**	1.2	**86.7**	<0.001
	8	C	<5	**16.5**	0.8	**14.0**	0.8	**84.9**	0.001
Bending	8	A1	0	**229.8**	16.9	**173.6**	17.5	**75.8**	<0.001
strength (MPa)	16	A2	<5	**227.8**	27.7	**248.6**	36.8	**109.1**	0.014
	16	B	<5	**201.3**	29.3	**214.9**	29.3	**106.8**	0.017
	8	C	<5	**211.6**	9.9	**211.4**	33.6	**100.0**	**0.988**
Energy to	8	A1	0	**0.10**	0.03	**0.04**	0.01	**38.5**	<0.001
break point (J)	16	A2	<5	**0.12**	0.05	**0.16**	0.06	**132.2**	0.001
	16	B	<5	**0.08**	0.03	**0.11**	0.04	**130.2**	0.037
	8	C	<5	**0.07**	0.01	**0.09**	0.04	**127.0**	**0.123**

As expected, freeze-drying the cortical samples to a 0% residual moisture content induced a significant decrease in the bending strength, absorbed energy, and Young's modulus (Figure 3A). The strength of the totally dry cortical samples was reduced to approximately 76% of that of the unprocessed controls.

The residual fat percentages of the cortical samples are presented in Figure 3B. The efficiency of the three different cleansing methods did not differ with regard to cleansing adipose tissue from the bone. The residual fat content of processed cortical samples varied from 0.2% to 0.5%

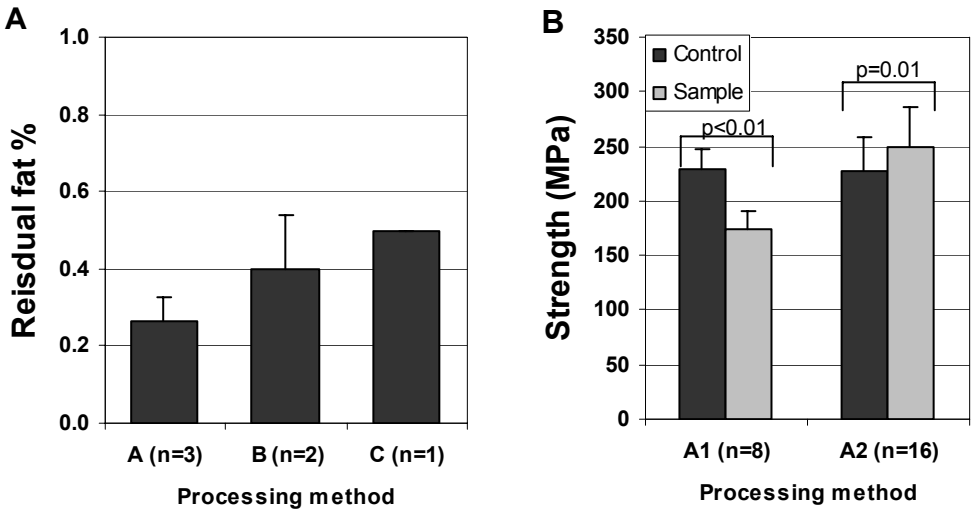

***Figure 3**. **A**) Mean results of the strength of cleansing method A-processed cortical samples with different residual moisture contents (A1 = residual moisture content 0%, A2 = residual moisture content <5%) compared with unprocessed controls. **B**) Residual fat percentages of processed cortical samples. Method A was the longest processing method (including a 20-h water incubation), Method B had double the incubation time in hydrogen peroxide and ethanol compared to A and C, Method C was the shortest method (study **I** copyright by Biologicals, reproduced with permission).*

5.6 Scaffold characterization

5.6.1 Immersion studies in stimulated body fluid (**II**, **III**)

For studies **II** and **III**, non-treated control composition (CC) bioactive glass scaffolds were used as a reference material (Figure 4A).

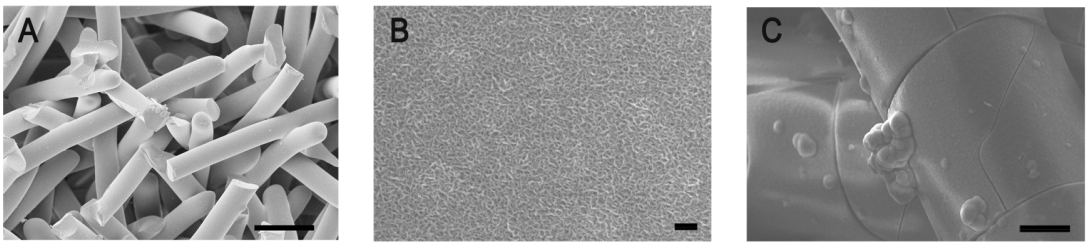

***Figure 4. A**) SEM image of CC scaffold. Scale 200µm. **B**) SEM image of thin Ca-P treated scaffold. Scale 600 nm **C**) SEM image of thick Ca-P treatment scaffold. Scale 25 µm.*

In study **II**, after immersion in Kokubo's SBF a thin homogenous Ca-P layer was observed (Figure 4B). Samples treated with a solution comprising 2-fold concentrated Kokubo's SBF produced a thick and irregular Ca-P layer (Figure 4C). In study **III**, the inhibitory effect of zinc ions on the degradation rate and on HA formation was observed when bioactive glass scaffolds were immersed in SBF. The samples containing 5 mol% of zinc presented a homogeneous, thin, amorphous Ca-P layer only after 2 wk of immersion (Figure 5A). The samples characterized concurrently, containing 0.25 and 0.5 mol% zinc, exhibited a thick HA layer with significant degradation of the core of each fiber (Figure 5B).

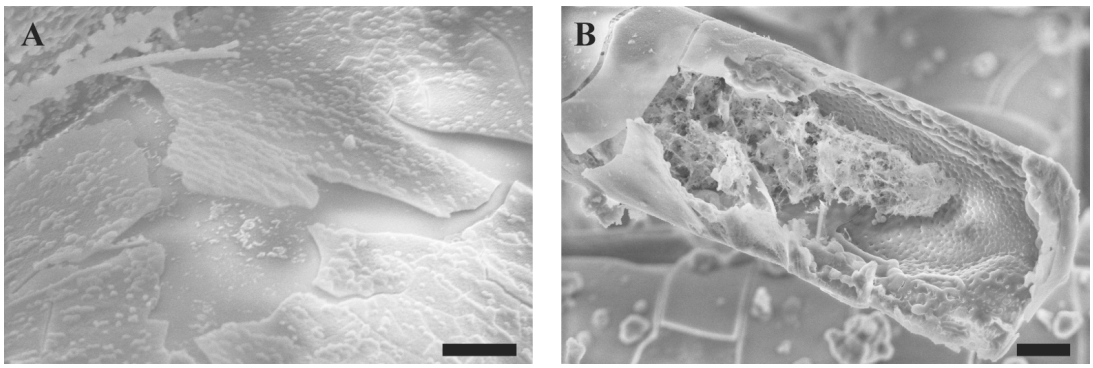

Figure 5. *A) Thin Ca-P layer over fiber containing 5 mol% ZnO after immersion in SBF for 14 d. Scale 6 µm* ***B****) Thick Ca-P outer layer on a significantly degraded fiber containing 0.5 mol% ZnO after immersion in SBF for 14 d. Scale 20 µm (study* ***III*** *copyright by Acta Biomaterialia, reproduced with permission).*

5.6.2 Ion release atomic absorption spectroscopy analysis (**III**)

The release of alkaline earth ions, *i.e.*, Ca^{2+} and Mg^{2+}, depended on the amount of zinc in the glass and on the immersion time in SBF. That is, the amount of ions released increased with the immersion time and was inversely proportional to the amount of substituted zinc. The amount of zinc released in the solution was proportional to the amount of zinc in the material (Figure 6A). When the amount was normalized with respect to the percentage of zinc substituted, however, the ability of the material to release zinc ions was inversely proportional to the amount of zinc in the glass (Figure 6B).

A

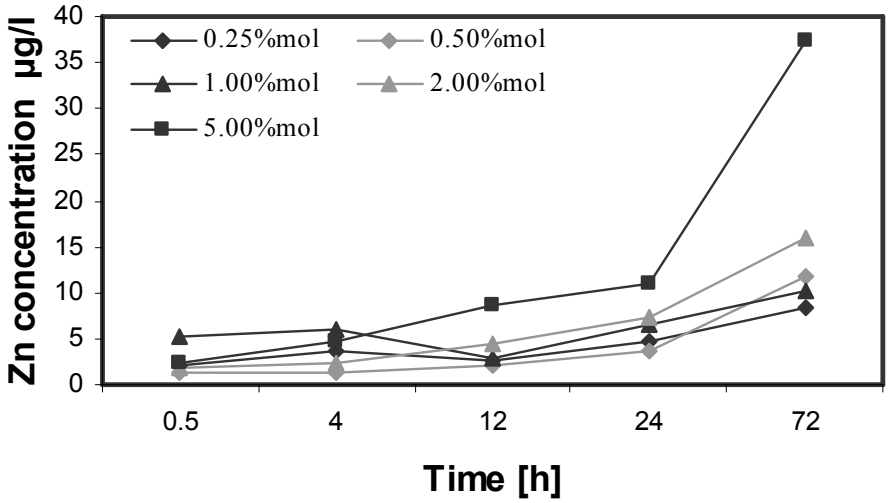

B

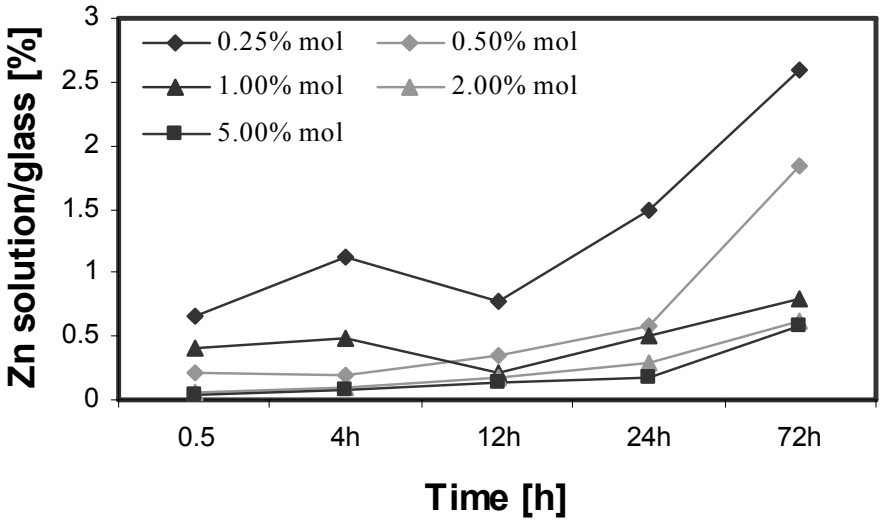

Figure 6. *A) Effect of total amount of zinc released in the solution (above) and* ***B****) ZnO on zinc release (below)(study* ***III*** *copyright by Acta Biomaterialia, reproduced with permission).*

5.6.3 Scaffold characterization of PLA and PLA/bioceramic composite scaffolds (**IV**)

The characteristics of the typical porous structure of the scaffolds can be seen in the SEM micrographs in Figure 7. Two different functional surfaces were formed during the freeze-drying of the scaffolds. The denser top surface of the scaffolds (Figure 7A), also referred to as the skin layer, was formed on all scaffold types when the frozen solvent sublimated from the top surface during the freeze-drying process. The β-TCP and bioactive glass granules were mainly dispersed into the

porous bottom surface during manufacturing, although some granules were observed in the middle of the scaffold (Figure 7B). The granule distribution on the porous surface and the difference between 10wt% and 20wt% filler material is shown in Figures 7C, E (10%) and 7D, F (20%). The interconnectivity of the pores is shown in Figure 8.

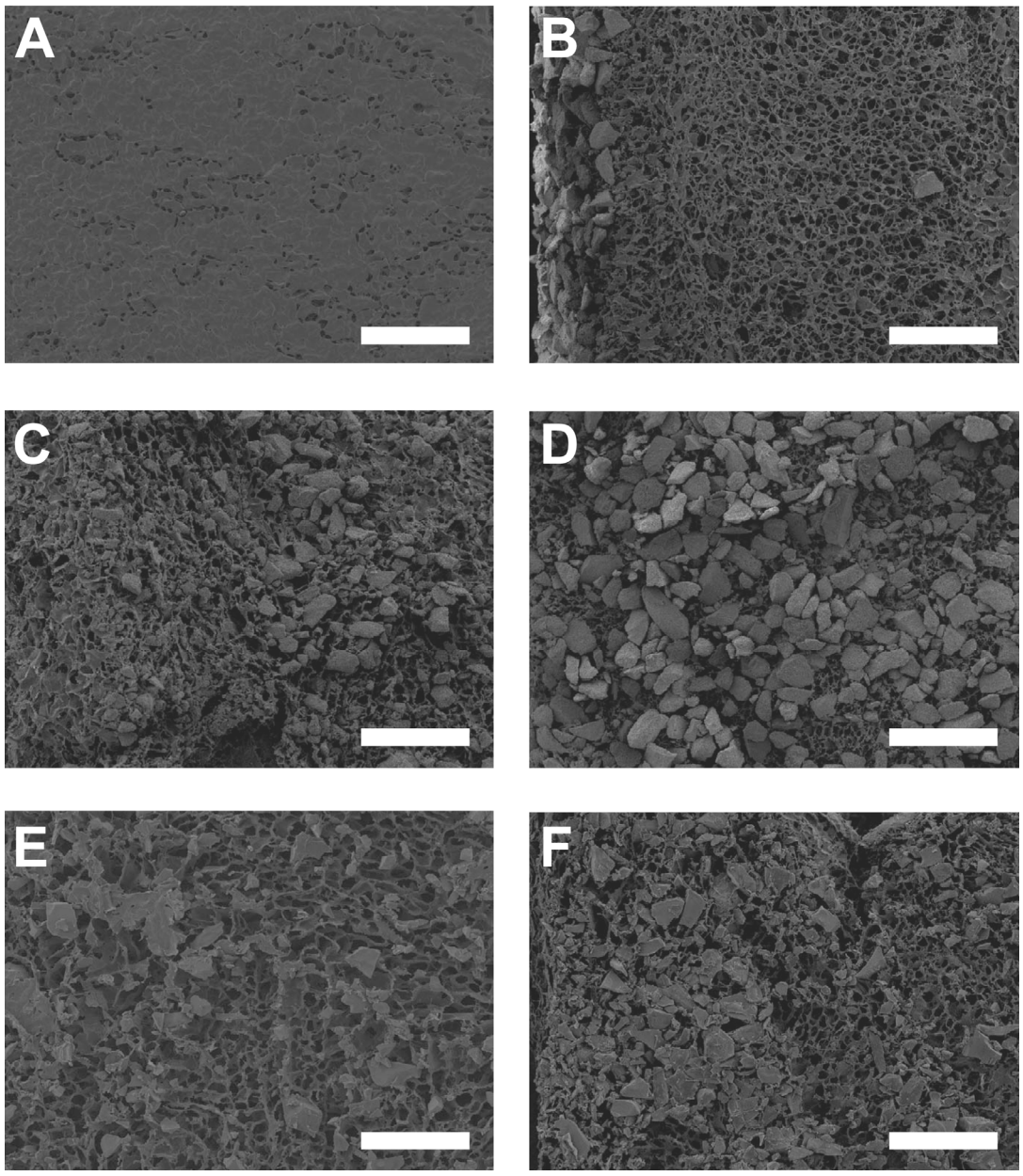

Figure 7. *SEM images of A) dense top surface of PLA scaffold B) cross-section of PLA/20 β-TCP scaffold, C) porous bottom surface of PLA/10 β-TCP scaffold, D) porous bottom surface of PLA/20 β-TCP scaffold. E) porous bottom surface of PLA/10 bioactive glass scaffold, F) porous bottom surface of PLA/20 bioactive glass scaffold. Scale 500 µm.*

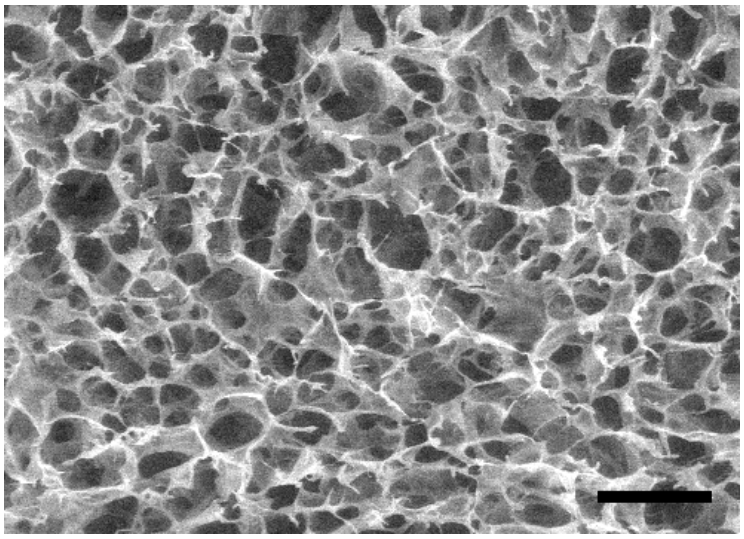

Figure 8. *E-SEM image of porous bottom surface of PLA scaffold. Scale 100 µm (study **IV** copyright by Tissue Engineering, reproduced with permission).*

5.7 Adipose stem cell viability, attachment, and morphology on biomaterials (**II**, **III**, **IV**)

In studies **II**, **III** and **IV,** live/dead staining was performed to study the attachment and viability of ASCs. Live/dead staining of ASCs seeded on bioactive glass scaffolds in studies **II** and **III** revealed only a few dead cells (thick Ca-P and 1 mol% zinc scaffold) or no dead cells at the 3-h time-point (Figure 9). The number of cells was higher on each scaffold type at 2 wk compared to 3 h. There was a notable increase in the proportion of viable cells and there were only a few dead cells on each scaffold type after 2 wk in culture. ASCs were more evenly spread out on Ca-P treated and CC scaffolds than on zinc-releasing scaffolds. The ASCs formed clustered structures, especially at the junctions of glass fibers on the zinc-releasing scaffolds. Qualitative analysis of the number of cells attached and spread out on each scaffold indicated that there was a higher cell number on CC scaffolds compared to zinc scaffolds, but revealed no differences between CC and Ca-P treated scaffolds.

As observed in studies **II** and **III** and also in study **IV**, the number of viable cells was increased at 2 wk in comparison to that at the 3-h time-point (Figure 10). In study **IV**, the proportion of dead cells at the 3-h time-point was higher than that in studies **II** and **III** on the cell seeding surfaces of all tested scaffold types, although at both time-points (3 h and 2 wk), the number of viable cells was greater than the number of dead cells. In addition, at 3 h the cells were attached only in the region close to the porous bottom surface (*i.e.*, cell seeding area in study **IV**), whereas in studies **II** and **III**, the cells were spread throughout the bioactive glass scaffolds by 3 h. Visual inspection of the different scaffold types revealed no differences in the number of cells or cell viability at the 3-h or 2-wk time-points, similar to the findings of study **II**. In study **IV**, during the 2-wk culture period, the cells migrated

from the porous bottom surface towards the inner parts of the scaffolds, which confirmed the interconnectivity of the pores. Only a few cells were observed, however, on the dense top surface in each scaffold type. The cell density at the region close to the porous surface was higher than that in the core of each scaffold type. At the region close to the surface, cells had formed cluster structures on all scaffold types and especially huge clusters were formed on PLA/10β-TCP, and on both PLA/bioactive glass scaffolds. The ASCs had the most uniform spatial distribution on PLA/20β-TCP scaffolds.

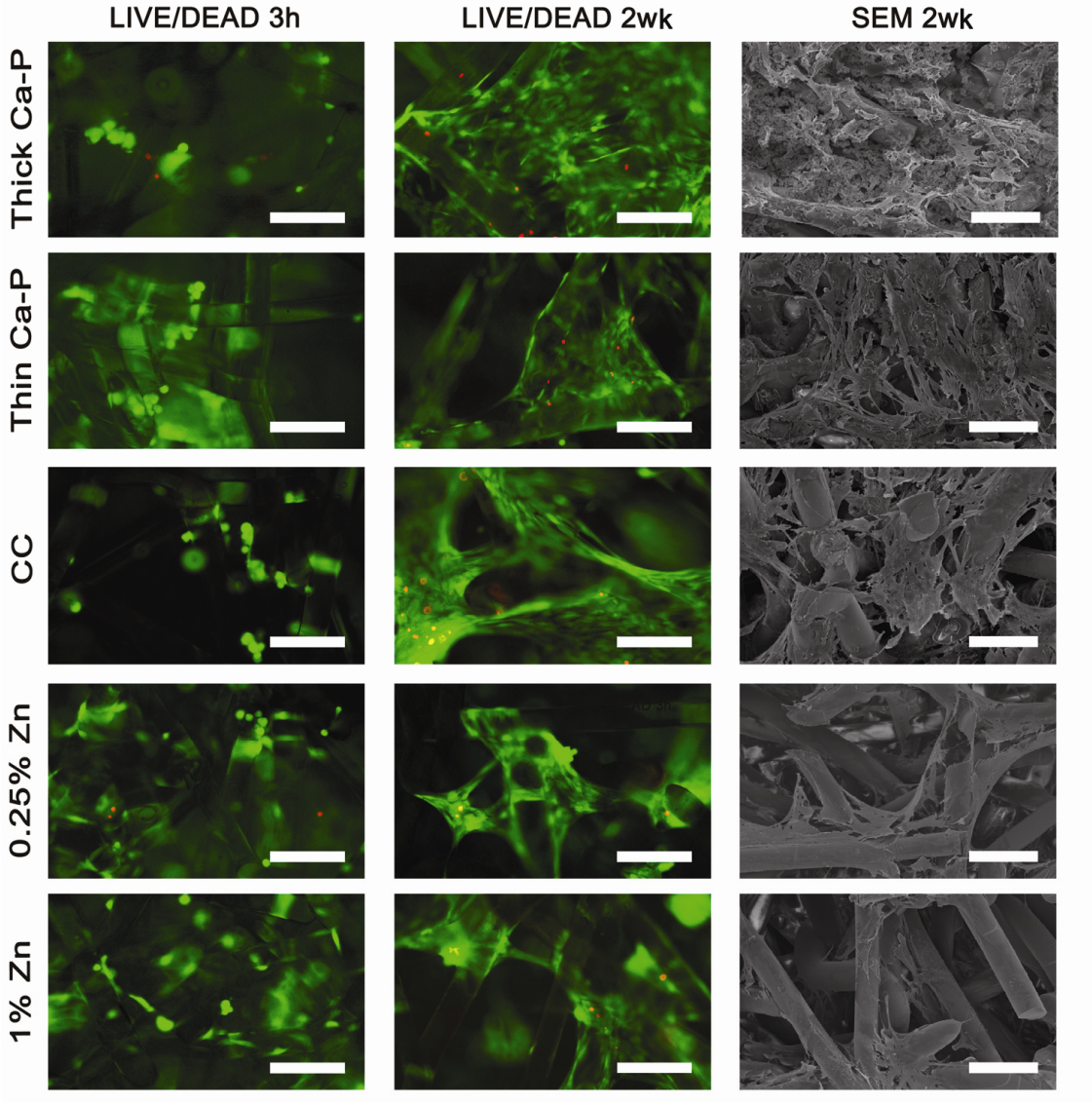

Figure 9. *Fluorescence images of viable (green fluorescence) and dead (red fluorescence) ASCs attached to bioactive glass scaffolds at 3 h and 2 wk as can be seen on with SEM images of ASCs grown on the surface of the bioactive glass scaffolds at 2 wk. Scale 200 µm.*

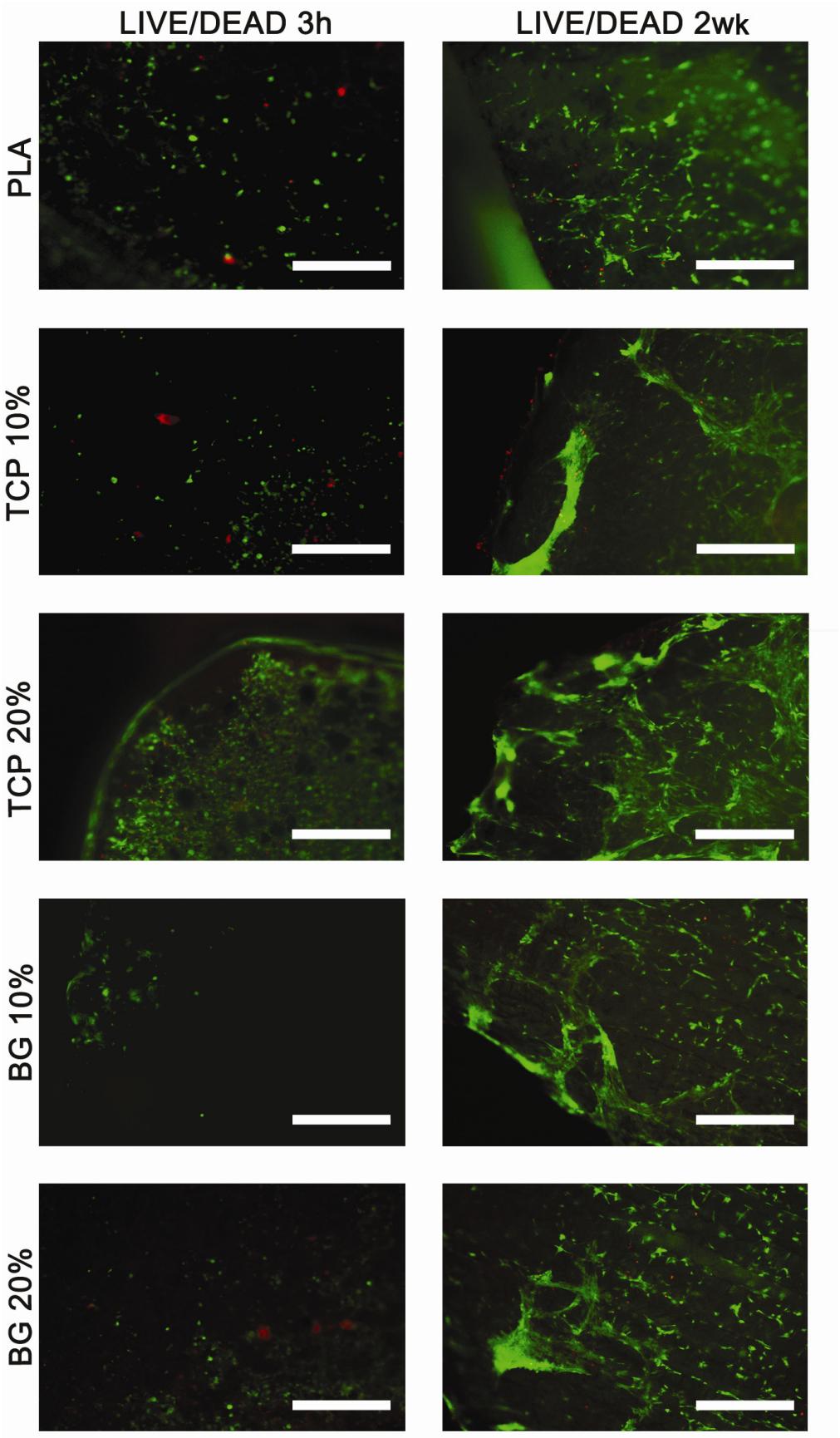

Figure 10. *Fluorescence images of viable (green fluorescence) and dead (red fluorescence) ASCs attached to porous bottom surface of PLA, PLA/β-TCP (TCP) and PLA/bioactive glass (BG) composite scaffolds at 3 h and 2 wk. Scale 500 µm.*

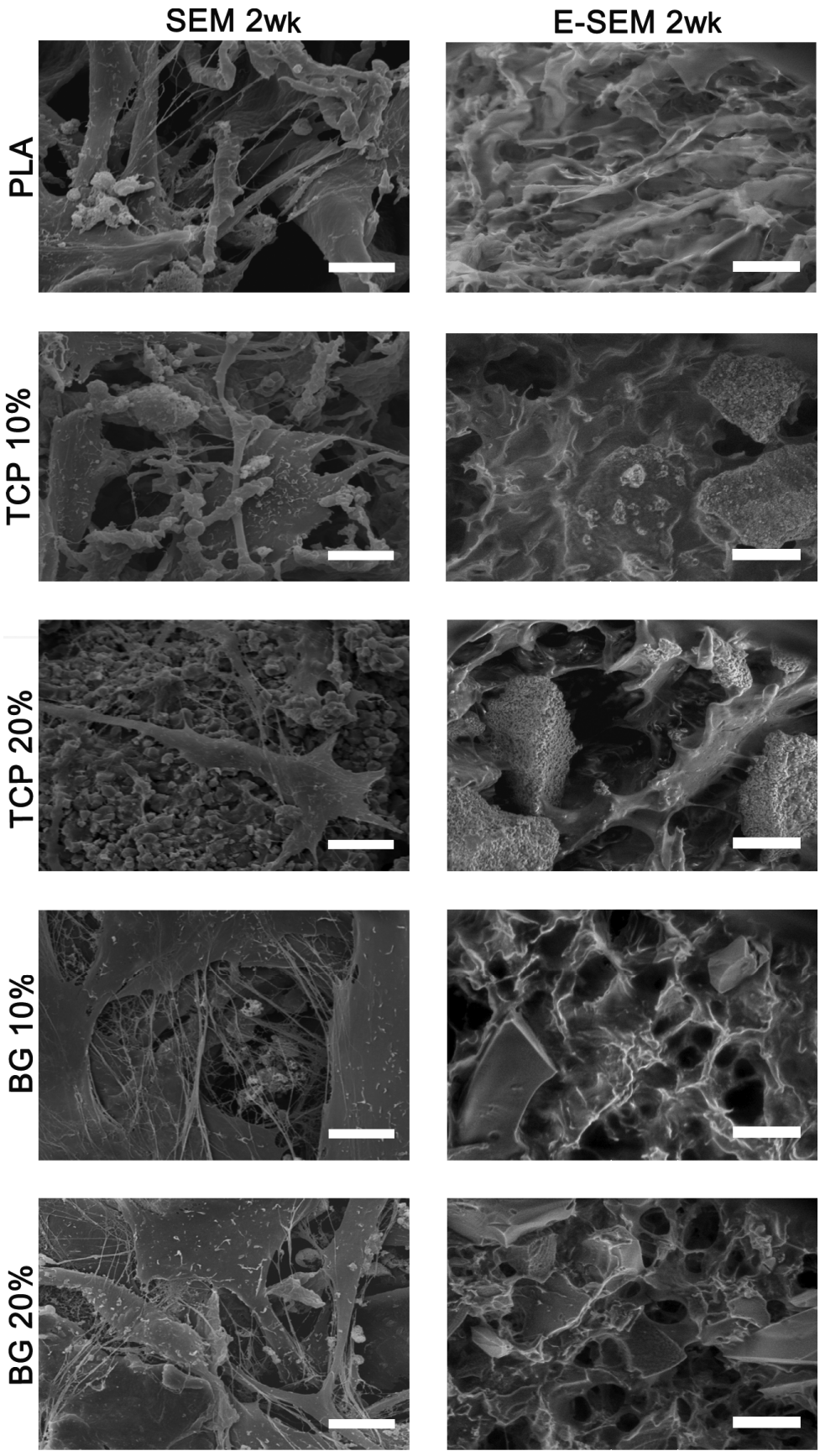

Figure 11. *SEM and E-SEM images of ASCs grown on the surface of PLA, PLA/β-TCP (TCP), PLA/ the bioactive glass (BG) scaffolds after 2 wk in culture. Scale10 μm in SEM images and 50 μm in E-SEM images.*

SEM imaging was performed to examine the morphology of the cells in studies **II**, **III**, and **IV** at 2 wk. In studies **II**, **III**, and **IV**, the ASC morphology was not affected by Ca-P treatment, or by the addition of zinc addition to bioactive glass scaffolds, β-TCP, or bioactive glass components in the PLA scaffolds (Figures 9 and 11). ASCs were attached and also spread to the middle regions of the scaffold in all the scaffold types studied. SEM images show ASCs stretching along the glass fibers and forming bridges from one glass fiber to another on the surface of each of the studied bioactive glass scaffolds (Figure 9, studies **II**, **III**). The cells were especially well distributed across the Ca-P treated and CC scaffolds. The lower cell number in the zinc-releasing scaffolds compared to other bioactive glass scaffolds, detected with live/dead staining, was verified also by SEM.

Images with high magnification (SEM images, Figure 11) show ASCs with an elongated phenotype and forming projections on the porous surface of the scaffolds (study **IV**). The β-TCP and bioactive glass granules were clearly distinguished on the porous surface of the scaffolds and the ASCs formed bridges between the granules on the PLA/β-TCP and PLA/bioactive glass composite scaffolds (E-SEM images, Figure 11). In each of the scaffold types in study **IV**, the majority of ASCs were spread on the region close to the porous bottom surface, which supports the live/dead staining findings.

5.8 Proliferation and osteogenic differentiation of adipose stem cells (**II**, **III**, **IV**)

The effect of different scaffold materials on ASC proliferation was assessed by measuring the total DNA content (studies **II**, **III**, **IV**). There were no significant differences in cell proliferation between the studied scaffold types at 1 or 2 wk in studies **II** and **III** (Figure 12). Both the thin and thick Ca-P treated scaffolds had a higher number of cells at 2 wk (thin p=0.004 and thick p=0.02) than at 1 wk (Figure 12A). The cell number in CC scaffolds also increased with time, but not significantly in study **II**. In study **III**, however, the DNA content was significantly higher (p=0.013) in CC scaffolds at 2 wk compared to 1 wk (Figure 12B). Also, in the zinc-releasing scaffolds, the cell number tended to increase with time, but not significantly. Similarly, in study **IV**, the culture duration (1 wk *vs* 2 wk) did not significantly affect ASC proliferation, although the DNA content of the ASCs increased on PLA/β-TCP composites and PLA scaffolds over time. In contrast, the relative DNA content did not increase when the cells were cultured on bioactive glass composites for 2 wk compared to 1 wk.

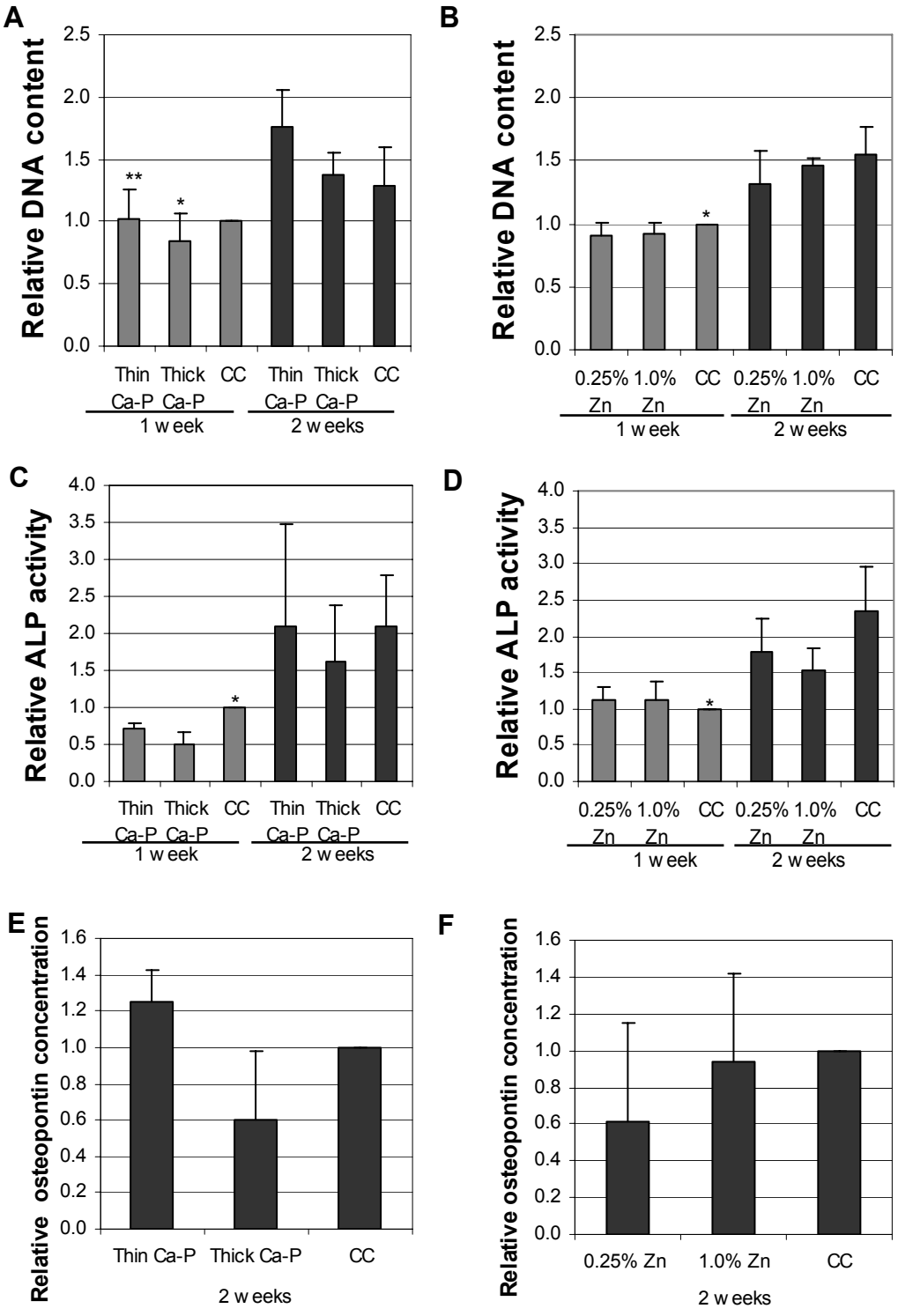

Figure 12. *Relative DNA content, ALP activity, and osteopontin concentration of ASCs cultured on different bioactive glass scaffolds. Results are expressed as mean +SD (n=3, except in figures B and D n=4).* ***A)*** ***p<0.01 with respect to the 2-wk DNA sample of thin Ca-P treated scaffolds; *p<0.05 with respect to the 2-wk DNA sample of thick Ca-P treated scaffolds* ***B)*** *and* ***D)*** **p<0.05 with respect to the 2-wk DNA/ALP sample CC scaffolds* ***C)*** ** p<0.05 with respect to the 1 wk ALP sample of thin Ca-P and thick Ca-P treatment* ***E)*** **p<0.05 with respect to thick Ca-P treatment* ***F)*** *No significant differences were found (studies* ***II***, ***III*** *copyright by Acta Biomaterialia, reproduced with permission).*

At the 2-wk time-point, ASC proliferation was significantly higher in both of the PLA/β-TCP scaffolds than in the other three scaffold types (**IV,** Figure 13A). Conversely, proliferation of ASCs cultured on PLA/bioactive glass scaffolds was significantly lower than that on the other scaffold types. No significant differences were detected between the two concentrations of both β-TCP and bioactive glass (*i.e.,* 10 wt% *vs* 20 wt%).

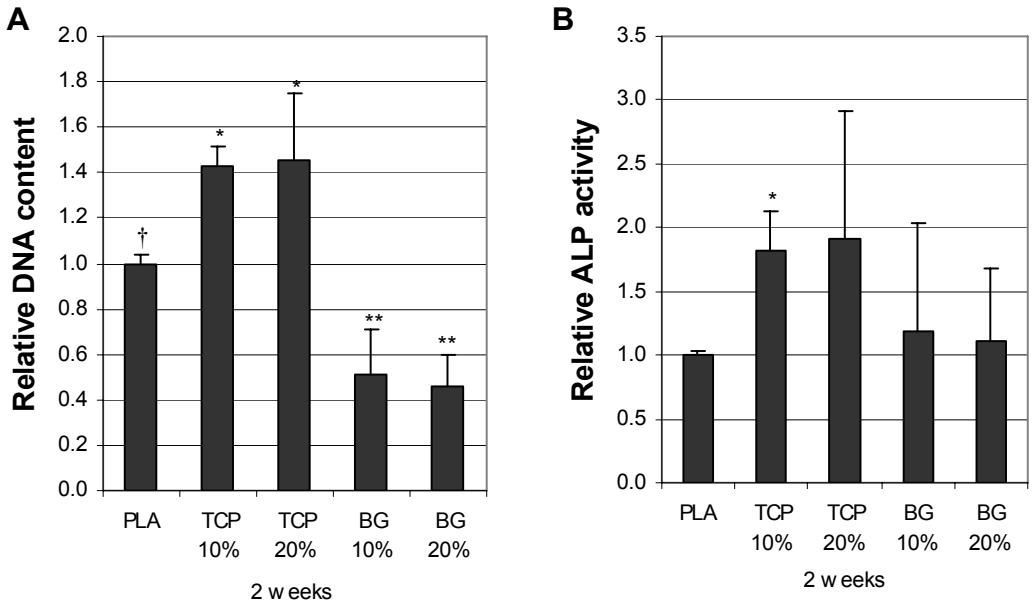

Figure 13*. Relative DNA content and ALP activity of ASCs cultured for 2 wk on PLA, PLA/β-TCP (TCP), and PLA/Bioactive glass (BG) scaffolds. Results are expressed as mean +SD (n=4).* ***A)*** **p<0.05 with respect to PLA, bioactive glass 10 and 20 wt%, **p<0.05 with respect to PLA, β-TCP 10, and 20 wt%, †p<0.05 with respect to β-TCP 10 and 20 wt%, and bioactive glass 10 and 20 wt%.* ***B)*** **p<0.05 with respect to PLA, bioactive glass 10 and 20wt% (study* ***IV*** *copyright by Tissue Engineering, reproduced with permission).*

Concurrent measurement of ALP activity (studies **II**, **III**, **IV**) and osteopontin concentration (studies **II**, **III)** indicated early osteogenic differentiation of ASCs in all studies. There was significant stimulation of ALP activity at 1 wk on CC scaffolds compared to both the thin (p=0.044) and the thick (p=0.003) treated Ca-P scaffolds (Figure 12C). ALP activity increased with time, but no significant stimulation was observed in any scaffold type in study **II**. In study **III**, however, the ALP activity as well as the ASC proliferation significantly increased (p=0.023) on CC scaffolds at 2 wk compared to 1 wk (Figure 12D**)**. The addition of zinc to the bioactive glass scaffolds did not increase the ASC ALP activity. In contrast, ALP activity on CC scaffolds was over 30% higher than that on 1 mol% zinc scaffolds. Furthermore, adding zinc to bioactive glass scaffolds did not enhance ASC osteopontin secretion (Figure 12F). In study **II**, there was a significant difference in the osteopontin concentration (p=0.036) between the thin and thick Ca-P scaffolds at 2 wk (Figure. 12E). No significant differences in the staining were observed between the bioactive glass scaffolds at 2 wk in studies **II** and **III**.

In study **IV**, the ALP activity of ASCs cultured on PLA and bioactive glass composite scaffolds was two times higher at 2 wk than at 1 wk. A statistically significant increase at the 2-wk time-point when ASCs were cultured on PLA/20 β-TCP scaffolds ($p=0.034$), although ALP activity of ASCs cultured on PLA/10 β-TCP scaffolds was also three times higher at 2 wk than at 1 wk.

At 2 wk, relative ALP activity of ASCs cultured on PLA/10 β-TCP scaffolds was the same magnitude as that of ASCs cultured on PLA/20 β-TCP scaffolds, but it was significantly higher compared to that on the other scaffold types (PLA, $p=0.017$, bioactive glass 10 wt%, $p=0.023$ and bioactive glass 20 wt%, $p=0.022$; **IV**, Figure 13B). After the 2-wk culturing period, due to the lower number of cells in PLA/bioactive glass scaffolds than in PLA scaffolds, the relative ALP activity of ASCs cultured on PLA/bioactive glass and PLA scaffolds was at the same level. These findings indicate the relative ALP/DNA ratio was greater on PLA/bioactive glass scaffolds than on PLA and PLA/β-TCP scaffolds.

6. Discussion

6.1 Sterilized allograft bone as a bone reconstruction material

Treatments to improve the quality and safety of repairing bone defects must be aimed at stimulating bone regeneration. Restoration of skeletal function with autologous bone remains the most commonly used procedure; however, allografts are often required in the reconstruction of major bone defects as the quantity of bone harvested from autologous skeletal donor sites is limited and may result in major morbidity. The reason for the superiority of autologous bone is the osteoblasts in the graft, which make it osteogenic. Thus, the aim of bone tissue engineering is to produce cell-biomaterial constructs that are osteogenic *in vivo*.

The results of study **I** indicated that chemical cleansing combined with PES did not adversely affect the biomechanical properties of cortical bone samples. Only Young's modulus of the cortical samples decreased slightly, although significantly, in all processing groups. Consistent with this finding, Scheffler *et al.* also reported that the mechanical properties of bone-patellar tendon-bone grafts (BTB) were not significantly altered after sterilization with PES (Scheffler et al. 2005). The results of several other *in vitro* studies indicate that PES is a reliable sterilization method that is feasible to utilize, and there are no adverse effects on the structural and biologic incorporation properties of allograft bone treated with PES (Pruss et al. 2001, Pruss et al. 2002, Pruss et al. 2003).

The defatting step prior to PES sterilization is a prerequisite for the effective penetration of sterilization medium into the bone tissue. The delipidation process is often performed using a chloroform–methanol combination (Thoren et al. 1995, Pruss et al. 1999), and hydrogen peroxide in combination with nonionic detergents and alcohol, which is an effective cleansing method for cortical allografts (DePaula et al. 2005). In addition, Lomas *et al.* demonstrated that the majority of blood and marrow components can be removed from whole femoral head allografts by a combination of sonication, centrifugation, and warm water washing (Lomas et al. 2000). Pulse lavage alone is also an effective method for defatting morselized allograft bone (Haimi et al. 2008). Our results indicated that the processing method used in efficiently reduced adipose tissue from cortical bone and no additional delipidation steps were necessary.

Although processing and cleansing allograft bone is often recommended, in many countries, including Finland, most allograft bone is used as unprocessed fresh-frozen bone (Hirn 2001, Yates et al. 2005). The most commonly used form of fresh-frozen bone is morselized femoral head, obtained from living donors, who can be double-tested for viruses. Therefore, the use of fresh-frozen bone is virologically

and bacteriologically safe (Aspenberg 1998, Hirn 2001). Laboratory screening for viruses and bacteria may sometimes fail and without proper cleansing of the graft of cellular antigens, the risk of a host immunologic response is significantly increased.

Besides traditional gamma irradiation, chemical sterilization methods have become popular and widely used. One example of a chemical sterilization method is Biocleanse (Regeneration Technologies, Alachua, FL), an automated low-temperature chemical sterilization procedure that utilizes hydrogen peroxide gas and plasma, which has been used successfully to sterilize bone and BTB grafts without any significant effects on the mechanical properties (Jones et al. 2007a, Mikhael et al. 2008). Although these chemical sterilization methods have become popular and widely used, gamma irradiation is still often used as a terminal sterilization method for allograft bone. The concern in using gamma irradiation is the fact that the recommended standard dose (25-35 kGy) significantly impairs the fracture resistance of bone and significantly reduces the ultimate stress-strain properties of the bone (Currey et al. 1997, Cornu et al. 2000, Akkus and Rimnac 2001). Low and moderate dose (10-30 kGy) gamma sterilized massive bone allografts which are used for replacement of bone defects fail at higher rate than nonsterilized matching grafts (Lietman et al. 2000). In addition, even low dose (15 kGy) gamma irradiation significantly reduces the osteoinduction of human morselized bone grafts when implanted in nude rats and mice. The mechanism underlying the reduced osteoinduction was thought to be the decreased expression of BMP-7 and core binding factor α1, which are crucial to the *in vivo* bone formation process (Chen et al. 2007).

The results of the mechanical testing of cortical bone in study **I** suggest that chemical sterilization may be a better choice than gamma sterilization for cortical bone allografts. This study was limited, however, as the effects of the chemical cleansing procedures combined with PES on cortical bone were only evaluated *in vitro*. There are many applications in orthopedic surgery where cancellous bone is used as bone gap filling material. Despite this, cortical grafts are also used for large defects where weight-bearing properties are needed (Galea and Kearney 2005). The mechanical properties were studied only after sterilization, but prior to implantation. The long-term mechanical integrity of PES-sterilized cortical bone can only be verified *in vivo* studies. Further, the effect of PES on bone remodeling *in vivo* should also be studied. This is especially important because a recent study on anterior cruciate ligament sterilization with PES showed that PES slowed the remodeling activity compared to non-sterilized allografts (Scheffler et al. 2008).

6.2 Adipose stem cell culture related methodologic considerations

A specific model to characterize and culture human ASCs for bone tissue engineering applications was established in these studies. The surface marker expression data were consistent with previous results for ASCs (Gronthos et al. 2001, Gimble and Guilak 2003, Strem et al. 2005), indicating positive expression

for markers substantiating the mesenchymal origin of cells and negative expression of markers of a hematopoietic or angiogenic origin of the cells.

ASC proliferation and osteogenic differentiation on the bioactive materials in this study were confirmed, without the need for dexamethasone, ß-glycerophosphate, and ascorbate-2-phosphate, which are basic osteogenic agents considered necessary for ASC differentiation towards bone (Halvorsen et al. 2001, Zuk et al. 2002, de Girolamo et al. 2007, Bunnell et al. 2008). The osteogenic process was followed by the assessment of ALP activity and osteopontin concentration. These assays demonstrated that the ALP activity of ASCs was higher at 2 wk than at 1 wk and osteopontin was secreted at 2 wk, indicating that these stem cells differentiate osteogenically, similarly to those previously described (Zuk et al. 2001, Zuk et al. 2002).

ALP is considered to be a reliable marker of osteoblast function (Beck et al. 1998, Park et al. 2007) and is widely used as such. Many studies report a correlation between *in vitro* ALP expression and *in vivo* bone formation (James et al. 1996, Zhang et al. 1997, Chen et al. 2005, Siddappa et al. 2007). ALP activity is not an optimal biochemical marker for *in vivo* osteogenesis, however, because there are also studies, reporting no correlation between the level of ALP expression and *in vivo* bone formation (Yamamoto et al. 1991, Mendes et al. 2004). Instead, both ALP activity and cell proliferation ability together may be a more reliable way of predicting *in vivo* bone formation. The correlation between proliferation and *in vivo* bone formation is not well studied; only one study reported that high proliferative activity of osteoblast-like cells correlated with the *in vivo* osteoinductive capacity of demineralized bone matrix (Adkisson et al. 2000). In addition, the fact that seeding ASCs on different biomaterial scaffolds significantly enhances bone formation compared to empty scaffolds is widely reported in the literature (Hicok et al. 2004, Cui et al. 2007, Yoon et al. 2007, Jeon et al. 2008).

Our hypothesis is that cell proliferation ability is crucial when implanting cell-seeded constructs into bone defects. If only a few of the applied cells proliferate inside the scaffold, regardless of their level of differentiation, bone formation is not likely to occur if the number of cells is not sufficient. Further *in vivo* studies are needed to test this hypothesis. The main limitation of the present studies is the fact that only *in vitro* experiments were performed. Reliable conclusions on the suitability of the biomaterials for the treatment of bone defects can be drawn after *in vivo* studies are performed. Late bone-specific markers, such as osteocalcin and bone sialoprotein, should also be examined *in vitro* (Aubin et al. 1995).

6.3 Adipose stem cell seeded on scaffolds in bone tissue engineering applications

Many previous studies on bioactive glass have uniformly shown the stimulatory effect on osteoblast function *in vitro* (Xynos et al. 2000a, Xynos et al. 2000b, Gao et al. 2001, Xynos et al. 2001, Bosetti et al. 2003, Radin et al. 2005). The findings are contradictory, however, as one study demonstrated that the positive effects of

bioactive glass on bone growth in human patients are not mediated by the accelerated differentiation of MSCs *in vitro* (Reilly et al. 2007). In studies **II** and **III,** the bioactive glass had a stimulatory effect on human ASC proliferation and differentiation into osteogenic lineages.

A number of studies demonstrated that the biomaterial must have the ability to form an apatite layer for bone bonding to occur (Höland et al. 1985, Nakamura et al. 1985). Ca-P coating of various biomaterials such as biodegradable polymers, ceramics, and titanium enhance osteoblast proliferation, activation, and differentiation into mature osteoblasts (ter Brugge et al. 2002, Bigi et al. 2005, Vaahtio et al. 2006). One hypothesis to explain this stimulatory effect of Ca-P is the dissolution of calcium and phosphate, leading to the supersaturation of calcium ions. This subsequently leads to re-precipitation of Ca-P, resulting in a transformed surface that stimulates osteogenic differentiation of the osteoprogenitor cells (Zeng et al. 1999). Furthermore, surface reactive glass composites, which contain Ca-P particles, bond chemically to bone, leading to direct lamellar bone repair (Kangasniemi et al. 1994, Suominen et al. 1996).

In contrast, there are a few *in vivo* studies showing that the Ca-P layer does not induce bone formation (Ekholm et al. 2005, Holmbom et al. 2005). In fact, these studies demonstrate that apatite coating caused a strong inflammatory reaction and less osteoid tissue (Ekholm et al. 2005). In addition, HA-coated cellulose sponges implanted subcutaneously in rats have shown to attract macrophages and fibroblasts and favor angiogenesis (Tommila et al. 2008). The differences between the findings of these *in vivo* studies may be due to the fact that different animal models were used. The crystallinity of the Ca-P coatings also varied in these studies. Many studies indicate that the crystallinity of a biomaterial surface affects cell function (Ball et al. 2001, Oliveira et al. 2002, ter Brugge et al. 2002). Proliferation and osteogenic differentiation of human osteoblast-like cells and rat MSCs is inhibited on more amorphous Ca-P coatings. Our results in study **II**, however, showed that scaffolds treated with a thick, more crystalline Ca-P layer inhibited ALP activity, osteopontin release, and proliferation of ASCs compared to thin Ca-P treated scaffolds with a more amorphous Ca-P layer. Direct comparison of our results to these previous studies is impossible because different cell types such as osteoblast-like cells, bone marrow cells, and osteoblasts were used and the Ca-P coatings were produced on either titanium or starch, whereas we studied the effect of a Ca-P layer on bioactive glass scaffolds on human ASCs. One explanation for the inhibitory effect on osteogenic differentiation of thick Ca-P treated scaffolds may be the higher release of calcium ions from these scaffolds. It has also been previously reported that ALP activity of human osteoblasts decreases in response to high calcium concentrations (Xynos et al 2000b), which is consistent with normal physiology. Our conclusion from the results of study **II** was that Ca-P treatment of bioactive glass delays early osteogenic differentiation of ASCs. This is a novel observation for human ASCs, but it is consistent with the results of previous *in vivo* animal studies (Ekholm et al. 2005, Holmbom et al. 2005). Inhibition of the degradation product release *i.e.,* ion release, from Ca-P treated scaffolds, may account for our observation. These degradation products of bioactive glass are involved in the osteostimulative properties of the material (Ducheyne and Qiu 1999, Kaufmann et

al. 2000, Xynos et al. 2000b, Välimäki et al. 2005b). Slower dissolution kinetics of zinc-releasing bioactive glass scaffolds was also the key finding in study **III,** which may explain why zinc-releasing scaffolds inhibited osteogenic differentiation and proliferation of ASCs compared to CC scaffolds. Also, we showed that the addition of zinc slows down the degradation of bioactive glass, hindering the ion release from the material, which is consistent with previously reported results (Lusvardi et al. 2002).

Incorporation of other polyvalent metals such as aluminum into bioactive glass has also shown to increase the durability of bioactive glass with respect to leaching (Greenspan and Hench 1976). However, i*n vivo* the bone bonding of aluminum containing bioactive glass is inhibited, because aluminum interferes with the Ca-P formation (Andersson et al. 1990, Andersson et al. 1992). Aluminum may inhibit the Ca-P formation either by reducing the surface available for Ca-P formation or by formation of aluminum-containing crystals (Andersson et al. 1993). Similarly, zinc-ions have been demonstrated to incorporate in the Ca-P layer forming on the bioactive glass, inhibiting its further formation (Jaroch and Clupper 2007). Classically, the bioactivity of a biomaterial has been defined as the ability to form a Ca-P layer. However, we feel that the definition is too narrow: It does not take into account the material's dissolution kinetics, which has a major impact on the ASC proliferation and differentiation. This impact was shown in our studies **II** and **III**. Furthermore, contradictory findings on the effect of Ca-P on bone formation exist as discussed above. In conclusion, the Ca-P formation ability of bioactive glass should not be considered the only indicator of bioactivity.

Aluminum has shown to play a role in bone fragility, neurotoxicity, and onset of Alzheimer's disease (Mjoberg et al. 1997, Ferreira et al. 2008). Although aluminum may be used to delay the degradation profile of bioactive glass, the disadvantages related to this polyvalent metal severely limit its use. These disadvantages related to aluminum have also restricted the use of commercially available glass ionomer cements, which contain aluminum ions as essential elements for the setting process of the cement (Blades et al. 1998). However, in a recent glass ionomer cement study, zinc was successfully used instead of aluminum as a network modifying oxide (Boyd and Towler 2005).

Adding zinc to bioceramic materials has shown to stimulate the proliferation and osteoblastic differentiation of osteoprogenitor cells (Ishikawa et al. 2002, Ikeuchi et al. 2003, Storrie and Stupp 2005, Du et al. 2006). Even low concentrations of zinc (0.075 mg/L, Ishikawa *et al*. and 0.235 mg/L, Du *et al*.) released from biomaterials have been shown to stimulate osteoblast proliferation, compared to control materials without zinc releasing ability (Ishikawa et al. 2002, Du et al. 2006). Contrary to previous studies, a recent study by Popp *et al*. showed that supplementation of the culture medium with soluble zinc (concentration between 0.20 mg/L and 2.62 mg/L) did not affect proliferation or osteogenic differentiation of osteoprogenitor cells (Popp et al. 2007). A limitation of the Popp *et al.* study, however, was that they did not use control medium with a zinc concentration of 0, therefore the stimulatory effect of the additional zinc could not be analyzed. The maximum concentration used in their study was higher than the maximum zinc release from the 1 mol% zinc scaffolds that we used (1.0 mg/L).

In study **III,** CaO was substituted with ZnO, allowing the molar percentage of all other components to be kept constant. Contrary to our study, Aina *et al*. modified 45S5 bioactive glass by adding ZnO in such a way that the amount of all components was adjusted and SiO_2, in particular, varied from 45 wt% to 37 wt% (Aina et al. 2007). Thus, the authors significantly modified the degradation rate of the original glass and at least partially compensated for the effect of ZnO as a degradation inhibitor. We suggest that the stimulatory effect of zinc ions with the chosen zinc-release concentrations may have been observed on ASCs if 3D scaffolds with a tailored, faster degrading composition were used in study **III**.

Live/dead staining and SEM imaging in study **IV** showed that cell density in the region close to the surface was higher compared to that in the core of each scaffold type; a feature attributed to the heterogeneous structure of the composite scaffolds. The bioactive glass and β-TCP particles were clustered on the porous side of the composite scaffold, which made this region more hydrophilic. This feature of the composite scaffolds may be advantageous because a previous study revealed that bone formation is enhanced *in vivo* when osteoblasts have higher exposure to bioactive HA nanoparticles at the polymer/bioceramic composite scaffold surface (Kim et al. 2006b).

Increasing percentages of β-TCP added to a PLA matrix stimulates the proliferation and differentiation of human MSCs and osteogenic cells . Our results in study **IV** were similar in the sense that both proliferation and total ALP activity of ASCs were significantly increased on PLA/β-TCP scaffolds compared to PLA scaffolds.

The results from study **IV** suggest that bioactive glass particles do not stimulate total ALP activity of ASCs more than PLA alone, although the relative ALP activity of a single cell, *i.e.,* the ALP/DNA ratio on PLA/bioactive glass scaffolds, was higher than that in PLA and PLA/β-TCP scaffolds. Similar results were obtained by Leach *et al*. who showed that PLGA scaffolds coated with bioactive glass had no effect on ALP activity or osteocalcin production of human MSCs, compared with uncoated scaffolds (Leach et al. 2006). This result is contradictory to a previous study, however, where osteoblast-like cells grown on α-TCP had a significantly higher ALP/DNA ratio compared to bioactive glass (Mayr-Wohlfart et al. 2001). This finding is also in contrast to the findings from studies **II** and **III**, where there was a uniform stimulatory effect of bioactive glass. The results of the studies cannot be directly compared, however, because different glass compositions were used in studies **II** and **III** and in study **IV** (Table 3). The main difference was that B_2O_3, TiO_2, and P_2O_5 were not included in the bioactive glass composition used in study **IV** and therefore the bioactive glass properties may not be the same as the CC bioactive glass used in studies **II** and **III**. Bioactive glass used in study **IV** has decreased reaction kinetics compared to CC bioactive glass, because bioactive glasses with higher silica content (55-60 wt%) react more slowly (Välimäki and Aro 2006).

Table 3. *Bioactive glass compositions (wt%) used in studies II, III and IV and six other well known bioactive glasses and their compositions (wt%): 45S5 Bioglass® (Hench 2006) also known as Biogran® by BIOMET* 3i™ *(http://biomet3i.com/English/products/Regenerative/Biogran-Is-The-Ideal-Graft-Material.cfm), S53P4 (Andersson et al. 1990) known also as BonAlive™ by Vivoxid Oy (http://www.vivoxid.com/?n=9097&PRODUCTS), 13-93 (Brink 1997), 1-98 (Itälä et al. 2001a), 58S and 77S (Ogino et al. 1980).*

Bioactive glass	Na_2O	K_2O	MgO	CaO	SiO_2	P_2O_5	B_2O_3	TiO_2
CC bioactive glass (**II** and **III**)	11.0-12.0	16.0-17.0	3.0-4.0	12.0-14.0	50.0-51.0	3.0-4.0	1.0-2.0	0-1.0
bioactive glass used in study **IV**	5.0	7.5	3.0	25.0	59.5	0	0	0
45S5, Bioglass®, Biogran®	24.5	0	0	24.5	45.0	6.0	0	0
S53P4, BonAlive™	23.0	0	0	20.0	53.0	4.0	0	0
13-93	6.0	12	5	20.0	53.0	4.0	0	0
1-98	6.0	11.0	5.0	22.0	53.0	2.0	1.0	0
58S	0	0	0	33.0	58.0	9.0	0	0
77S	0	0	0	14.0	77.0	9.0	0	0

High Na_2O content improves bioactivity of bioactive glass but makes it more difficult to process (Hench et al. 1971, Brink 1997). However, both of the bioactive glasses used in studies **II**, **III** and **IV** were at the large working range (Brink 1997). Another difference between these studies was that different cell concentrations were used; in studies **II** and **III**, the cell concentration was approximately 510 cells per mm^3, and in study **IV**, the cell concentration was approximately 660 cells per mm^3. Furthermore, different cell lines were used in the experiments. Despite these limitations, evaluation of the cell spreading and attachment from the live/dead images could be performed between these studies. ASCs appeared to be more evenly distributed in the middle parts of bioactive glass scaffolds used in studies **II** and **III** than in the middle parts of scaffolds used in study **IV**. The viable cell density on bioactive glass scaffolds (especially on CC scaffolds) was also higher than on scaffolds used in study **IV**. On this basis, and according to the results from studies **II** and **III**, the CC scaffolds appear to provide the best conditions for ASCs to grow and differentiate into osteogenic lineages.

6.4 Future perspectives

In the future, allograft bone may be replaced by tissue-engineered constructs because they offer new solutions to the disadvantages related to allografts, such as the risk of bacterial contamination and virus transmission. In addition, tissue engineered bones can be tailored to grow into the desired shapes and sizes. The need for graft substitutes will continue to increase due to the aging population. The regeneration of large, especially weight-bearing skeletal defects with tissue engineering solutions, however, will most likely require several more years of

research. Further expertise in the field of bioreactors is also needed to produce tissue -engineered bone products in a more cost-effective and standardized manner. The present studies focused on developing new potential tissue engineering solutions for treatment of small bone defects by using ASCs in combination with bioactive biomaterials. The *in vitro* experiments performed here were the first phase of the development process and the next phase would be *in vivo* studies, eventually aiming toward clinical treatments. Based on the *in vitro* results of this study, bioactive glass scaffolds and PLA/β-TCP scaffolds have the highest potential for future hard tissue engineering applications. With a chemically active surface, bioactive glasses possess a high potential in orthopedic surgery, but their applications are limited due to their weak mechanical properties. Thus, the use of composite biomaterials will be needed to develop scaffolds with the desired properties, *e.g.*, for load bearing bone applications.

The first tissue-engineered applications have been used successfully applied in clinical practice. Our group at Regea has performed a few novel clinical treatments in which ASCs were used in combination with biomaterials to treat complicated bone defects with encouraging results. For example, a new hemimaxilla was successfully reconstructed via ectopic bone formation (Mesimäki et al. submitted). The number of clinical trials based on these adult stem cells in combination with biomaterials and signaling molecules is expected to grow rapidly in the near future.

The risk of cancer has to be considered when stem cells are used in clinical practice. Human bone marrow-derived MSCs cultured in autologous serum or FBS to late passage may display localized genetic alterations (Dahl et al. 2008), indicating that the *in vitro* expansion period should be as short as possible. In addition, Houghton *et al*. showed that epithelial cancers can originate from bone marrow-derived cells (Houghton et al. 2004). It has been suggested that bone-marrow derived endothelial precursors are essential during tumor angiogenesis (Lyden et al. 2001, Ciarrocchi et al. 2007, Nolan et al. 2007). However, a recent study of Purhonen *et al*., contradicted this demonstrating that no bone marrow-derived endothelial cell progenitors were involved in angiogenesis during tumor growth i.e. cancer growth does not require these cells. It was also shown that endothelial differentiation is not a typical in vivo function of normal bone marrow-derived stem cells (Purhonen et al. 2008). More studies are required before making final conclusions on the cancer risk of stem cells.

The main challenge in clinical treatments using autologous stem cells will be the patient variation. The capacity of MSCs to differentiate appears to decrease with increasing age (Quarto et al. 1995, D'Ippolito et al. 1999). In addition, Tokalov´s findings of age-related changes in the number of MSCs must be taken into account in considering these cells for clinical use (Tokalov et al. 2007). Although there are no reports on patient variation of human ASCs in the literature, the variation between patients was evident in all ASC experiments of the present work. In each repeated experiment we used a different patient pool consisting of 2 to 4 patient samples. The biologic variation may have been reduced using more parallel samples in the same experiment. This experimental model, however, more closely represents an actual life situation of donor variations in clinics. To achieve clinical success with ASCs, a quantitative bioassay must be developed to screen and verify the

adequate differentiation and proliferation capability of ASCs. Numerous issues related to ASC-biomaterial constructs must be resolved before the full potential of ASC-biomaterial constructs can be realized.

7. Conclusions

On the basis of these studies, the following conclusions can be drawn:

I. Chemical cleansing methods combined with PES were efficient for use with allograft bone. Decreasing the incubation time did not affect the fat cleansing efficiency of the chemical cleansing processes studied. The different processing methods combined with PES and freeze-drying to <5% residual moisture content did not have adverse effects on the biomechanical properties of cortical allograft bone. With a residual moisture content of 0%, the biomechanical properties were significantly reduced in comparison to unprocessed controls.

II. Ca-P surface treatment of bioactive glass did not significantly affect cell viability and proliferation. Our results indicated, however, that Ca-P surface treatment of bioactive glass scaffolds inhibits ion release, causing a delay in early osteogenic differentiation of ASCs. The osteogenic differentiation of ASCs was further delayed in thick Ca-P treated scaffolds compared to thin Ca-P treated scaffolds.

III. Zinc inhibited the degradation profile of the bioactive glass scaffolds. ASC viability was not affected by the addition of zinc to the bioactive glass scaffolds. The proliferation and osteogenic differentiation of the ASCs, however, were inhibited because the dissolution kinetics of bioactive glass was affected by the addition of zinc.

IV. There were no differences between different scaffold types on cell viability or morphology. The PLA/bioactive glass scaffolds provided the weakest support for ASC proliferation, although ASCs exhibited the highest ALP/DNA ratio when cultured on PLA/bioactive glass scaffolds. Our results indicated that PLA/β-TCP composite scaffolds significantly enhanced ASC proliferation and total ALP activity, compared to PLA alone or composite forms of PLA/bioactive glass scaffolds.

The results of studies **II** and **III** confirmed the osteostimulative effect of bioactive glass on human ASCs. This stimulating effect, however, was crucially related to the composition of the bioactive glass as indicated by comparing the results of studies **II** and **III** to those of study **IV**. Control composition bioactive glass and PLA/β-TCP composite scaffolds demonstrated the best potential for clinical bone tissue

engineering applications, but these scaffolds must be further studied in *in vivo* models. For allograft processing, the potential of the methods examined in the present studies combined with PES also require further *in vivo* research.

Acknowledgements

This study was performed at Regea – Institute for Regenerative Medicine, Tampere University and Department of Biomedical Engineering, Tampere University of Technology during the years 2006-2008.

I owe my deep gratitude to my supervisor, Professor Riitta Suuronen, MD, DDS, PhD, for the opportunity to work under her supervision. Her enthusiastic and inspiring guidance and endless optimism for this work enabled the efficient progression of this project. Her expertise, confidence, and support of this work have been invaluable.

I would also like to express my sincere gratitude to my supervisor, Professor Minna Kellomäki, Dr. Tech., for leading me to the field of biomaterials and tissue engineering in my earlier years as a master's degree student. Her scientific expertise and constructive criticism have been greatly appreciated.

I am deeply grateful to my third supervisor, Susanna Miettinen, PhD, the leader of the "Mese group", for introducing me to the fascinating world of adult stem cells. I admire her for her extensive knowledge of stem cell biology and translational applications of stem cells. Without her helpful advice, constructive criticism, and support, this project would not have been possible. I am proud to have had the chance to perform research under her supervision.

I would like to thank the official examiners of this thesis, Adjunct Professor Heimo Ylänen, PhD, and Professor Risto Penttinen, PhD, for their valuable criticism when reviewing this thesis.

I owe special thanks to Annika Vienonen, PhD, for guiding me in the research field of allograft bone processing and motivating my early steps in this project. Special thanks to Professor George Sándor, MD, DDS, PhD, for his comments and support during the process of writing the manuscripts that resulted from this thesis. I want to warmly thank Loredana Moimas, PhD, for sharing her experience and knowledge on bioactive glass and her valuable assistance with writing the manuscripts. I owe my gratitude also to Janne Nurmi, PhD; Eija Pirhonen, PhD; Mika Pelto, MSc; Martti Hirn, MD, PhD; and Heini Huhtala, MSc, for their helpful advice.

I want to express gratitude to all my co-authors for their contribution to this work. I am grateful to Hannu Kuokkanen and Sari Räty for providing the adipose tissue samples for my research. I especially want to thank Niina Suuriniemi, MSc, for excellently conducting the heaviest laboratory work load for study **IV**. I warmly thank Ms. Miia Juntunen, Ms. Anna-Maija Honkala, and Minna Salomäki, MSc, for their outstanding technical assistance in the cell culture laboratory. I would also like to thank Mr. Rami Peurakoski and Mrs. Jaana Leppäniemi for excellent technical help with machining the allograft bone samples. I thank Mr. Arto Koistinen for his

important technical assistance and guidance in the use of the E-SEM equipment and Professor Lauri Pelliniemi, MD, PhD for his assistance with the SEM imaging.

Special thanks belong also to all my dear colleagues, especially to Bettina Lindroos, MSc, for her friendship and number of hours that she spent helping me with this thesis. I am grateful for Mr. Henrik Mannerström for his patient consultation with graphic processing. I also want to thank my student Aliisa Pälli, MSc, and Ms. Noora Kaipola for their endless helpfulness with important practical things related to this work.

I owe my warmest thanks to all of my friends for their never-failing support and counterbalancing my life. Especially Emilia, Eveliina, Kaisa, Katja, Heidi, Kia, and Esko – I am grateful for you for being my friends during these busy years and giving my life joy and happiness! Sonja, Sami, and Matti Suuronen, thank you for keeping my mind clear when I was writing this manuscript by playing Canasta and Badminton with me.

I wish to thank my parents, Raija-Liisa and Heikki, and my brother Kari and his family for their endless encouragement and support. Finally, I want to dedicate this thesis to Tuomas and Saga because without their love this work would not have been possible.

This research was financially supported by the competitive research funding of the Pirkanmaa Hospital District, the Finnish Funding Agency for Technology and Innovation (TEKES), and the Finnish Cultural Foundation and the City of Tampere.

8. References

Adkisson HD, Strauss-Schoenberger J, Gillis M, Wilkins R, Jackson M and Hruska KA (2000): Rapid quantitative bioassay of osteoinduction. J Orthop Res 18: 503-511.

Aho AJ, Suominen E, Alanen A, Yli-Urpo A, Knuuti J and Aho HJ (2003): Remodeling of the tibia after grafting of a large cavity with particulate bioactive glass-hydroxylapatite--case report on treatment of fibrous dysplasia with 13 years' follow-up. Acta Orthop Scand 74: 766-770.

Aina V, Perardi A, Bergandi L, Malavasi G, Menabue L, Morterra C and Ghigo D (2007): Cytotoxicity of zinc-containing bioactive glasses in contact with human osteoblasts. Chem Biol Interact 167: 207-218.

Akkus O and Belaney RM (2005): Sterilization by gamma radiation impairs the tensile fatigue life of cortical bone by two orders of magnitude. J Orthop Res 23: 1054-1058.

Akkus O and Rimnac CM (2001): Fracture resistance of gamma radiation sterilized cortical bone allografts. J Orthop Res 19: 927-934.

An YH (2000): Mechanical properties of bone. In: Mechanical Testing of Bone and the Bone-Implant Interface. Eds. Y. H. An and R. A. Draughn. Boca Raton, CRC Press**:** 41-64.

Anderegg CR, Alexander DC and Freidman M (1999): A bioactive glass particulate in the treatment of molar furcation invasions. J Periodontol 70: 384-387.

Andersson OH, Rosenqvist J and Karlsson KH (1993): Dissolution, leaching, and Al2O3 enrichment at the surface of bioactive glasses studied by solution analysis. J Biomed Mater Res 27: 941-948.

Andersson ÖH, Liu G, Kangasniemi K and Juhanoja J (1992): Evaluation of the acceptance of glass in bone. J Mater Sci Mater Med 3: 145-150.

Andersson ÖH, Liu G, Karlsson KH, Niemi L, Miettinen J and Juhanoja J (1990): In vivo behaviour of glasses in the SiO_2-Na_2O-CaO-P_2O_5-Al_2O_3-B_2O_3-system. J Mater Sci Mater Med 1: 219-227.

Aro HT and Aho AJ (1993): Clinical use of bone allografts. Ann Med 25: 403-412.

Arstila H, Fröberg L, Hupa L, Vedel E, Yländen H and Hupa M (2005): The sintering range of porous bioactive glasses. Glass Technol 46: 138-141.

Arstila H, Hupa L, Karlsson KH and Hupa M (2008): Influence of heat treatment on crystallization of bioactive glasses. J Non-Cryst Solids 354: 722-728.

Arstila H, Vedel E, Hupa L and Hupa M (2007): Factors affecting crystallization of bioactive glasses. J Eur Ceram Soc 27: 1543-1546.

Ashammakhi N, Renier D, Arnaud E, Marchac D, Ninkovic M, Donaway D, Jones B, Serlo W, Laurikainen K, Tormala P and Waris T (2004): Successful use of biosorb osteofixation devices in 165 cranial and maxillofacial cases: a multicenter report. J Craniofac Surg 15: 692-701; discussion 702.

Aspenberg P (1998): Bank bone, infections and HIV. Acta Orthop Scand 69: 557-558.

Aubin JE, Liu F, Malaval L and Gupta AK (1995): Osteoblast and chondroblast differentiation. Bone 17: 77S-83S.

Aunoble S, Clement D, Frayssinet P, Harmand MF and Le Huec JC (2006): Biological performance of a new beta-TCP/PLLA composite material for applications in spine surgery: in vitro and in vivo studies. J Biomed Mater Res A 78: 416-422.

Aust L, Devlin B, Foster SJ, Halvorsen YD, Hicok K, du Laney T, Sen A, Willingmyre GD and Gimble JM (2004): Yield of human adipose-derived adult stem cells from liposuction aspirates. Cytotherapy 6: 7-14.

Bacigalupo A, Tong J, Podesta M, Piaggio G, Figari O, Colombo P, Sogno G, Tedone E, Moro F, Van Lint MT and et al. (1992): Bone marrow harvest for marrow transplantation: effect of multiple small (2 ml) or large (20 ml) aspirates. Bone Marrow Transplant 9: 467-470.

Balamurugan A, Balossier G, Michel J, Kannan S, Benhayoune H, Rebelo AH and Ferreira JM (2007): Sol gel derived SiO(2)-CaO-MgO-P(2)O(5) bioglass system--preparation and in vitro characterization. J Biomed Mater Res B Appl Biomater 83: 546-553.

Ball MD, Downes S, Scotchford CA, Antonov EN, Bagratashvili VN, Popov VK, Lo WJ, Grant DM and Howdle SM (2001): Osteoblast growth on titanium foils coated with hydroxyapatite by pulsed laser ablation. Biomaterials 22: 337-347.

Banfi A, Muraglia A, Dozin B, Mastrogiacomo M, Cancedda R and Quarto R (2000): Proliferation kinetics and differentiation potential of ex vivo expanded human bone marrow stromal cells: Implications for their use in cell therapy. Exp Hematol 28: 707-715.

Barbour SA and King W (2003): The safe and effective use of allograft tissue--an update. Am J Sports Med 31: 791-797.

Barry FP and Murphy JM (2004): Mesenchymal stem cells: clinical applications and biological characterization. Int J Biochem Cell Biol 36: 568-584.

Beck GR, Jr., Sullivan EC, Moran E and Zerler B (1998): Relationship between alkaline phosphatase levels, osteopontin expression, and mineralization in differentiating MC3T3-E1 osteoblasts. J Cell Biochem 68: 269-280.

Bergsma EJ, Rozema FR, Bos RR and de Bruijn WC (1993): Foreign body reactions to resorbable poly(L-lactide) bone plates and screws used for the fixation of unstable zygomatic fractures. J Oral Maxillofac Surg 51: 666-670.

Bigi A, Bracci B, Cuisinier F, Elkaim R, Fini M, Mayer I, Mihailescu IN, Socol G, Sturba L and Torricelli P (2005): Human osteoblast response to pulsed laser deposited calcium phosphate coatings. Biomaterials 26: 2381-2389.

Blades MC, Moore DP, Revell PA and Hill R (1998): In vivo skeletal response and biomechanical assessment of two novel polyalkenoate cements following femoral implantation in the female New Zealand White rabbit. J Mater Sci Mater Med 9: 701-706.

Block JE and Thorn MR (2000): Clinical indications of calcium-phosphate biomaterials and related composites for orthopedic procedures. Calcif Tissue Int 66: 234-238.

Boccaccini A and Maquet V (2003): Bioresorbable and bioactive polymer/Bioglass® composites with tailored pore structure for tissue engineering applications. Compos Sci Tech 63: 2417-2429

Bohner M (2000): Calcium orthophosphates in medicine: from ceramics to calcium phosphate cements. Injury 31 Suppl 4: 37-47.

Bohner M (2001): Physical and chemical aspects of calcium phosphates used in spinal surgery. Eur Spine J 10 Suppl 2: S114-121.

Bonucci E (2000): Basic Composition and Structure of Bone. In: Mechanical Testing of Bone and the Bone-Implant Interface. Eds. Y. H. An and R. A. Draughn. Boca Raton, CRC Press**:** 3-22.

Bosetti M and Cannas M (2005): The effect of bioactive glasses on bone marrow stromal cells differentiation. Biomaterials 26: 3873-3879.

Bosetti M, Zanardi L, Hench L and Cannas M (2003): Type I collagen production by osteoblast-like cells cultured in contact with different bioactive glasses. J Biomed Mater Res A 64: 189-195.

Boyce T, Edwards J and Scarborough N (1999): Allograft bone. The influence of processing on safety and performance. Orthop Clin North Am 30: 571-581.

Boyd D and Towler MR (2005): The processing, mechanical properties and bioactivity of zinc based glass ionomer cements. J Mater Sci Mater Med 16: 843-850.

Brink M (1997): The influence of alkali and alkaline earths on the working range for bioactive glasses. J Biomed Mater Res 36: 109-117.

Brink M, Turunen T, Happonen RP and Yli-Urpo A (1997): Compositional dependence of bioactivity of glasses in the system Na2O-K2O-MgO-CaO-B2O3-P2O5-SiO2. J Biomed Mater Res 37: 114-121.

Bruder SP, Kraus KH, Goldberg VM and Kadiyala S (1998): The effect of implants loaded with autologous mesenchymal stem cells on the healing of canine segmental bone defects. J Bone Joint Surg Am 80: 985-996.

Buckwalter JA, Glimcher MJ, Cooper RR and Recker R (1996): Bone biology. I: Structure, blood supply, cells, matrix, and mineralization. Instr Course Lect 45: 371-386.

Bunnell BA, Estes BT, Guilak F and Gimble JM (2008): Differentiation of adipose stem cells. Methods Mol Biol 456: 155-171.

Butler AM, Morgan DA, Verheul R and Walsh WR (2005): Mechanical properties of gamma irradiated morselized bone during compaction. Biomaterials 26: 6009-6013.

Buttery LDK and Bishop AE (2005): Introduction to tissue engineering. In: Biomaterials, artificial organs and tissue engineering. Eds. L. L. Hench and J. R. Jones. Cambridge, Woodhead Publishing Limited**:** 193-200.

Caplan AI (1994): The mesengenic process. Clin Plast Surg 21: 429-435.

Caplan AI and Bruder SP (2001): Mesenchymal stem cells: building blocks for molecular medicine in the 21st century. Trends Mol Med 7: 259-264.

Chen J, Sotome S, Wang J, Orii H, Uemura T and Shinomiya K (2005): Correlation of in vivo bone formation capability and in vitro differentiation of human bone marrow stromal cells. J Med Dent Sci 52: 27-34.

Chen JB, Yu Y, Yang JL, Morgan DA and Walsh WR (2007): BMP-7 and CBFA1 in allograft bone in vivo bone formation and the influence of gamma-irradiation. J Biomed Mater Res A 80: 435-443.

Choumerianou DM, Dimitriou H and Kalmanti M (2008): Stem cells: promises versus limitations. Tissue Eng Part B Rev 14: 53-60.

Christodoulou I, Buttery LD, Saravanapavan P, Tai G, Hench LL and Polak JM (2005): Dose- and time-dependent effect of bioactive gel-glass ionic-dissolution products on human fetal osteoblast-specific gene expression. J Biomed Mater Res B Appl Biomater 74: 529-537.

Ciarrocchi A, Jankovic V, Shaked Y, Nolan DJ, Mittal V, Kerbel RS, Nimer SD and Benezra R (2007): Id1 restrains p21 expression to control endothelial progenitor cell formation. PLoS ONE 2: e1338.

Conrad EU, Ericksen DP, Tencer AF, Strong DM and Mackenzie AP (1993): The effects of freeze-drying and rehydration on cancellous bone. Clin Orthop Relat Res: 279-284.

Cornell CN (1999): Osteoconductive materials and their role as substitutes for autogenous bone grafts. Orthop Clin North Am 30: 591-598.

Cornu O, Banse X, Docquier PL, Luyckx S and Delloye C (2000): Effect of freeze-drying and gamma irradiation on the mechanical properties of human cancellous bone. J Orthop Res 18: 426-431.

Coury AJ (2004): Degradation of Materials in the Biological Environment: Chemical and biochemical degradation of polymers. In: Biomaterials Science An Introduction to Materials in Medicine. Eds. B. D. Ratner, A. S. Hoffman, F. J. Schoen and J. E. Lemons. San Diego, Elsevier Academic Press**:** 411-430.

Cowan CM, Shi YY, Aalami OO, Chou YF, Mari C, Thomas R, Quarto N, Contag CH, Wu B and Longaker MT (2004): Adipose-derived adult stromal cells heal critical-size mouse calvarial defects. Nat Biotechnol 22: 560-567.

Cui L, Liu B, Liu G, Zhang W, Cen L, Sun J, Yin S, Liu W and Cao Y (2007): Repair of cranial bone defects with adipose derived stem cells and coral scaffold in a canine model. Biomaterials.

Currey JD (1969a): The mechanical consequences of variation in the mineral content of bone. J Biomech 2: 1-11.

Currey JD (1969b): The relationship between the stiffness and the mineral content of bone. J Biomech 2: 477-480.

Currey JD (1988): The effects of drying and re-wetting on some mechanical properties of cortical bone. J Biomech 21: 439-441.

Currey JD, Foreman J, Laketic I, Mitchell J, Pegg DE and Reilly GC (1997): Effects of ionizing radiation on the mechanical properties of human bone. J Orthop Res 15: 111-117.

D'Ippolito G, Schiller PC, Ricordi C, Roos BA and Howard GA (1999): Age-related osteogenic potential of mesenchymal stromal stem cells from human vertebral bone marrow. J Bone Miner Res 14: 1115-1122.

Daculsi G, Laboux O, Malard O and Weiss P (2003): Current state of the art of biphasic calcium phosphate bioceramics. J Mater Sci Mater Med 14: 195-200.

Dahl JA, Duggal S, Coulston N, Millar D, Melki J, Shahdadfar A, Brinchmann JE and Collas P (2008): Genetic and epigenetic instability of human bone marrow mesenchymal stem cells expanded in autologous serum or fetal bovine serum. Int J Dev Biol 52: 1033-1042.

de Girolamo L, Sartori MF, Albisetti W and Brini AT (2007): Osteogenic differentiation of human adipose-derived stem cells: comparison of two different inductive media. J Tissue Eng Regen Med 1: 154-157.

De Girolamo L, Sartori MF, Arrigoni E, Rimondini L, Albisetti W, Weinstein RL and Brini AT (2008): Human adipose-derived stem cells as future tools in tissue

regeneration: osteogenic differentiation and cell-scaffold interaction. Int J Artif Organs 31: 467-479.

de Groot K, Wolke JG and Jansen JA (1998): Calcium phosphate coatings for medical implants. Proc Inst Mech Eng [H] 212: 137-147.

DePaula CA, Truncale KG, Gertzman AA, Sunwoo MH and Dunn MG (2005): Effects of hydrogen peroxide cleaning procedures on bone graft osteoinductivity and mechanical properties. Cell Tissue Bank 6: 287-298.

Dominici M, Le Blanc K, Mueller I, Slaper-Cortenbach I, Marini F, Krause D, Deans R, Keating A, Prockop D and Horwitz E (2006): Minimal criteria for defining multipotent mesenchymal stromal cells. The International Society for Cellular Therapy position statement. Cytotherapy 8: 315-317.

Dorozhkin SV and Epple M (2002): Biological and medical significance of calcium phosphates. Angew Chem Int Ed Engl 41: 3130-3146.

Du RL, Chang J, Ni SY, Zhai WY and Wang JY (2006): Characterization and in vitro bioactivity of zinc-containing bioactive glass and glass-ceramics. J Biomater Appl 20: 341-360.

Ducheyne P and Qiu Q (1999): Bioactive ceramics: the effect of surface reactivity on bone formation and bone cell function. Biomaterials 20: 2287-2303.

EAMST/EATB (1997). Common standards for musculoskeletal tissue banking. European Association of Musculo Skeletal Transplantation, European Association of Tissue Bank
Vienna, Austria.

Eastlund T (2006): Bacterial infection transmitted by human tissue allograft transplantation. Cell Tissue Bank 7: 147-166.

Einhorn TA (1998): The cell and molecular biology of fracture healing. Clin Orthop Relat Res: S7-21.

Ekholm E, Tommila M, Forsback AP, Martson M, Holmbom J, Aaritalo V, Finnberg C, Kuusilehto A, Salonen J, Yli-Urpo A and Penttinen R (2005): Hydroxyapatite coating of cellulose sponge does not improve its osteogenic potency in rat bone. Acta Biomater 1: 535-544.

El-Ghannam A, Ducheyne P and Shapiro IM (1999): Effect of serum proteins on osteoblast adhesion to surface-modified bioactive glass and hydroxyapatite. J Orthop Res 17: 340-345.

Elabd C, Chiellini C, Massoudi A, Cochet O, Zaragosi LE, Trojani C, Michiels JF, Weiss P, Carle G, Rochet N, Dechesne CA, Ailhaud G, Dani C and Amri EZ (2007): Human adipose tissue-derived multipotent stem cells differentiate in vitro and in vivo into osteocyte-like cells. Biochem Biophys Res Commun 361: 342-348.

Elshahat A, Shermak MA, Inoue N, Chao EY and Manson P (2004): The use of Novabone and Norian in cranioplasty: a comparative study. J Craniofac Surg 15: 483-489.

Eppley BL, Pietrzak WS and Blanton MW (2005): Allograft and alloplastic bone substitutes: a review of science and technology for the craniomaxillofacial surgeon. J Craniofac Surg 16: 981-989.

Evans FG and Lebow M (1951): Regional differences in some of the physical properties of the human femur. J Appl Physiol 3: 563-572.

Ferreira PC, Piai Kde A, Takayanagui AM and Segura-Munoz SI (2008): Aluminum as a risk factor for Alzheimer's disease. Rev Lat Am Enfermagem 16: 151-157.

Filgueiras MR, La Torre G and Hench LL (1993): Solution effects on the surface reactions of a bioactive glass. J Biomed Mater Res 27: 445-453.

Franks F (1998): Freeze-drying of bioproducts: putting principles into practice. Eur J Pharm Biopharm 45: 221-229.

Freyman TM, Yannas IV and Gibson LJ (2001): Cellular materials as porous scaffolds for tissue engineering. Progr Mater Sci 46: 273-282.

Friedenstein AJ, Chailakhyan RK and Gerasimov UV (1987): Bone marrow osteogenic stem cells: in vitro cultivation and transplantation in diffusion chambers. Cell Tissue Kinet 20: 263-272.

Friedenstein AJ, Petrakova KV, Kurolesova AI and Frolova GP (1968): Heterotopic of bone marrow.Analysis of precursor cells for osteogenic and hematopoietic tissues. Transplantation 6: 230-247.

Friedenstein AJ, Piatetzky S, II and Petrakova KV (1966): Osteogenesis in transplants of bone marrow cells. J Embryol Exp Morphol 16: 381-390.

Fuchs E and Segre JA (2000): Stem cells: a new lease on life. Cell 100: 143-155.

Galea G and Kearney JN (2005): Clinical effectiveness of processed and unprocessed bone. Transfus Med 15: 165-174.

Gao T, Aro HT, Ylanen H and Vuorio E (2001): Silica-based bioactive glasses modulate expression of bone morphogenetic protein-2 mRNA in Saos-2 osteoblasts in vitro. Biomaterials 22: 1475-1483.

Garcia AJ, Ducheyne P and Boettiger D (1998): Effect of surface reaction stage on fibronectin-mediated adhesion of osteoblast-like cells to bioactive glass. J Biomed Mater Res 40: 48-56.

Gimble J and Guilak F (2003): Adipose-derived adult stem cells: isolation, characterization, and differentiation potential. Cytotherapy 5: 362-369.

Giordano RA, Wu BM, Borland SW, Cima LG, Sachs EM and Cima MJ (1996): Mechanical properties of dense polylactic acid structures fabricated by three dimensional printing. J Biomater Sci Polym Ed 8: 63-75.

Greenspan DC and Hench LL (1976): Chemical and mechanical behavior of bioglass-coated alumina. J Biomed Mater Res 10: 503-509.

Grieb TA, Forng RY, Stafford RE, Lin J, Almeida J, Bogdansky S, Ronholdt C, Drohan WN and Burgess WH (2005): Effective use of optimized, high-dose (50 kGy) gamma irradiation for pathogen inactivation of human bone allografts. Biomaterials 26: 2033-2042.

Gronthos S, Franklin DM, Leddy HA, Robey PG, Storms RW and Gimble JM (2001): Surface protein characterization of human adipose tissue-derived stromal cells. J Cell Physiol 189: 54-63.

Gürpinar ÖA and Onur MA (2005): In Vitro Investigation of Cell Compatibility of Pure ß-TCP Granules. J Bioac Compat Polym 20: 183-196.

Haimi S, Wahlman M, Mannila M, Virtanen V and Hirn M (2008): Pulse-lavage washing is an effective method for defatting of morselized allograft bone in the operating theater. Acta Orthop 79: 94-97.

Halvorsen YC, Wilkison WO and Gimble JM (2000): Adipose-derived stromal cells--their utility and potential in bone formation. Int J Obes Relat Metab Disord 24 Suppl 4: S41-44.

Halvorsen YD, Franklin D, Bond AL, Hitt DC, Auchter C, Boskey AL, Paschalis EP, Wilkison WO and Gimble JM (2001): Extracellular matrix mineralization and osteoblast gene expression by human adipose tissue-derived stromal cells. Tissue Eng 7: 729-741.

Hattori H, Masuoka K, Sato M, Ishihara M, Asazuma T, Takase B, Kikuchi M and Nemoto K (2006): Bone formation using human adipose tissue-derived stromal cells and a biodegradable scaffold. J Biomed Mater Res B Appl Biomater 76: 230-239.

Hattori H, Sato M, Masuoka K, Ishihara M, Kikuchi T, Matsui T, Takase B, Ishizuka T, Kikuchi M, Fujikawa K and Ishihara M (2004): Osteogenic potential of human adipose tissue-derived stromal cells as an alternative stem cell source. Cells Tissues Organs 178: 2-12.

Hautamäki MP, Aho AJ, Alander P, Rekola J, Gunn J, Strandberg N and Vallittu PK (2008): Repair of bone segment defects with surface porous fiber-reinforced polymethyl methacrylate (PMMA) composite prosthesis: histomorphometric incorporation model and characterization by SEM. Acta Orthop 79: 555-564.

Heath JW and Young B (2000): Wheater's Functional Histology. London, Churchill Livingstone.

Heikkilä JT, Mattila KT, Andersson ÖH, Knuuti J, Yli-Urpo A and Aho AJ (1995): Behaviour of bioactive glass in human bone. In: Bioceramics. Eds. L. L. Hench, J. Wilson and D. Greenspan. Pergamon, Elsevier. 8**:** 35-41.

Hench LL (2006): The story of Bioglass. J Mater Sci Mater Med 17: 967-978.

Hench LL and Best S (2004): Classes of materials used in medicine: Ceramics, glasses, and glass-ceramics. In: Biomaterials Science An Introduction to Materials in Medicine. Eds. B. D. Ratner, A. S. Hoffman, F. J. Schoen and J. E. Lemons. San Diego, Elsevier Academic Press**:** 153-169.

Hench LL and Polak JM (2002): Third-generation biomedical materials. Science 295: 1014-1017.

Hench LL, Splinter RJ and Allen WC (1971): Bonding Mechanism at the interface of ceramic prosthetic materials. J Biomed Mater Res Symposium 2: 117-141.

Hench LL and West J (1996): Biological applications of bioactive glasses. Life Chem Rep 13: 187-241

Hicok KC, Du Laney TV, Zhou YS, Halvorsen YD, Hitt DC, Cooper LF and Gimble JM (2004): Human adipose-derived adult stem cells produce osteoid in vivo. Tissue Eng 10: 371-380.

Hiltunen K, Seppälä JN, Itäivaara M and Häirkönen M (1997): The biodegradation of lactic acid-based
poly(ester-urethanes). J Environ Polym Degr 5: 167-173.

Hing KA, Best SM, Tanner KE, Revell PA and Bonfield W (1998): Histomorphological and biomechanical characterization of calcium phosphates in the osseous environment. Proc Inst Mech Eng [H] 212: 437-451.

Hirn MY (2001): Processing of morsellised femoral heads with high-pressure saline. Acta Orthop Scand 72: 411-412.

Hoffman AS (2004): Classes of materials used in medicine: Introduction. In: Biomaterials Science An Introduction to Materials in Medicine
Eds. B. D. Ratner, A. S. Hoffman, F. J. Schoen and J. E. Lemons. San Diego, Elsevier Academic Press**:** 67-79.

Holmbom J, Sodergard A, Ekholm E, Martson M, Kuusilehto A, Saukko P and Penttinen R (2005): Long-term evaluation of porous poly(epsilon-caprolactone-co-L-lactide) as a bone-filling material. J Biomed Mater Res A 75: 308-315.

Holmes RE (1979): Bone regeneration within a coralline hydroxyapatite implant. Plast Reconstr Surg 63: 626-633.

Horwitz EM, Gordon PL, Koo WK, Marx JC, Neel MD, McNall RY, Muul L and Hofmann T (2002): Isolated allogeneic bone marrow-derived mesenchymal cells engraft and stimulate growth in children with osteogenesis imperfecta: Implications for cell therapy of bone. Proc Natl Acad Sci U S A 99: 8932-8937.

Houghton J, Stoicov C, Nomura S, Rogers AB, Carlson J, Li H, Cai X, Fox JG, Goldenring JR and Wang TC (2004): Gastric cancer originating from bone marrow-derived cells. Science 306: 1568-1571.

Hulbert SF, Young FA, Mathews RS, Klawitter JJ, Talbert CD and Stelling FH (1970): Potential of ceramic materials as permanently implantable skeletal prostheses. J Biomed Mater Res 4: 433-456.

Höland W, Vogel W, Naumann K and Gummel J (1985): Interface reactions between machinable bioactive glass-ceramics and bone. J Biomed Mater Res 19: 303-312.

Ikeuchi M, Ito A, Dohi Y, Ohgushi H, Shimaoka H, Yonemasu K and Tateishi T (2003): Osteogenic differentiation of cultured rat and human bone marrow cells on the surface of zinc-releasing calcium phosphate ceramics. J Biomed Mater Res A 67: 1115-1122.

Ishaug-Riley SL, Crane-Kruger GM, Yaszemski MJ and Mikos AG (1998): Three-dimensional culture of rat calvarial osteoblasts in porous biodegradable polymers. Biomaterials 19: 1405-1412.

Ishaug-Riley SL, Crane GM, Gurlek A, Miller MJ, Yasko AW, Yaszemski MJ and Mikos AG (1997): Ectopic bone formation by marrow stromal osteoblast transplantation using poly(DL-lactic-co-glycolic acid) foams implanted into the rat mesentery. J Biomed Mater Res 36: 1-8.

Ishaug SL, Crane GM, Miller MJ, Yasko AW, Yaszemski MJ and Mikos AG (1997): Bone formation by three-dimensional stromal osteoblast culture in biodegradable polymer scaffolds. J Biomed Mater Res 36: 17-28.

Ishikawa K, Miyamoto Y, Yuasa T, Ito A, Nagayama M and Suzuki K (2002): Fabrication of Zn containing apatite cement and its initial evaluation using human osteoblastic cells. Biomaterials 23: 423-428.

Ito A, Ojima K, Naito H, Ichinose N and Tateishi T (2000): Preparation, solubility, and cytocompatibility of zinc-releasing calcium phosphate ceramics. J Biomed Mater Res 50: 178-183.

Itälä A, Koort J, Ylänen HO, Hupa M and Aro HT (2003): Biologic significance of surface microroughing in bone incorporation of porous bioactive glass implants. J Biomed Mater Res A 67: 496-503.

Itälä A, Nordström EG, Ylänen H, Aro HT and Hupa M (2001a): Creation of microrough surface on sintered bioactive glass microspheres. J Biomed Mater Res 56: 282-288.

Itälä AI, Ylänen HO, Ekholm C, Karlsson KH and Aro HT (2001b): Pore diameter of more than 100 microm is not requisite for bone ingrowth in rabbits. J Biomed Mater Res 58: 679-683.

Jagur-Grodzinski J (1999): Biomedical application of functional polymers. Reac Func Polym 39: 99-138.

James IE, Dodds RA, Olivera DL, Nuttall ME and Gowen M (1996): Human osteoclastoma-derived stromal cells: correlation of the ability to form mineralized nodules in vitro with formation of bone in vivo. J Bone Miner Res 11: 1453-1460.

Jaroch DB and Clupper DC (2007): Modulation of zinc release from bioactive sol-gel derived SiO(2)-CaO-ZnO glasses and ceramics. J Biomed Mater Res A 82: 575-588.

Jeon O, Rhie JW, Kwon IK, Kim JH, Kim BS and Lee SH (2008): In vivo bone formation following transplantation of human adipose-derived stromal cells that are not differentiated osteogenically. Tissue Eng Part A 14: 1285-1294.

Jones DB, Huddleston PM, Zobitz ME and Stuart MJ (2007a): Mechanical properties of patellar tendon allografts subjected to chemical sterilization. Arthroscopy 23: 400-404.

Jones JR (2005): Scaffolds for tissue engineering. In: Biomaterials, articial organs and tissue engineering. Eds. L. L. Hench and J. R. Jones. Cambridge, Woodhead Publishing Limited**:** 201-214.

Jones JR, Tsigkou O, Coates EE, Stevens MM, Polak JM and Hench LL (2007b): Extracellular matrix formation and mineralization on a phosphate-free porous bioactive glass scaffold using primary human osteoblast (HOB) cells. Biomaterials 28: 1653-1663.

Kamitakahara M, Ohtsuki C, Inada H, Tanihara M and Miyazaki T (2006): Effect of ZnO addition on bioactive CaO-SiO2-P2O5-CaF2 glass-ceramics containing apatite and wollastonite. Acta Biomater 2: 467-471.

Kangasniemi IM, Vahatalo K, Happonen RP, Yli-Urpo A and de Groot K (1994): In vivo reactions of Ca,P particle containing surface reactive glasses. J Biomed Mater Res 28: 993-1002.

Karjomaa S, Suortti T, Lempiäinen R, Selin JF and Itäivaara M (1998): Microbial degradation of poly-(L-lactic acid) oligomers. Polymer Degrad Stabil 59: 333-336

Kasten P, Beyen I, Niemeyer P, Luginbuhl R, Bohner M and Richter W (2008): Porosity and pore size of beta-tricalcium phosphate scaffold can influence protein production and osteogenic differentiation of human mesenchymal stem cells: An in vitro and in vivo study. Acta Biomater.

Kaufmann EA, Ducheyne P and Shapiro IM (2000): Effect of varying physical properties of porous, surface modified bioactive glass 45S5 on osteoblast proliferation and maturation. J Biomed Mater Res 52: 783-796.

Kim HW, Kim HE and Knowles JC (2006a): Production and potential of bioactive glass nanofiber as a next generation biomaterial. Adv Funct Mater 16: 1529-1535.

Kim HW, Lee HH and Chun GS (2008): Bioactivity and osteoblast responses of novel biomedical nanocomposites of bioactive glass nanofiber filled poly(lactic acid). J Biomed Mater Res A 85: 651-663.

Kim SS, Sun Park M, Jeon O, Yong Choi C and Kim BS (2006b): Poly(lactide-co-glycolide)/hydroxyapatite composite scaffolds for bone tissue engineering. Biomaterials 27: 1399-1409.

Kitoh H, Kitakoji T, Tsuchiya H, Mitsuyama H, Nakamura H, Katoh M and Ishiguro N (2004): Transplantation of marrow-derived mesenchymal stem cells and platelet-rich plasma during distraction osteogenesis--a preliminary result of three cases. Bone 35: 892-898.

Kline LB and Hull RN (1960): The virucidal properties of peracetic acid. Am J Clin Pathol 33: 30-33.

Kokubo T, Ito S, Huang ZT, Hayashi T, Sakka S, Kitsugi T and Yamamuro T (1990a): Ca,P-rich layer formed on high-strength bioactive glass-ceramic A-W. J Biomed Mater Res 24: 331-343.

Kokubo T, Kushitani H, Sakka S, Kitsugi T and Yamamuro T (1990b): Solutions able to reproduce in vivo surface-structure changes in bioactive glass-ceramic A-W. J Biomed Mater Res 24: 721-734.

Lassila LV, Nohrstrom T and Vallittu PK (2002): The influence of short-term water storage on the flexural properties of unidirectional glass fiber-reinforced composites. Biomaterials 23: 2221-2229.

Leach JK, Kaigler D, Wang Z, Krebsbach PH and Mooney DJ (2006): Coating of VEGF-releasing scaffolds with bioactive glass for angiogenesis and bone regeneration. Biomaterials 27: 3249-3255.

Lee JA, Parrett BM, Conejero JA, Laser J, Chen J, Kogon AJ, Nanda D, Grant RT and Breitbart AS (2003): Biological alchemy: engineering bone and fat from fat-derived stem cells. Ann Plast Surg 50: 610-617.

LeGeros RZ, Lin S, Rohanizadeh R, Mijares D and LeGeros JP (2003): Biphasic calcium phosphate bioceramics: preparation, properties and applications. J Mater Sci Mater Med 14: 201-209.

Lendeckel S, Jodicke A, Christophis P, Heidinger K, Wolff J, Fraser JK, Hedrick MH, Berthold L and Howaldt HP (2004): Autologous stem cells (adipose) and fibrin glue used to treat widespread traumatic calvarial defects: case report. J Craniomaxillofac Surg 32: 370-373.

Lensch MW, Daheron L and Schlaeger TM (2006): Pluripotent stem cells and their niches. Stem Cell Rev 2: 185-201.

Lietman SA, Tomford WW, Gebhardt MC, Springfield DS and Mankin HJ (2000): Complications of irradiated allografts in orthopaedic tumor surgery. Clin Orthop Relat Res: 214-217.

Lo H, Ponticiello MS and Leong KW (1995): Fabrication of controlled release biodegradable foams by phase separation. Tissue Engineering 1: 15-28.

Lomas R, Drummond O and Kearney JN (2000): Processing of whole femoral head allografts: a method for improving clinical efficacy and safety. Cell Tissue Bank 1: 193-200.

Lovelace TB, Mellonig JT, Meffert RM, Jones AA, Nummikoski PV and Cochran DL (1998): Clinical evaluation of bioactive glass in the treatment of periodontal osseous defects in humans. J Periodontol 69: 1027-1035.

Lusvardi G, Malavasi G, Menabue L and Menziani MC (2002): Synthesis, characterization, and molecular dynamics simulation of Na2O-CaO-SiO2-ZnO glasses. J Phys Chem B 106: 9753-9760

Lyden D, Hattori K, Dias S, Costa C, Blaikie P, Butros L, Chadburn A, Heissig B, Marks W, Witte L, Wu Y, Hicklin D, Zhu Z, Hackett NR, Crystal RG, Moore MA, Hajjar KA, Manova K, Benezra R and Rafii S (2001): Impaired recruitment of bone-marrow-derived endothelial and hematopoietic precursor cells blocks tumor angiogenesis and growth. Nat Med 7: 1194-1201.

Mainil-Varlet P, Rahn B and Gogolewski S (1997): Long-term in vivo degradation and bone reaction to various polylactides. 1. One-year results. Biomaterials 18: 257-266.

Mano JF, Sousa RA, Boesel LF, Neves NM and Reis RL (2004): Bioinert, biodegradable and injectable polymeric matrix composites for hard tissue replacement: state of the art and recent developments. Compos Sci Tech 64: 789-817.

Maquet V, Boccaccini AR, Pravata L, Notingher I and Jerome R (2004): Porous poly(alpha-hydroxyacid)/Bioglass composite scaffolds for bone tissue engineering. I: Preparation and in vitro characterisation. Biomaterials 25: 4185-4194.

Martin C, Winet H and Bao JY (1996): Acidity near eroding polylactide-polyglycolide in vitro and in vivo in rabbit tibial bone chambers. Biomaterials 17: 2373-2380.

Mathineu LM, Bourban PE and Manson JAE (2006): Processing of homogeneous ceramic/polymer blends for bioresorbable composites. Compos Sci Tech 66: 1606-1614.

Matsumoto MA, Filho HN, Padovan LE, Kawakami RY and De Assis Taveira LA (2005): Tissue response to poly-L-lactide acid-polyglycolic acid absorbable screws in autogenous bone grafts: a histologic morphological analysis. Clin Oral Implants Res 16: 112-118.

Mayr-Wohlfart U, Fiedler J, Gunther KP, Puhl W and Kessler S (2001): Proliferation and differentiation rates of a human osteoblast-like cell line (SaOS-2) in contact with different bone substitute materials. J Biomed Mater Res 57: 132-139.

Mendes SC, Tibbe JM, Veenhof M, Both S, Oner FC, van Blitterswijk CA and de Bruijn JD (2004): Relation between in vitro and in vivo osteogenic potential of cultured human bone marrow stromal cells. J Mater Sci Mater Med 15: 1123-1128.

Meretoja VV, Helminen AO, Korventausta JJ, Haapa-aho V, Seppala JV and Narhi TO (2006): Crosslinked poly(epsilon-caprolactone/D,L-lactide)/bioactive glass

composite scaffolds for bone tissue engineering. J Biomed Mater Res A 77: 261-268.

Merwin GE (1986): Bioglass middle ear prosthesis: preliminary report. Ann Otol Rhinol Laryngol 95: 78-82.

Mesimäki K, Lindroos B, Törnwall J, Lindqvist C, Kontio R, Miettinen S and Suuronen R (submitted): Novel Maxillary Reconstruction with Ectopic Bone Formation by GMP Adipose Stem Cells.

Migliaresi C and Alexander H (2004): Classes of materials used in medicine: Composites. In: Biomaterials Science An Introduction to Materials in Medicine. Eds. B. D. Ratner, A. S. Hoffman, F. J. Schoen and J. E. Lemons. San Diego, Elsevier Academic Press**:** 181-196.

Mihalko WM, Beaudoin AJ, Cardea JA and Krause WR (1992): Finite-element modelling of femoral shaft fracture fixation techniques post total hip arthroplasty. J Biomech 25: 469-476.

Mikhael MM, Huddleston PM, Zobitz ME, Chen Q, Zhao KD and An KN (2008): Mechanical strength of bone allografts subjected to chemical sterilization and other terminal processing methods. J Biomech 41: 2816-2820.

Mikos AG, Lu L, Temenoff JS and Tessmar JK (2004): Tissue engineering: Synthetic bioresorbable polymer scaffolds. In: Biomaterials Science An Introduction to Materials in Medicine. Eds. B. D. Ratner, A. S. Hoffman, F. J. Schoen and J. E. Lemons. San Diego, Elsevier Academic Press**:** 735-749.

Mikos AG, Thorsen AJ, Czerwonka LA, Bao Y, Langer R, Winslow DN and Vacanti JP (1994): Preparation and characterization of poly(L-lactic acid) foams. Polymer 35: 1068-1077.

Mjoberg B, Hellquist E, Mallmin H and Lindh U (1997): Aluminum, Alzheimer's disease and bone fragility. Acta Orthop Scand 68: 511-514.

Moimas L, Biasotto M, Di Lenarda R and Schmid C (2006a). In situ Tissue Engineering, effect of a porous bioactive glass scaffold on bone healing: in vivo rabbit study. 10th Ceramics, Cells and Tissues - Materials for Tissue Engineering, Chemistry and Microstructure: The Role for Ceramics, Faenza, Italy, Consiglio Nazionale Delle Ricerche.

Moimas L, De Rosa G, Sergo V and Schmid C (2006b): Bioactive porous scaffolds for tissue engineering applications: investigation on the degradation process by Raman spectroscopy and scanning electron microscopy. J Appl Biomater Biomech 4: 102-109.

Moimas L, Markkula K, Schmid C and Pirhonen E (2004). Three-dimensional Porous Bioactive Glass Fibre Scaffolds, FluidDynamic and Geometrical Characterization. 9th Ceramics, Cells and Tissues - Materials for Tissue Engineering, Chemistry and Microstructure: The Role for Ceramics, Faenza, Italy, Consiglio Nazionale Delle Ricerche.

Muschler GF, Nitto H, Boehm CA and Easley KA (2001): Age- and gender-related changes in the cellularity of human bone marrow and the prevalence of osteoblastic progenitors. J Orthop Res 19: 117-125.

Nakamura T, Yamamuro T, Higashi S, Kokubo T and Itoo S (1985): A new glass-ceramic for bone replacement: evaluation of its bonding to bone tissue. J Biomed Mater Res 19: 685-698.

Natali AN and Meroi EA (1989): A review of the biomechanical properties of bone as a material. J Biomed Eng 11: 266-276.

Nather A, Thambyah A and Goh JC (2004): Biomechanical strength of deep-frozen versus lyophilized large cortical allografts. Clin Biomech (Bristol, Avon) 19: 526-533.

Navarro M, Ginebra MP, Planell JA, Zeppetelli S and Ambrosio L (2004): Development and cell response of a new biodegradable composite scaffold for guided bone regeneration. J Mater Sci Mater Med 15: 419-422.

Niemela T, Niiranen H and Kellomaki M (2008): Self-reinforced composites of bioabsorbable polymer and bioactive glass with different bioactive glass contents. Part II: In vitro degradation. Acta Biomater 4: 156-164.

Niemeyer P, Krause U, Fellenberg J, Kasten P, Seckinger A, Ho AD and Simank HG (2004): Evaluation of mineralized collagen and alpha-tricalcium phosphate as scaffolds for tissue engineering of bone using human mesenchymal stem cells. Cells Tissues Organs 177: 68-78.

Nolan DJ, Ciarrocchi A, Mellick AS, Jaggi JS, Bambino K, Gupta S, Heikamp E, McDevitt MR, Scheinberg DA, Benezra R and Mittal V (2007): Bone marrow-derived endothelial progenitor cells are a major determinant of nascent tumor neovascularization. Genes Dev 21: 1546-1558.

Ogino M, Ohuchi F and Hench LL (1980): Compositional dependence of the formation of calcium phosphate films on bioglass. J Biomed Mater Res 14: 55-64.

Okii N, Nishimura S, Kurisu K, Takeshima Y and Uozumi T (2001): In vivo histological changes occurring in hydroxyapatite cranial reconstruction--case report. Neurol Med Chir (Tokyo) 41: 100-104.

Oliveira AL, Alves CM and Reis RL (2002): Cell adhesion and proliferation on biomimetic calcium-phosphate coatings produced by a sodium silicate gel methodology. J Mater Sci Mater Med 13: 1181-1188.

Ovesen J, Moller-Madsen B, Thomsen JS, Danscher G and Mosekilde L (2001): The positive effects of zinc on skeletal strength in growing rats. Bone 29: 565-570.

Park A, Wu B and Griffith LG (1998): Integration of surface modification and 3D fabrication techniques to prepare patterned poly(L-lactide) substrates allowing regionally selective cell adhesion. J Biomater Sci Polym Ed 9: 89-110.

Park BW, Hah YS, Kim DR, Kim JR and Byun JH (2007): Osteogenic phenotypes and mineralization of cultured human periosteal-derived cells. Arch Oral Biol 52: 983-989.

Peltola M, Kinnunen I and Aitasalo K (2008): Reconstruction of orbital wall defects with bioactive glass plates. J Oral Maxillofac Surg 66: 639-646.

Peltoniemi H, Ashammakhi N, Kontio R, Waris T, Salo A, Lindqvist C, Gratz K and Suuronen R (2002): The use of bioabsorbable osteofixation devices in craniomaxillofacial surgery. Oral Surg Oral Med Oral Pathol Oral Radiol Endod 94: 5-14.

Peter SJ, Miller MJ, Yasko AW, Yaszemski MJ and Mikos AG (1998): Polymer concepts in tissue engineering. J Biomed Mater Res 43: 422-427.

Pittenger MF, Mackay AM, Beck SC, Jaiswal RK, Douglas R, Mosca JD, Moorman MA, Simonetti DW, Craig S and Marshak DR (1999): Multilineage potential of adult human mesenchymal stem cells. Science 284: 143-147.

Popp JR, Love BJ and Goldstein AS (2007): Effect of soluble zinc on differentiation of osteoprogenitor cells. J Biomed Mater Res A 81: 766-769.

Pruss A, Baumann B, Seibold M, Kao M, Tintelnot K, von Versen R, Radtke H, Dorner T, Pauli G and Gobel UB (2001): Validation of the sterilization procedure of allogeneic avital bone transplants using peracetic acid-ethanol. Biologicals 29: 59-66.

Pruss A, Gobel UB, Pauli G, Kao M, Seibold M, Monig HJ, Hansen A and von Versen R (2003): Peracetic acid-ethanol treatment of allogeneic avital bone tissue transplants--a reliable sterilization method. Ann Transplant 8: 34-42.

Pruss A, Kao M, Kiesewetter H, von Versen R and Pauli G (1999): Virus safety of avital bone tissue transplants: evaluation of sterilization steps of spongiosa cuboids using a peracetic acid-methanol mixture. Biologicals 27: 195-201.

Pruss A, Perka C, Degenhardt P, Maronna U, Buttner-Janz K, Paul B, Muller K, Klumpp C, Bruck JC and Von Versen R (2002): Clinical efficacy and compatibility of allogeneic avital tissue transplants sterilized with a peracetic acid/ethanol mixture. Cell Tissue Bank 3: 235-243.

Puelacher WC, Vacanti JP, Ferraro NF, Schloo B and Vacanti CA (1996): Femoral shaft reconstruction using tissue-engineered growth of bone. Int J Oral Maxillofac Surg 25: 223-228.

Purhonen S, Palm J, Rossi D, Kaskenpaa N, Rajantie I, Yla-Herttuala S, Alitalo K, Weissman IL and Salven P (2008): Bone marrow-derived circulating endothelial precursors do not contribute to vascular endothelium and are not needed for tumor growth. Proc Natl Acad Sci U S A 105: 6620-6625.

Quarto R, Thomas D and Liang CT (1995): Bone progenitor cell deficits and the age-associated decline in bone repair capacity. Calcif Tissue Int 56: 123-129.

Radin S, Ducheyne P, Rothman B and Conti A (1997): The effect of in vitro modeling conditions on the surface reactions of bioactive glass. J Biomed Mater Res 37: 363-375.

Radin S, Reilly G, Bhargave G, Leboy PS and Ducheyne P (2005): Osteogenic effects of bioactive glass on bone marrow stromal cells. J Biomed Mater Res A 73: 21-29.

Rao MS and Mattson MP (2001): Stem cells and aging: expanding the possibilities. Mech Ageing Dev 122: 713-734.

Reck R (1981): Tissue reactions to glass ceramics in the middle ear. Clin Otolaryngol Allied Sci 6: 63-65.

Reilly GC, Radin S, Chen AT and Ducheyne P (2007): Differential alkaline phosphatase responses of rat and human bone marrow derived mesenchymal stem cells to 45S5 bioactive glass. Biomaterials 28: 4091-4097.

Ren J, Ren T, Zhao P, Huang Y and Pan K (2007): Repair of mandibular defects using MSCs-seeded biodegradable polyester porous scaffolds. J Biomater Sci Polym Ed 18: 505-517.

Rho JY, Kuhn-Spearing L and Zioupos P (1998): Mechanical properties and the hierarchical structure of bone. Med Eng Phys 20: 92-102.

Robey PG (1996): Bone matrix proteoglycans and glycoproteins. In: Principles of Bone Biology. Eds. J. P. Bilezikian, L. G. Raisz and G. A. Rodan. San Diego, Academic press**:** 155-165.

Rodbell M (1964): Metabolism of Isolated Fat Cells. I. Effects of Hormones on Glucose Metabolism and Lipolysis. J Biol Chem 239: 375-380.

Rodriguez JP, Gonzalez M, Rios S and Cambiazo V (2004): Cytoskeletal organization of human mesenchymal stem cells (MSC) changes during their osteogenic differentiation. J Cell Biochem 93: 721-731.

Rosenberg AE (2005): Bones, joints, and soft tissue tumors. In: Robbins and Cotran pathologic basis of disease. Eds. V. Kumar, A. K. Abbas and N. Fausto. Philadelphia, Elsevier Saunders**:** 1273-1324.

Ross MH, Kaye GI and Pawlina W (2003): Histology A Text and Atlas. Baltimore, Philadelphia, Lippincott Williams & Wilkins.

Santos EM, Radin S, Shenker BJ, Shapiro IM and Ducheyne P (1998): Si-Ca-P xerogels and bone morphogenetic protein act synergistically on rat stromal marrow cell differentiation in vitro. J Biomed Mater Res 41: 87-94.

Schantz JT, Hutmacher DW, Lam CX, Brinkmann M, Wong KM, Lim TC, Chou N, Guldberg RE and Teoh SH (2003): Repair of calvarial defects with customised tissue-engineered bone grafts II. Evaluation of cellular efficiency and efficacy in vivo. Tissue Eng 9 Suppl 1: S127-139.

Scheffler SU, Gonnermann J, Kamp J, Przybilla D and Pruss A (2008): Remodeling of ACL allografts is inhibited by peracetic acid sterilization. Clin Orthop Relat Res 466: 1810-1818.

Scheffler SU, Scherler J, Pruss A, von Versen R and Weiler A (2005): Biomechanical comparison of human bone-patellar tendon-bone grafts after sterilization with peracetic acid ethanol. Cell Tissue Bank 6: 109-115.

Schoen FJ (2004): Tissue engineering: Introduction. In: Biomaterials Science An Introduction to Materials in Medicine. Eds. B. D. Ratner, A. S. Hoffman, F. J. Schoen and J. E. Lemons. San Diego, Elsevier Academic Press**:** 709-712.

Seal BL, Otero TC and Panitch A (2001): Polymeric biomaterials for tissue and organ regeneration. Mater Sci Eng: 147 - 230.

Shamblott MJ, Edwards BE and Gearhart JD (2000): Pluripotent Stem Cells. In: Principles of Tissue Engineering. Eds. R. P. Lanza, R. Langer and J. Vacanti. San Diego, Academic Press**:** 369-381.

Siddappa R, Licht R, van Blitterswijk C and de Boer J (2007): Donor variation and loss of multipotency during in vitro expansion of human mesenchymal stem cells for bone tissue engineering. J Orthop Res 25: 1029-1041.

Stamboulis A, Hench LL and Boccaccini AR (2002): Mechanical properties of biodegradable polymer sutures coated with bioactive glass. J Mater Sci Mater Med 13: 843-848.

Storrie H and Stupp SI (2005): Cellular response to zinc-containing organoapatite: an in vitro study of proliferation, alkaline phosphatase activity and biomineralization. Biomaterials 26: 5492-5499.

Strem BM, Hicok KC, Zhu M, Wulur I, Alfonso Z, Schreiber RE, Fraser JK and Hedrick MH (2005): Multipotential differentiation of adipose tissue-derived stem cells. Keio J Med 54: 132-141.

Suominen E, Aho AJ, Vedel E, Kangasniemi I, Uusipaikka E and Yli-Urpo A (1996): Subchondral bone and cartilage repair with bioactive glasses, hydroxyapatite, and hydroxyapatite-glass composite. J Biomed Mater Res 32: 543-551.

Suuronen R, Kallela I and Lindqvist C (2000): Bioabsorbable plates and screws: Current state of the art in facial fracture repair. J Craniomaxillofac Trauma 6: 19-27; discussion 28-30.

Suuronen R, Kontio R, Ashammakhi N, Lindqvist C and Laine P (2004): Bioabsorbable self-reinforced plates and screws in craniomaxillofacial surgery. Biomed Mater Eng 14: 517-524.

Södergård A, Pantke M and Selin JF (1996): Environmental degradation of peroxide modified poly(L-lactide). International Biodeterioration & Biodegradation 38: 101-106.

Takahashi Y, Yamamoto M and Tabata Y (2005): Osteogenic differentiation of mesenchymal stem cells in biodegradable sponges composed of gelatin and beta-tricalcium phosphate. Biomaterials 26: 3587-3596.

Takizawa T, Akizuki S, Horiuchi H and Yasukawa Y (1998): Foreign body gonitis caused by a broken poly-L-lactic acid screw. Arthroscopy 14: 329-330.

Tang ZL, Wasserloos K, St Croix CM and Pitt BR (2001): Role of zinc in pulmonary endothelial cell response to oxidative stress. Am J Physiol Lung Cell Mol Physiol 281: L243-249.

ter Brugge PJ, Wolke JG and Jansen JA (2002): Effect of calcium phosphate coating crystallinity and implant surface roughness on differentiation of rat bone marrow cells. J Biomed Mater Res 60: 70-78.

Thompson IA (2005): Biocomposites. In: Biomaterials, artificial organs and tissue engineering. Eds. L. L. Hench and J. R. Jones. Cambridge, Woodhead Publishing Limited**:** 48-58.

Thoren K, Aspenberg P and Thorngren KG (1995): Lipid extracted bank bone. Bone conductive and mechanical properties. Clin Orthop Relat Res: 232-246.

Tokalov SV, Gruner S, Schindler S, Wolf G, Baumann M and Abolmaali N (2007): Age-related changes in the frequency of mesenchymal stem cells in the bone marrow of rats. Stem Cells Dev 16: 439-446.

Tomford WW (1995): Transmission of disease through transplantation of musculoskeletal allografts. J Bone Joint Surg Am 77: 1742-1754.

Tommila M, Jokinen J, Wilson T, Forsback AP, Saukko P, Penttinen R and Ekholm E (2008): Bioactive glass-derived hydroxyapatite-coating promotes granulation tissue growth in subcutaneous cellulose implants in rats. Acta Biomater 4: 354-361.

Turunen T, Peltola J, Yli-Urpo A and Happonen RP (2004): Bioactive glass granules as a bone adjunctive material in maxillary sinus floor augmentation. Clin Oral Implants Res 15: 135-141.

Törmälä P (1992): Biodegradable self-reinforced composite materials; manufacturing structure and mechanical properties. Clin Mater 10: 29-34.

Törmälä P, Pohjonen T and Rokkanen P (1998): Bioabsorbable polymers: materials technology and surgical applications. Proc Inst Mech Eng [H] 212: 101-111.

Vaahtio M, Peltola T, Hentunen T, Ylanen H, Areva S, Wolke J and Salonen JI (2006): The properties of biomimetically processed calcium phosphate on bioactive ceramics and their response on bone cells. J Mater Sci Mater Med 17: 1113-1125.

Wakitani S, Goto T, Pineda SJ, Young RG, Mansour JM, Caplan AI and Goldberg VM (1994): Mesenchymal cell-based repair of large, full-thickness defects of articular cartilage. J Bone Joint Surg Am 76: 579-592.

Vallittu PK (1997): Oxygen inhibition of autopolymerization of polymethylmethacrylate-glass fibre composite. J Mater Sci Mater Med 8: 489-492.

van der Donk S, Weernink T, Buma P, Aspenberg P, Slooff TJ and Schreurs BW (2003): Rinsing morselized allografts improves bone and tissue ingrowth. Clin Orthop Relat Res: 302-310.

Wang M (2003): Developing bioactive composite materials for tissue replacement. Biomaterials 24: 2133-2151.

Wang S, Cui W and Bei J (2005): Bulk and surface modifications of polylactide. Anal Bioanal Chem 381: 547-556.

Waris E, Ashammakhi N, Kaarela O, Raatikainen T and Vasenius J (2004): Use of bioabsorbable osteofixation devices in the hand. J Hand Surg [Br] 29: 590-598.

Werner HP and Wewalka G (1973): [Destruction of spores in alcohol by peracetic acid (author's transl)]. Zentralbl Bakteriol [Orig B] 157: 387-391.

Verrier S, Blaker JJ, Maquet V, Hench LL and Boccaccini AR (2004): PDLLA/Bioglass composites for soft-tissue and hard-tissue engineering: an in vitro cell biology assessment. Biomaterials 25: 3013-3021.

Wildemann B, Kadow-Romacker A, Pruss A, Haas NP and Schmidmaier G (2007): Quantification of growth factors in allogenic bone grafts extracted with three different methods. Cell Tissue Bank 8: 107-114.

Williams DF (1986): Definitions in Biomaterials. Proceedings of a Consensus Conference of the European Society for Biomaterials. New York, Elsevier.

Virolainen P, Heikkila J, Hirn M, Aro HT and Aho AJ (2003): 30 years of bone banking at Turku bone bank. Cell Tissue Bank 4: 43-48.

von Doernberg MC, von Rechenberg B, Bohner M, Grunenfelder S, van Lenthe GH, Muller R, Gasser B, Mathys R, Baroud G and Auer J (2006): In vivo behavior of calcium phosphate scaffolds with four different pore sizes. Biomaterials 27: 5186-5198.

Välimäki VV and Aro HT (2006): Molecular basis for action of bioactive glasses as bone graft substitute. Scand J Surg 95: 95-102.

Välimäki VV, Moritz N, Yrjans JJ, Vuorio E and Aro HT (2006): Effect of zoledronic acid on incorporation of a bioceramic bone graft substitute. Bone 38: 432-443.

Välimäki VV, Yrjans JJ, Vuorio E and Aro HT (2005a): Combined effect of BMP-2 gene transfer and bioactive glass microspheres on enhancement of new bone formation. J Biomed Mater Res A 75: 501-509.

Välimäki VV, Yrjans JJ, Vuorio EI and Aro HT (2005b): Molecular biological evaluation of bioactive glass microspheres and adjunct bone morphogenetic protein 2 gene transfer in the enhancement of new bone formation. Tissue Eng 11: 387-394.

Xynos ID, Edgar AJ, Buttery LD, Hench LL and Polak JM (2000a): Ionic products of bioactive glass dissolution increase proliferation of human osteoblasts and induce insulin-like growth factor II mRNA expression and protein synthesis. Biochem Biophys Res Commun 276: 461-465.

Xynos ID, Edgar AJ, Buttery LD, Hench LL and Polak JM (2001): Gene-expression profiling of human osteoblasts following treatment with the ionic products of Bioglass 45S5 dissolution. J Biomed Mater Res 55: 151-157.

Xynos ID, Hukkanen MV, Batten JJ, Buttery LD, Hench LL and Polak JM (2000b): Bioglass 45S5 stimulates osteoblast turnover and enhances bone formation In vitro: implications and applications for bone tissue engineering. Calcif Tissue Int 67: 321-329.

Yamaguchi M, Oishi H and Suketa Y (1987): Stimulatory effect of zinc on bone formation in tissue culture. Biochem Pharmacol 36: 4007-4012.

Yamamoto T, Ecarot B and Glorieux FH (1991): In vivo osteogenic activity of isolated human bone cells. J Bone Miner Res 6: 45-51.

Yang XB, Webb D, Blaker J, Boccaccini AR, Maquet V, Cooper C and Oreffo RO (2006): Evaluation of human bone marrow stromal cell growth on biodegradable polymer/bioglass composites. Biochem Biophys Res Commun 342: 1098-1107.

Yao J, Radin S, Reilly G, Leboy PS and Ducheyne P (2005): Solution-mediated effect of bioactive glass in poly (lactic-co-glycolic acid)-bioactive glass composites on osteogenesis of marrow stromal cells. J Biomed Mater Res A 75: 794-801.

Yates P, Thomson J and Galea G (2005): Processing of whole femoral head allografts: validation methodology for the reliable removal of nucleated cells, lipid and soluble proteins using a multi-step washing procedure. Cell Tissue Bank 6: 277-285.

Ylänen H, Karlsson KH, Itälä A and Aro HT (2000): Effect of immersion in SBF on porous bioactive bodies made by sintering bioactive glass microspheres
J Non-Crystalline Solids 275: 107-115.

Ylänen HO, Helminen T, Helminen A, Rantakokko J, Karlsson KH and Aro HT (1999): Porous bioactive glass matrix in reconstruction of articular osteochondral defects. Ann Chir Gynaecol 88: 237-245.

Yoon E, Dhar S, Chun DE, Gharibjanian NA and Evans GR (2007): In vivo osteogenic potential of human adipose-derived stem cells/poly lactide-co-glycolic acid constructs for bone regeneration in a rat critical-sized calvarial defect model. Tissue Eng 13: 619-627.

Zeng H, Chittur KK and Lacefield WR (1999): Dissolution/reprecipitation of calcium phosphate thin films produced by ion beam sputter deposition technique. Biomaterials 20: 443-451.

Zhang M, Powers RM, Jr. and Wolfinbarger L, Jr. (1997): A quantitative assessment of osteoinductivity of human demineralized bone matrix. J Periodontol 68: 1076-1084.

Zioupos P, Smith CW and An YH (2000): Factors Affecting Mechanical Properties of Bone. In: Mechanical Testing of Bone and the Bone-Implant Interface. Eds. Y. H. An and R. A. Draughn. Boca Raton, CRC Press**:** 65-86.

Zuk PA, Zhu M, Ashjian P, De Ugarte DA, Huang JI, Mizuno H, Alfonso ZC, Fraser JK, Benhaim P and Hedrick MH (2002): Human adipose tissue is a source of multipotent stem cells. Mol Biol Cell 13: 4279-4295.

Zuk PA, Zhu M, Mizuno H, Huang J, Futrell JW, Katz AJ, Benhaim P, Lorenz HP and Hedrick MH (2001): Multilineage cells from human adipose tissue: implications for cell-based therapies. Tissue Eng 7: 211-228.

Available online at www.sciencedirect.com
ScienceDirect
Biologicals 36 (2008) 99–104
IABS BIOLOGICALS
www.elsevier.com/locate/biologicals

The effect of chemical cleansing procedures combined with peracetic acid–ethanol sterilization on biomechanical properties of cortical bone

Suvi Haimi [a,*], Annika Vienonen [a], Martti Hirn [b], Mika Pelto [c], Vesa Virtanen [d], Riitta Suuronen [a]

[a] Regea Institute for Regenerative Medicine, University of Tampere and Tampere University Hospital, Tampere, Finland
[b] Clinic of Orthopaedics, Tampere University Hospital, Tampere, Finland
[c] Institute of Biomaterials, Tampere University of Technology, Tampere, Finland
[d] Laboratory of Biotechnology, University of Oulu, Sotkamo, Finland

Received 23 February 2007; revised 12 June 2007; accepted 15 June 2007

Abstract

Peracetic acid–ethanol sterilization (PES) with a preceding delipidation step is an effective sterilization method for allograft bone, but its influence on biomechanical properties of bone has not been studied. The aim of this study was to evaluate the effects of different incubation times of water, hydrogen peroxide and alcohol cleansing procedures combined with PES on biomechanical properties of freeze-dried cortical bone. These effects were studied by performing three-point bending tests on cortical samples. The lyophilized cortical samples were rehydrated prior to mechanical testing. The bending strength and the absorbed energy of the processed cortical samples were increased slightly but the Young's modulus was decreased compared to unprocessed samples. However, when the residual moisture content of the processed cortical samples was reduced from <5% to 0% all the biomechanical properties studied were significantly decreased. Hexane elution was used to determine the residual fat content of the processed cortical bone. Reducing the incubation time in cleansing had no effect on the residual fat content of the bone samples. Our in vitro study indicates that the cleansing procedure proposed combined with PES affects the biomechanical properties of cortical bone only on a limited scale.
© 2007 The International Association for Biologicals. Published by Elsevier Ltd. All rights reserved.

Keywords: Allograft bone; Peracetic acid; Chemical processing; Mechanical testing

1. Introduction

Allograft bone has been widely used in orthopaedic surgery. Bone transplants are particularly useful for different reconstruction procedures such as joint reconstruction and they are vital for many deficiencies due to trauma or extensive tumour surgery [1–3]. Allografts have many advantages over autograft bone, e.g. lack of donor site morbidity and almost unlimited availability [1,4,5]. However, the potential of the viral transmission by allograft bone remains a great concern. The need to ensure maximum safety has led to a search for different sterilization methods. At the moment the most commonly used methods are various chemical sterilizations and irradiation procedures such as beta and gamma [5,6]. So far no optimal sterilization method has been found. All methods currently in use compromise either the safety of the allograft bone or the biological and biomechanical properties of the allograft [7,8].

Before chemical sterilization allograft bone must be defatted to improve the effectiveness of the sterilization [9]. Removal of lipids has been also shown to increase the incorporation of bone allografts [10]. Peracetic acid–ethanol sterilization (PES) is a potential sterilization method for

* Corresponding author. Regea Institute for Regenerative Medicine, University of Tampere, Biokatu 12, 33520 Tampere, Finland. Tel.: +358 44 029 1203; fax: +358 3 3551 8498.
E-mail address: suvi.haimi@regea.fi (S. Haimi).

1045-1056/07/$34.00 © 2007 The International Association for Biologicals. Published by Elsevier Ltd. All rights reserved.
doi:10.1016/j.biologicals.2007.06.001

allograft bone and it has been proven to effectively inactivate viruses, fungi and bacteria [9,11]. In addition it has been reported that PES does not cause any significant reductions in the osteoconductivity of demineralized bone matrix or affect its osteointegration properties [12]. In the present work the effects of different incubation times of water, hydrogen peroxide and alcohol cleansing procedures combined with PES on the biomechanical properties of freeze-dried cortical bone were investigated. The processed bone samples were compared to unprocessed frozen bone samples. Our hypothesis was that chemical cleansing combined with PES does not adversely affect the biomechanical properties of cortical bone.

The final tissue product is freeze-dried to improve the chemical stability [7,13,14]. It has been claimed that freeze-dried tissue should contain no more than 6% moisture, permitting storage at RT for 5 years after processing [7]. The negative effect of freeze-drying on the biomechanical properties of allograft bone is well known, but so far the effects of different residual moisture contents of cortical bone have not been taken into account in any study [15–17]. Our second objective was to study the effect of different residual moisture contents (<5% and 0%) on the biomechanical properties of cortical bone.

In order to optimize the cleansing procedures we tested three variations of cleansing method used in the National Blood Service, Tissue Service, UK. The efficiency of these three cleansing methods combined with PES in removing fat from allograft bone was therefore compared.

2. Materials and methods

2.1. Bone material and preparation of the bone samples

Four pairs of proximal tibias, four pairs of distal tibias and one pair of proximal femurs were received from 6 male donors of 19–62 years of age and from 2 female donors of 31 and 45 years of age from Tampere University Hospital bone bank. The donors had no medical history of diseases or traumas, which could affect the biomechanical properties of the examined bones. The donors were brain dead heart-beating donors who had been tested to be negative in bacteriological and viral screening according to the standards of the European Association of Tissue Banks (EATB and EAMST 1997). The allografts were harvested in the operation theatre with full aseptic precautions and were stored at −75 °C. The study was approved by the ethical commission of Pirkanmaa Hospital District.

Pairs of bones from the same donor were examined because the biomechanical properties of bone from different donors may vary. The unprocessed controls and the samples for processing were taken equally from the contralateral sides of bone from the same donor to ensure that possible differences due to anatomical heterogeneity in the bones would not affect the results. This procedure enabled comparable analysis of the paired specimens.

Longitudinal cortical specimens were cut from the diaphysial part of the bones, using a grinding machine (model 40BKS; Scantool 40, Brovst, Denmark) and then they were further shaped with a band saw (model DW738; Dewalt, Italy) and finally ground down to final dimensions of $40.0 \times 4.0 \times 2.0$ mm, using a milling machine. The dimensions of the specimens were measured with a sliding gauge. Five to twelve pairs (mean 6) of cortical samples were obtained from each bone pair. The bone samples were continuously irrigated with distilled water throughout machining. When not being handled, all the samples were kept frozen at −75 °C. The 96 cortical samples obtained were evenly divided to serve as a processing sample or as an unprocessed control according to Fig. 1.

2.2. Cleansing procedures

The cleansing procedure A was based on a cleansing procedure used in the National Blood Service, Tissue Service, UK. The cortical samples were placed in a 1 l glass container with 800 ml of a treatment solution. The first step of the cleansing procedure was sonicating the samples with distilled water in a temperature-controlled ultrasonic bath (model DU-14; Nickel Electro Ltd., UK) for 15 min at 54 °C. This was

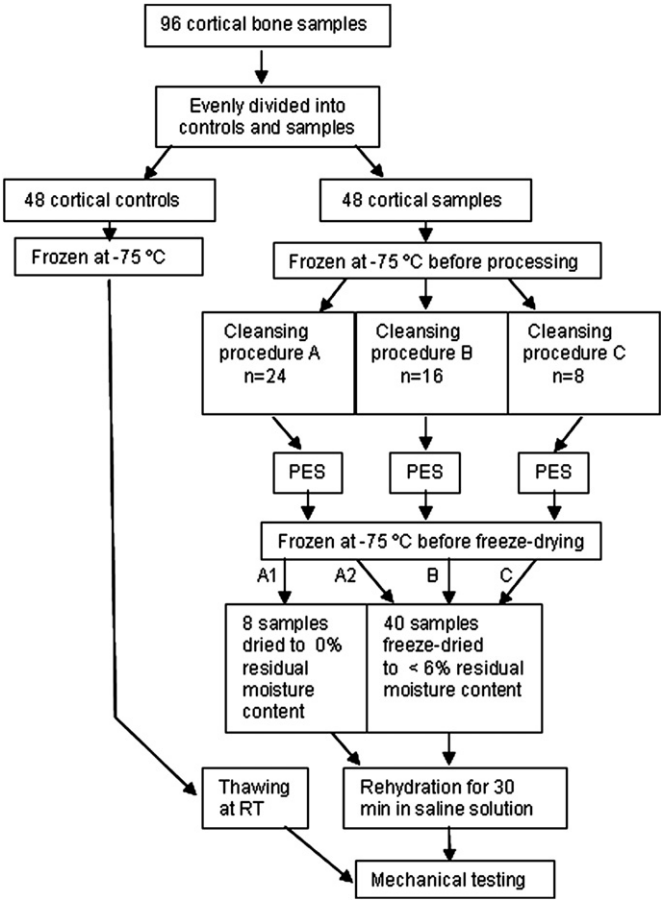

Fig. 1. Experimental design for mechanical testing. One processing group consists of 8 cortical samples.

followed by four washes in distilled water (60 min, 10 min, 10 min, 10 min) under agitation (200 rpm) on a temperature-controlled shaker (model SM 30 A/B/C; Edmund Bühler GmbH, Germany) at 60 °C. The following two steps were also performed in ultrasonic bath. The samples were soaked for 10 min in 3% hydrogen peroxide followed by a 10 min soak in 70% ethanol at room temperature (RT). The chemical treatments were followed by five washes in distilled water (10 min, 10 min, overnight 20 h, 10 min, 10 min) under constant agitation (200 rpm) on the shaker at 60 °C.

Cleansing procedures B and C were modifications of the procedure A. In cleansing procedure B the incubation times with hydrogen peroxide and 70% ethanol incubations were doubled, but the overnight (20 h) and the following two 10 min water washes were omitted. In cleansing procedure C only the overnight (20 h) and the following two 10 min water washes were omitted. Twenty four samples (three separate procedures were performed, in which 8 samples were processed) were processed with cleansing procedure A, 16 samples (two separate procedures were performed, in which 8 samples were processed) were processed with cleansing procedure B, and 8 samples were processed with cleansing procedure C. The samples and controls were individually packed in permeable specimen bags (Thermo, UK) to avoid sample mix-up.

2.3. Sterilization with PES

All the processed samples were sterilized with 1% PES solution according to the method previously described [11]. Briefly, PES procedure was performed under constant agitation (on the shaker at low pressure, 200 mbar) at RT in a desiccator for 4 h. PES solution was removed by washing the bone samples four times for 10 min in distilled water under agitation (on the shaker at low pressure 200 mbar) at RT in a desiccator. At the end of the procedure, the absence of peracetic acid was confirmed by a Merkoquant® test (Merck KGaA) with a sensitivity of 5 ppm.

2.4. Freeze-drying

All the processed cortical samples were freeze-dried in the freeze-dryer (model Heto drywinner with CT 110 Cooling Trap, Jouan Nordic, Denmark). Eight samples processed using cleansing method A were dried to 0% residual moisture content. These 8 samples (A1) were freeze-dried for 27 h (the temperature of the condenser was −110 °C and working vacuum was approximately 1 mbar). The residual moisture was removed with hygroscopic P_2O_5 treatment in a desiccator for 9 days at low pressure (200 mbar). The removal of residual moisture was completed when the weight of the cortical samples was stabilized. Based on this analysis, all the other samples were freeze-dried for 5 h to reach a final residual moisture content of 4.5% for cortical samples.

2.5. Mechanical testing

The mechanical tests were carried out at RT. The cortical samples were loaded into a mechanical testing machine (model 4411; Instron, United Kingdom). The data were analysed by Instron series IX software version 8.31. The machine sensors allowed measurement of the travel and load throughout the procedure. All the freeze-dried cortical samples were rehydrated for 30 min in physiological saline solution. The frozen controls were thawed at RT and tested wet.

In the three-point bending test the cortical samples were subjected to a combination of tension and compression when being loaded. The samples were oriented so that the periosteal surface was in tension and the endosteal surface in compression (Fig. 2). The three-point bending test was carried out as described earlier by Currey et al. except that the crosshead speed was 1 mm/min [8]. The dimensions of each sample were entered into the software program before testing. Young's modulus of elasticity was calculated from the linear part of the stress–strain curve. The bending strength was calculated from the following formula, $\sigma = 3FL/2bd^2$, where F is the external force affecting the sample, L is the gauge length (32 mm), b is the sample width and d is the sample thickness. The energy absorbed by the sample at the break point was measured by the area that was under the load–deformation curve.

2.6. Residual lipid content determination

After mechanical testing, the efficiency of the whole processing method for cleansing fat cells from the bone was determined by measuring the residual fat content with ultrasonic hexane elution. Then all processed and freeze-dried cortical samples were ground with a grinder (model Polymix A10; Kinematica, Switzerland). From each processing group

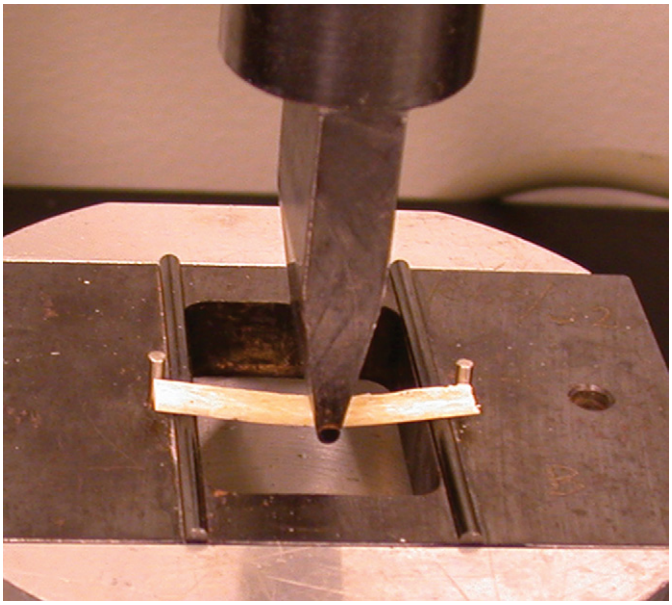

Fig. 2. Three-point bending test of cortical bone.

separately, all the cortical samples were pooled to yield one sample. Lipids from the bone powder samples were extracted in hexane. Thereafter the hexane was evaporated and the resultant residual weight was expressed as the percentage of the extracted original dried cortical bone powder weight.

2.7. Statistical analysis

The statistical analysis of the results was carried with SPSS version 13. The mechanical results of samples and controls were compared using paired *t*-test. The effects of different cleansing processes combined with PES on the biomechanical properties of cortical samples were compared using one-way ANOVA. According to the test of homogeneity of variances, ANOVA was not an appropriate test for comparison of the Young's modulus values of cortical samples, therefore Mann–Whitney *U* test was used instead for these measured values. The power calculations were carried out with PS-Power and Sample Size Calculations version 2.1.30.

3. Results

3.1. Mechanical testing

The mechanical results are summarized in Table 1. No statistical difference (all p values were >0.05) was found between the effects of the different processing methods on the biomechanical properties of the cortical samples. All the three different processing methods significantly reduced the Young's modulus of the cortical samples (freeze-dried to <5% residual moisture content) compared to the unprocessed samples. The bending strength and the absorbed energy of the cortical samples were slightly but still significantly improved by the processing methods compared to the unprocessed controls.

There was a significant decrease in the bending strength, absorbed energy and the Young's modulus of the cortical samples freeze-dried to 0% residual moisture content (Fig. 3). The strength of the totally dry cortical samples was reduced to about 76% of that of the controls.

3.2. Lipid content determination

The residual fat percentages of the cortical samples are presented in Fig. 4. There were no differences between the efficiency of cleansing methods A, B and C in cleansing adipose tissue from the bone. The residual fat content of processed cortical samples varied between 0.2% and 0.5%.

4. Discussion

We studied the effects of different incubation times of water, hydrogen peroxide and alcohol combined with PES and freeze-drying on the biomechanical properties of cortical bone. The bactericidal, fungicidal, virucidal and sporicidal effects of peracetic acid have long been well known. The preceding delipidation step is a prerequisite for effective penetration of a sterilization medium into the bone tissue [9]. The addition of ethanol to the peracetic acid sterilizing medium reduces the surface tension. Negative pressure removes the gas vesicles, which prevent complete tissue penetration of the sterilizing medium [11]. A reliable comparison of the biomechanical properties between processed samples and unprocessed controls requires that the sample and control are taken from the same individual and from the adjacent anatomical locations, which have as identical biomechanical properties as possible. The mean bending strength and Young's modulus obtained from the unprocessed cortical controls were of the same magnitude as those previously reviewed in the literature [8,18]. Therefore the conclusions drawn from the mechanical results obtained from processed cortical samples can be considered reliable.

In our study the Young's modulus of the processed cortical samples decreased significantly in all processing groups. We assume that the deterioration of rigidity of the cortical samples was due to a weak demineralization effect of PES. When bone

Table 1
Mechanical results of cortical bone

	n	Method	Residual moisture (%)	Controls mean	Controls SD	Specimen mean	Specimen SD	%	*p*
Young's modulus (GPa)	8	A1	0	**15.3**	1.5	**14.1**	1.1	**92.7**	0.026
	16	A2	<5	**16.9**	1.1	**14.3**	1.2	**84.3**	<0.001
	16	B	<5	**15.4**	1.4	**13.4**	1.2	**86.7**	<0.001
	8	C	<5	**16.5**	0.8	**14.0**	0.8	**84.9**	0.001
Bending strength (MPa)	8	A1	0	**229.8**	16.9	**173.6**	17.5	**75.8**	<0.001
	16	A2	<5	**227.8**	27.7	**248.6**	36.8	**109.1**	0.014
	16	B	<5	**201.3**	29.3	**214.9**	29.3	**106.8**	0.017
	8	C	<5	**211.6**	9.9	**211.4**	33.6	**100.0**	**0.988**
Energy to break point (J)	8	A1	0	**0.10**	0.03	**0.04**	0.01	**38.5**	<0.001
	16	A2	<5	**0.12**	0.05	**0.16**	0.06	**132.2**	0.001
	16	B	<5	**0.08**	0.03	**0.11**	0.04	**130.2**	0.037
	8	C	<5	**0.07**	0.01	**0.09**	0.04	**127.0**	**0.123**

The mean values of the cortical controls and processed specimens (methods A, B and C) are given. n = number of pairs of specimens, % = mean value of the processed samples expressed as a percentage of the mean value of the controls, p = probability resulting from a paired *t*-test on the differences between the paired specimens (not significant values in bold face).

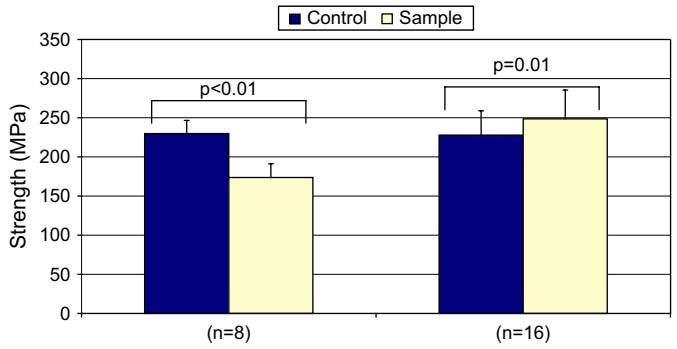

Fig. 3. Mean results of the strengths of cleansing method A processed cortical samples with different residual moisture contents (A1 = residual moisture content 0%, A2 = residual moisture content <5%) compared with unprocessed controls.

is demineralized, its stiffness decreases and it therefore becomes softer and tougher [19]. The demineralization effect could also be the reason why the absorbed energy of the processed cortical samples (freeze-dried to <5% of residual moisture) was significantly higher than the absorbed energy of unprocessed controls. The ability of the material to absorb energy improves when material becomes tougher [20]. There was a slight increase in bending strength which cannot be explained based on literature. PES may cause a slight demineralization effect but in that case the bending strength should have decreased as seen in some other studies [19,21]. The pH value of the PES solution we used was 2.3, which is much higher than the pH value of demineralization solution Lewandrowski et al. used (0.5 N HCl pH 0.3) [19]. Therefore the demineralization effect of PES can only be considered weak and our results cannot be entirely compared to other demineralization studies.

Gamma radiation has been widely used in cortical bone allograft sterilization, but the standard radiation dose, which is recommended for bone allograft has been reported to alter the biomechanical properties of the allograft. The studies suggest that bone becomes more brittle, the ultimate stress–strain and toughness are significantly reduced as a result of radiation sterilization [8,22]. The alteration of the biomechanical properties as a result of chemical cleansing combined with PES appears minor compared to gamma radiation. This was supported by Scheffler et al. who have showed that PES does not impair the biomechanical properties of human bone–patellar tendon bone grafts, even though they used different defatting method than we did [23]. Therefore the chemical sterilization we used can be considered as a better alternative than gamma sterilization at least for strut grafts.

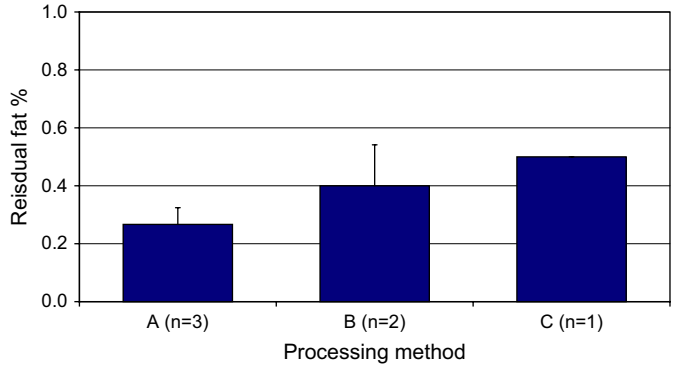

Fig. 4. Residual fat percentages of the processed cortical samples. Method A was the longest processing method (including 20 h water incubation), method B had double hydrogen peroxide and ethanol incubation compared to A and C, and method C was the shortest method.

This was the first study in which the effect of different residual moisture contents on the biomechanical properties of cortical bone was shown to be crucial. In several studies freeze-drying has been reported to impair the biomechanical properties of bone [7,15–17,24,25]. Our results corroborate with this finding. We found that processing and freeze-drying of cortical samples to 0% residual moisture content significantly reduced the strength and decreased the absorbed energy and the Young's modulus of the samples compared to those of unprocessed controls.

There were no differences in the delipidation efficiency of different chemical processing methods combined with PES. The shortest processing method (C) was sensed to be as efficient as the two other tested methods (A, B) in cleansing adipose tissue from cortical bone. The residual fat content variation between all the processed cortical samples was 0.2–0.5%. Pietrzak and Woodell-May studied the fat content of processed cortical bone using the same lipid content determination method as that used in this study. The residual fat content of these processed samples varied between 0% and 6.7% [26]. It can be concluded that our processing substantially reduces fat from cortical bone, although the fat content of cortical bone is initially very low.

Our results suggest that it is advisable not to freeze-dry processed bone grafts too dry, under 1% residual moisture. The biomechanical weakening of allograft bone may lead to unsuccessful healing in situations such as fracture repair, where mechanical strength is needed. Reducing the incubation times of chemical processes did not have an effect on the efficiency of the cleansing process to clean adipose tissue from the cortical bone. Our results showed that the different processing methods combined with PES had only slight effects on the biomechanical properties of cortical bone samples freeze-dried to <5% of residual moisture. However, in vivo studies have to be performed in order to investigate the effect of PES on the bone remodelling and allograft incorporation processes.

Acknowledgements

Special thanks to Heini Huhtala for her valuable statistical support. This research was supported by the competitive research funding of the Pirkanmaa Hospital District, the Employment and Economic Development Centre for Pirkanmaa, the City of Tampere and the Finnish Defence Forces.

References

[1] Barbour SA, King W. The safe and effective use of allograft tissue – an update. Am J Sports Med 2003;31:791–7.

[2] DePaula CA, Truncale KG, Gertzman AA, Sunwoo MH, Dunn MG. Effects of hydrogen peroxide cleaning procedures on bone graft osteoinductivity and mechanical properties. Cell Tissue Bank 2005;6:287–98.

[3] Pruss A, Kao M, von Garrel T, Frommelt L, Gurtler L, Benedix F, et al. Virus inactivation in bone tissue transplants (femoral heads) by moist heat with the 'Marburg bone bank system'. Biologicals 2003;31:75–82.

[4] Butler AM, Morgan DA, Verheul R, Walsh WR. Mechanical properties of gamma irradiated morselized bone during compaction. Biomaterials 2005;26:6009–13.

[5] Grieb TA, Forng RY, Stafford RE, Lin J, Almeida J, Bogdansky S, et al. Effective use of optimized, high-dose (50 kGy) gamma irradiation for pathogen inactivation of human bone allografts. Biomaterials 2005;26:2033–42.

[6] Vastel L, Meunier A, Siney H, Sedel L, Courpied JP. Effect of different sterilization processing methods on the mechanical properties of human cancellous bone allografts. Biomaterials 2004;25:2105–10.

[7] Boyce T, Edwards J, Scarborough N. Allograft bone: the influence of processing on safety and performance. Orthop Clin North Am 1999;30:571–81.

[8] Currey JD, Foreman J, Laketic I, Mitchell J, Pegg DE, Reilly GC. Effects of ionizing radiation on the mechanical properties of human bone. J Orthop Res 1997;15:111–7.

[9] Pruss A, Kao M, Kiesewetter H, von Versen R, Pauli G. Virus safety of avital bone tissue transplants: evaluation of sterilization steps of spongiosa cuboids using a peracetic acid–methanol mixture. Biologicals 1999;27:195–201.

[10] Thoren K, Aspenberg P, Thorngren KG. Lipid extracted bank bone: bone conductive and mechanical properties. Clin Orthop Relat Res 1995;232–46.

[11] Pruss A, Gobel UB, Pauli G, Kao M, Seibold M, Monig HJ, et al. Peracetic acid–ethanol treatment of allogeneic avital bone tissue transplants – a reliable sterilization method. Ann Transplant 2003;8:34–42.

[12] Pruss A, Perka C, Degenhardt P, Maronna U, Buttner-Janz K, Paul B, et al. Clinical efficacy and compatibility of allogeneic avital tissue transplants sterilized with a peracetic acid/ethanol mixture. Cell Tissue Bank 2002;3:235–43.

[13] Franks F. Freeze-drying of bioproducts: putting principles into practice. Eur J Pharm Biopharm 1998;45:221–9.

[14] Galea G, Kearney JN. Clinical effectiveness of processed and unprocessed bone. Transfus Med 2005;15:165–74.

[15] Conrad EU, Ericksen DP, Tencer AF, Strong DM, Mackenzie AP. The effects of freeze-drying and rehydration on cancellous bone. Clin Orthop Relat Res 1993;279–84.

[16] Cornu O, Banse X, Docquier PL, Luyckx S, Delloye C. Effect of freeze-drying and gamma irradiation on the mechanical properties of human cancellous bone. J Orthop Res 2000;18:426–31.

[17] Nather A, Thambyah A, Goh JC. Biomechanical strength of deep-frozen versus lyophilized large cortical allografts. Clin Biomech (Bristol, Avon) 2004;19:526–33.

[18] An YH. Mechanical properties of bone. In: An YH, Draughn RA, editors. Mechanical testing of bone and the bone–implant interface. Boca Raton: CRC Press; 2000. p. 41–64.

[19] Lewandrowski KU, Bonassar L, Uhthoff HK. Mechanical properties of perforated and partially demineralized bone grafts. Clin Orthop Relat Res 1998;238–46.

[20] Callister WD. Materials science and engineering, an introduction. 5th ed. New York: John Wiley & Sons, Inc.; 1999.

[21] Actis AB, Obwegeser JA, Ruperez C. Influence of different sterilization procedures and partial demineralization of screws made of bone on their mechanical properties. J Biomater Appl 2004;18:193–207.

[22] Akkus O, Rimnac CM. Fracture resistance of gamma radiation sterilized cortical bone allografts. J Orthop Res 2001;19:927–34.

[23] Scheffler SU, Scherler J, Pruss A, von Versen R, Weiler A. Biomechanical comparison of human bone–patellar tendon–bone grafts after sterilization with peracetic acid ethanol. Cell Tissue Bank 2005;6:109–15.

[24] Pelker RR, Friedlaender GE, Markham TC. Biomechanical properties of bone allografts. Clin Orthop Relat Res 1983;54–7.

[25] Simonian PT, Conrad EU, Chapman JR, Harrington RM, Chansky HA. Effect of sterilization and storage treatments on screw pullout strength in human allograft bone. Clin Orthop Relat Res 1994;290–6.

[26] Pietrzak WS, Woodell-May J. The composition of human cortical allograft bone derived from FDA/AATB-screened donors. J Craniofac Surg 2005;16:579–85.

This is a preprint of an article submitted to Acta Biomaterialia

Characterization of zinc-releasing three dimensional bioactive glass scaffolds and their effect on human adipose stem cell proliferation and osteogenic differentiation

Suvi Haimi[a], Giada Gorianc[b], Loredana Moimas[b,c], Bettina Lindroos[a], Heini Huhtala[d], Sari Räty[e], Hannu Kuokkanen[f], George K. Sándor[a], Chiara Schmid[b], Susanna Miettinen[a,*], Riitta Suuronen[a,g,h,*]

Corresponding author: Suvi Haimi

[a]*Regea Institute for Regenerative Medicine, University of Tampere, Tampere, Finland*
[b]*Department of Materials and Natural Resources, University of Trieste, Trieste, Italy*
[c]*Inion Oy, Tampere, Finland*
[d]*Tampere School of Public Health, University of Tampere, Tampere, Finland*
[e]*Department of Gastroenterology and Alimentary Tract Surgery, Tampere University Hospital, Tampere, Finland*
[f]*Department of Plastic Surgery of Tampere University Hospital, Tampere, Finland*
[g]*Department of Eye, Ear and Oral Diseases, Tampere University Hospital, Tampere, Finland*
[h]*Department of Biomedical Engineering, Tampere University of Technology, Tampere, Finland*
**Equal contribution*

Abstract

While the addition of Zinc ions to bioactive ceramics has been shown to enhance the proliferation and osteogenic differentiation of osteoblasts-like cells, contradictory results also exist. Therefore, the effect of zinc-releasing ceramics on cell proliferation and differentiation into osteogenic lineages requires further clarification. The aim of this study was to evaluate the effects of zinc addition on degradation profile of three dimensional bioactive glass scaffold, and on osteogenesis and proliferation of human adipose stem cells (hASC)s in these scaffolds. Bioactive glass scaffolds with the general composition of Na_2O, K_2O, MgO, CaO, B_2O_3, TiO_2, P_2O_5 and SiO_2 were prepared. The degradation was evaluated by scanning electron microscopy and elemental analysis. hASC viability, attachment, and proliferation were assessed with Live/dead staining, SEM imaging and DNA content measurement. The osteogenic differentiation of hASCs was analyzed by determination of alkaline phosphatase activity and osteopontin concentration. Degradation profile of bioactive glass was shown to slow down with the addition of zinc. The in vitro tests demonstrated that zinc addition to bioactive glass inhibited, although not significantly, the proliferation, ALP activity, and osteopontin production of hASCs at 2 weeks compared to control composition scaffolds. Our results suggest that the addition of zinc on bioactive glass inhibits osteostimulative properties of bioactive glass by slowing down its degradation rate.

1. Introduction

Zinc is known to play an important role in bone metabolism; its stimulatory effect on bone formation and its ability to promote the expression and maintenance of osteoblastic phenotypes has been shown in vitro [1-3]. Alimentary zinc diet depletion or supplementation has been shown to be responsible for variations in body weight, bone length and bone biomechanical properties in growing rats. The positive effect of zinc on bone metabolism has been associated with growth hormone (GH) or insulin-like growth factor 1 (IGF-1) [4].

Despite the numerous works reporting stimulating effects of zinc, there are also studies that show contradictory data on the effects of zinc ions on bone cells. Popp *et al*. studied the effect of Zn^{2+} supplemented osteogenic medium on osteoblastic proliferation and differentiation. They used concentrations of 0.20 mg/l, 0.65 mg/l and 2.62 mg/l and found no significant effects of such zinc amounts on rat bone marrow stromal cells [5]. Wang *et al.* have shown that the effect of zinc on the osteogenic and adipogenic differentiation of mouse primary bone marrow stromal cells (MSCs) and on the adipogenic trans-differentiation of mouse primary osteoblasts depends on ion concentration and incubation time, with zinc even having an inhibitory effect [6].

The use of synthetic bone substitutes for delivery of zinc ions has recently gained attention in research communities. There are numerous studies regarding the development and evaluation of zinc containing calcium phosphate ceramics both in vitro and in vivo [1,2,7-9]. There are also reports concerning the use of different bioactive glass compositions as short or long term zinc delivery vehicles [10-13].

Bioactive glass, due to its osteostimulative and bone bonding properties, has in fact been successfully used clinically in dental, craniomaxillofacial, and spine applications during the last few decades [14-19]. Its bone-bonding ability arises from the high rate of formation of hydroxyl-carbonate apatite (HCA) at the surface of the material after reaction with the surrounding biological fluids [20,21]. The bone-like, low crystalline HCA, together with the ionic products resulting from the degradation process of the material, are also correlated to the intrinsic and characteristic bioactive glass bone regeneration potential. They have been shown to be responsible for enhancing the proliferation and differentiation of osteoprogenitor cells [22].

There are number of bioactive glass compositions that have been investigated as possible zinc ion delivery vehicles. It has been proposed that due to the incorporation of zinc ions in the forming HCA layer, bioactive glass allows a tailored modulation of zinc release in the biological system, hence, avoiding the cytotoxicity related problems observed with the zinc containing calcium phosphate materials described above [23,24]. Despite the incorporation mechanism of zinc ions in HCA, the importance of the dosage as well as the possible cytotoxic effect of the zinc ion have also been reported for certain bioactive glass and glass-ceramic compositions [2,10].

There are many in vitro studies of the analysis of the zinc effect on cells, from rat to human, and from primary bone marrow stromal cells to osteoblasts. However, no prior study has involved the use of human adipose stem cells (hASCs), which have emerged as an attractive source of multipotent cells. They have shown ability to differentiate into osteogenic lineages in vitro [25,26] and have also been used to treat bone defects in clinical cases [27,28]. Additionally, the procurement of hACS is easy; their expansion in vitro is rapid and their harvest yield is approximately 40-fold higher compared to bone marrow mesenchymal stem cells[29].

Since there is much debate on the effects of zinc on cell proliferation and osteogenic differentiation, there is a clear need for more research to be carried out. Additionally, because zinc has been shown to favour crystallization of bioactive glass at lower temperatures with respect to zinc free glass [23,30], the effect of the ion on the manufacturing of zinc containing bioactive glass three dimensional (3-D) scaffolds also needs to be analyzed. This report represents the first attempt to verify the possibility of manufacturing zinc containing porous bioactive glass scaffolds suitable for bone tissue engineering applications and study the effect of zinc addition on construct degradation, osteogenic differentiation and proliferation of hASCs.

2. Materials and methods

2.1. Scaffold manufacturing

Bioactive glass with a composition of 10-12 mol% Na_2O, 10-12 mol% K_2O, 4-6 mol% MgO, 10-18 mol% CaO, 1-4 mol% P_2O_5, 1-2 mol% B_2O_3, 0-1 mol% TiO_2, 50-56 mol% SiO_2, and ZnO 0-5 mol% was manufactured. The family used in this study included glasses with 0, 0.25, 0.5, 1.0, 1.5, 2.0 and 5.0 mol% of ZnO, substituting CaO. In the cell culture experiments only 0, 0.25, and 1.0 mol% zinc containing bioactive glass scaffolds were studied. The glass manufacturing process consisted of melting of the reagents in a covered platinum crucible above 1360ºC, cooling down to room temperature, crushing, and remelting in order to get better material homogenization. The glass was then used for the manufacturing of 3 mm long and 75 μm thick bioactive glass fibres by melt spinning. The collected fibres were further packed into metallic moulds and sintered to obtain three-dimensional scaffolds with the desired structural and mechanical characteristics. Scaffolds with dimensions of 14 mm x 14 mm x 5 mm were used in the cell culture experiments.

Scaffolds characterized by a total porosity of 70% were chosen for the study based on the previous study of our group, where this porosity was shown to be suitable for hASC proliferation and osteogenic differentiation [31]. In addition, the same porosity was previously studied with respect to degradation [32], and in vivo behaviour [33].

2.2 Material and 3-D scaffold characterization

The compositional variation effect on the structure of the material was evaluated by Raman spectroscopy (S1000, Renishaw, New Mills, UK) and by Fourier Transform Infrared Attenuated Total Reflectance Spectroscopy (Perkin Elmer, Waltham, USA) with respect to eventually forming crystallites.

The effect of zinc addition on the degradation behaviour of the material was evaluated both in deionized water and in simulated body fluid (SBF). 110 mg of chopped fibres of the different compositions were immersed in 110 ml of deionized water and incubated at 37ºC for 0.5, 4, 12, 24 and 72 hours. At the time point, the fluid was filtered and the amounts of Zn^{2+}, Ca^{2+}, K^{+}, Mg^{2+} ions were identified by atomic absorption spectroscopy (AAS) (Perkin Elmer). The scaffolds were immersed and incubated in SBF [34] at 37ºC for different follow-up times (t=1h, 8h, 1d, 3d, 1w, 2w, 3w) with a surface area to volume ratio corresponding to 0.2 cm^{-1}. After the immersion, the scaffolds were gently washed by deionized water, flushed with ethanol and dried under laminar flow. The degradation was evaluated by scanning electron microscopy (SEM) (Stereoscan 430, Leica, Solms Germany). Elemental analysis (EDX Oxford Link, coupled to microscope)

was also performed to confirm the presence of the surface calcium phosphate layer. Fibres with diameters between min 0.25 and max 1 mm were immersed in SBF and incubated at 37ºC for different times (1, 3, 7 and 14 days). At each time point the fibres were washed with deionized water, flushed with ethanol and dried out. The fibres were weighed both before and after the immersion and the weight was recorded.

2.3. hASC isolation and culture

hASCs were isolated from adipose tissue samples obtained in surgical procedures from 9 patients (9 donors, mean age=48±9 years). The adipose tissue samples were received from the Department of Plastic Surgery and from the Department of Gastroenterology and Alimentary Tract Surgery, Tampere University Hospital. hASCs were isolated, cultured, and characterized by flow cytometric surface marker expression analysis as described previously [31].

2.4. Cell attachment, viability and morphology evaluation

Live/dead staining was used to assess hASC attachment and viability at 3 hours and 2 weeks as described previously [31]. Briefly, the viable cells (green fluorescence) and dead cells (red fluorescence) were studied using a fluorescence microscope after 45 min incubation in a mixture of 5 µM CellTracker™ green (5-chloromethylfluorescein diacetate [CMFDA]; Molecular Probes, Eugene, OR, USA) and 2.5 µM Ethidium Homodimer-1 (EH-1; Molecular Probes). The cell morphology was assessed at 2 weeks from a gold–palladium coated specimens by using SEM (Jeol JSM-5500, Sundbyberg, Sweden) as previously described [31].

2.5. Cell proliferation, quantitative analysis of alkaline phosphatase (ALP) activity and ALP staining

Cell proliferation was quantified using a CyQUANT® Cell proliferation assay kit (Molecular Probes, Invitrogen, Paisley, UK) as described earlier [35]. After 1 and 2 weeks in culture, ALP activity was determined as reported earlier [31]. At 2 weeks the hASC-biomaterial constructs were stained with a leukocyte ALP kit (Sigma-Aldrich, St. Louis, MO, USA) according to the manufacturer's protocols.

2.6. Human osteopontin immunoassay

Osteopontin was measured using the Quantikine® Human Osteopontin Immunoassay (RD Systems Europe Ltd, Abingdon, UK) according to the manufacturer's protocols. The fluorescence was measured in a microplate reader (Victor 1420).

2.7. Statistical analysis

All data was provided as mean ± standard deviation and $p < 0.05$ was considered significant. Statistical analysis of the results was performed with SPSS, version 13. The effect of culturing time was analyzed using a paired Student's *t*-test. The effect of zinc addition on the proliferation of hASCs, ALP activity and osteopontin concentration were compared using a one-way ANOVA, after checking for normal distribution and homogeneity of variance. Post hoc tests were performed to detect significant differences between groups. The experiments were repeated three to four times.

3. Results

3.1. Glass structure analysis

Both FTIR-ATR and Raman spectroscopy analysis showed that despite the introduction of ZnO up to 5%, no crystalline formation was seen in any spectra (Fig 1A). The glass structure even at the highest zinc substitution percentage was characterized by the characteristic bioactive glass vibrational bands.

3.2. Ion release AAS analysis

The release of alkaline earth ions, i.e. Ca and Mg was dependent on the amount of zinc in the glass and on the immersion time. In particular, the amount of released ions increased with the immersion time and it was in inverse relation with the amount of substituted zinc (Figs. 1B and 1C). The release of potassium was, on the contrary, independent from the amount of zinc and less dependent on immersion time than the alkaline earth ions (Fig. 1D). The amount of released zinc in the solution was proportional to the amount of zinc in the material (Fig. 1F). However, when the amount was rationalized with respect to the substituted zinc percentage, the ability of the material to release zinc ions was in an inverse relationship with the amount of zinc in the glass (Fig. 1E).

3.2. Immersion in simulated body fluid

The weight variation of the fibres immersed in SBF was inversely related to the amount of zinc in the material (Fig. 2A); in particular, only one 0.25% zinc containing fibre and none 0.5% zinc concentration fibres were left at the 14 day time point because all the others had degraded almost completely.

Scaffolds immersed in SBF showed an inhibitory effect of zinc ions on the degradation process and on the HCA formation. The samples containing 5 mol% of zinc presented only after 2 weeks immersion time a homogeneous, thin, amorphous calcium phosphate layer (Fig. 2B). At the same time point the samples characterized by 0.25 and 0.5 mol% zinc presented a thick HCA layer with significant degradation of the core of each fibre. (Fig. 2C) This resulted in a considerably alkaline and alkaline earth ions depleted glass, as evidenced by the elemental analyses (Figs. 2D, 2E). Figure 2D shows weak peaks corresponding to zinc, however, it is not possible to know if the zinc signal is due to Zn^{2+} ions included in the developing HCA layer or to the Zn^{2+} ions present in the underlying core glass.

3.3. Surface marker analysis

Based on the flow cytometric analysis of hASCs, positive surface marker expression was seen for the adhesion molecules CD9, CD29, CD34, CD49d, CD105, and CD166; receptor molecule CD44; surface enzymes CD10 and CD13; extracellular matrix protein CD90; complement regulatory protein CD59. hASCs showed moderately positive expression of putative stem cell marker STRO-1; major histocompatibility class I antigen HLA-ABC and fibroblast marker hFSP. Furthermore, hASCs were negative for the haematopoietic markers CD31 and CD45 and the vascular cell adhesion molecule CD106. These results were consistent with the literature [29,36].

3.4. Cell attachment and growth

Live/Dead staining was used to evaluate the viability of the cells. Live/Dead staining showed no dead cells at 3 hours on any studied scaffold type (Figs. 3A, C, E). The hASCs were more evenly spread on control composition scaffolds than on zinc scaffolds (Figs. 3B, D, F). The hASCs were clustered to the pointing parts of glass fibres especially on 0.25 and 1 mol% zinc scaffolds at 2 weeks. The majority of the hASCs were viable and there were only a few dead cells on each scaffold type after 2 weeks in culture. When qualitatively analysed, the cell density was higher in control composition scaffolds compared to zinc scaffolds at 2 weeks. The number of cells was increased at 2 weeks on each scaffold type compared to 3 hours.

3.5. Cell morphology

SEM imaging was used to examine the morphology of the cells. Figures 4A-F present SEM micrographs of hASCs on the 0.25 mol% zinc (4A, B), 1.0 mol% zinc (4C, D) and control composition bioactive glass scaffolds (4E, F). The cell morphology appeared unaffected by zinc addition. hASCs were well spread across all the 3-D scaffolds and showed elongated phenotype. Figures 4A, C and E demonstrate hASCs elongating along the fibres and forming bridges from one glass fibre to another on the surface of the scaffolds.

3.6. hASC proliferation and differentiation

To test the effects of zinc concentration on cell proliferation the total DNA content was measured. There were no significant differences between the three types of scaffolds (Fig. 5A). Control composition scaffold had significantly greater number of cells at 2 weeks ($p=0.013$) compared to 1 week.

Concurrent measurement of ALP activity and osteopontin concentration indicated early osteogenic differentiation, but did not reveal any stimulatory effect of zinc addition (Figs. 5B, C). In contrast, the ALP activity on control composition scaffolds was over 30% higher than on 1 mol% zinc scaffolds. The ALP activity as well as the DNA content of hASCs was significantly increased at 2 weeks compared to that at the 1 week in control composition scaffolds ($p=0.023$). No differences were observed in ALP staining (data not shown).

4. Discussion

The aim of this study was to investigate the effect of zinc addition on bioactive glass scaffold manufacturing, on their degradation, and on hASC attachment, proliferation, and osteogenic differentiation. The main concern was related to the substitution of CaO with ZnO to the bioactive glass, which was presumed to be related to the the change in the working range of the material. The main limitation of many bioactive glass compositions is their very limited working range with consequent crystallization of the material if thermally treated leading to significant modification of their bioactive properties. In the present study, no crystallization was observed even with the addition of 5% of ZnO, and glass fibres and production of completely amorphous 3-D scaffolds was successful. The Raman spectra in Fig. 1A, showed, in fact, the characteristics bioactive glass broad bands [37].

- 560-650 (cm^{-1}): Bond rocking vibration
  Oxygen atoms move perpendicularly at the Si-O-Si plane;
- 750-800 (cm^{-1}) weak: Bond bending vibration

Oxygens move perpendicularly to the Si-Si lines and Si-O-Si planes;

- 900-980 (cm^{-1}): Non bridging Si-O bonds (NBO)
  This bond is not in glass with a high content of silica and Hench demonstrated that it has an important role in the bioactivity [34]. These oxygen atoms do not do a bridge between network silica atoms breaking the continuity of the lattice.
- 1000-1200 (cm^{-1}): Asymmetric stretching mode O-Si-O bonds (BO)
  The oxygen that bridge two silica atoms moves parallel to the Si-Si line in the opposite direction of the near Si.

The effect of ZnO on the structure was followed when the areas below the BO and NBO vibrational bands were measured and the ratio between the BO and NBO values calculated for each composition. Despite the absence of statistical significance, the resultant ratio was inversely proportional to the amount of ZnO in the material. This means that zinc tends to act as network modifier in a stronger fashion than the Ca ions. However, this technique does not allow determination of what proportion of the Zn^{2+} ions act as network former, making the glass more durable, and in what proportion they act as network modifier.

Such information was collected by the analysis of the weight variation of fibres after immersion in SBF. Despite the differences in dimensions of the fibres used, as the weight variation was normalized to the surface area of the fibres, Fig. 2A gives us clear information on the stabilizing effect of zinc on the glass structure. Higher glass durability was also confirmed by the SEM analysis of the scaffolds after immersion in SBF. In fact, as expected, not only the degradation of the material is strongly retarded and the fibres appear to be only surface degraded after 14 days of immersion, but also HCA formation results delayed with time.

The information collected on the degradation behaviour of the zinc containing fibres and scaffolds was completed by the AAS analysis on the solution containing the degradation products. Interestingly, the substitution of CaO with ZnO did not seem to affect the release of alkali from the glass (see Fig. 1D), while being inversely proportional to the release of larger alkaline earth ions (Fig. 1B and 1C) and directly proportional to the release of zinc (Fig. 1E). This could be explained by ZnO acting both as network former and network modifier, which concurs with the Raman spectroscopy analysis and with the qualitative SEM analysis results.

The AAS data gave us valuable background information also for evaluation of the effect of the scaffolds on the hASCs. From the literature it is known that certain zinc concentrations can be cytotoxic to different cell types. Yamamoto et al. found that zinc concentration of 5.89 mg/l inhibits normal osteoblast function [38]. Ito et al. studied zinc doped β-tricalcium phosphate (ZnTCP) and showed that zinc released from the ZnTCP/AP ceramics significantly increased the proliferation of osteoblastic MC3T3-E1 cells with zinc release up-limit already at 3.53 mg/l when compared to those free from zinc [2]. Based on these results, 3-D scaffolds containing 0.25 and 1.0 mol% of ZnO were chosen for the in vitro culture with hASCs, to ensure that the cytotoxic limit of 3.53 mg/l was avoided.

As can be seen in Fig 1E, for zinc concentration below 1 mol%, the maximum amount of ions released in deionized water after 72 hours is approximately 0.01 mg/l. The immersion fluid did affect the degradation behaviour of the material but it was estimated that deionized water acts as worst situation environment if compared to SBF as it does not have any pH buffering ability. In addition, the AAS results relate to the immersion of 1 mg of material in 1 ml of medium while in the cell culture study

approximately 100 mg of material was immersed in 1 ml of medium. Based on the assumption that the surface area of the samples immersed in deionized water was comparable or higher than the one of the sintered sample, it was estimated that the maximum amount of Zn^{2+} ions in the solution in contact with the cells was below 1.0 mg/l, therefore far below the cytotoxic limit mentioned above [2].
Du et al. reported a stimulatory effect of ZnO in glass-ceramic on the proliferation of rat osteoblasts and they used similar concentrations of zinc (Zn^{2+} concentration released from zinc-containing glass-ceramic 0.235 mg/l and 0.915 mg/l) as we did [11]. Ishikawa et al. demonstrated that apatite cement that contained 5 wt% ZnTCP (zinc release 0.075 mg/l) had a significantly higher proliferation profile when compared to apatite cement with 0 wt% ZnTCP [7]. Limitation of both of these studies was that only the proliferation was evaluated with a short observation period of only 1 week. In contrast to these studies, Popp et al. did not find any effect of supplementing culture medium with soluble zinc on proliferation and osteogenic differentiation of osteoprogenitor cells. They concluded that sufficient amount of zinc for cell proliferation and differentiation is provided in normal serum [5]. In our study zinc addition to bioactive glass (maximum zinc release below 1.0 mg/l) decreased the cell number at 2 weeks compared to control composition as shown in Fig. 5A. However, there was only a minor difference in DNA content when compared to the control composition scaffolds. Furthermore zinc containing scaffolds inhibited, although not significantly, the ALP activity of hASCs at 2 weeks compared to control composition scaffolds. The osteopontin concentration was also higher in control composition scaffolds than in zinc scaffolds.
Possible explanations of the hASCs results obtained in this study can be derived from the material and degradation studies described previously. Bioactive glass degradation products are known to be responsible for the osteostimulative properties of the material [22,39,40]. Zinc-free 3-D bioactive glass fibre scaffolds with the same structural characteristics as the ones used in the present study have been shown to increase hASC proliferation and osteogenic differentiation in our previous study [31]. Zinc was verified to slow down the degradation of the material, and in particular it was shown that the amount of degradation products was inversely proportional to the amount of zinc in the material (Figs. 1B-D). It can therefore be deduced that the presence of zinc slows down the construct degradation in such a way that the intrinsic osteostimulative effect of the material is inhibited. This conclusion is not in contrast with the stimulatory effect of zinc ions. On the contrary, it gives additional information on the dependence of the results on the material used for the in situ release of the stimulant. In particular, in the present study CaO was substituted with ZnO, allowing the molar percentage of all other components to be constant. In the work of Aina et al. [10] 45S5 bioactive glass was modified with the addition of ZnO in such a way that the amount of all components was adjusted and in particular SiO_2 varied from 45 wt% to 37 wt%. This way the authors significantly modified the durability of the original glass and at least partially compensated the effect of ZnO as a degradation inhibitor. It can be expected that the stimulatory effect of zinc ions could be seen on hASCs if 3-D scaffolds with a tailored faster degrading composition would have been chosen.

5. Conclusions

The study showed that it is possible to manufacture 3-D amorphous porous zinc-containing bioactive glass scaffolds and that zinc has a clear inhibitory effect on the

degradation properties of the implants. With regards to the in vitro cell study, the ALP activity in control composition scaffolds was over one third higher than in 1 mol% zinc scaffolds at 2 weeks. The proliferation also decreased at 2 weeks in zinc-releasing scaffolds compared to control composition scaffolds. Furthermore, in Live/Dead staining confirmed that the cell number was qualitatively analyzed higher in control composition scaffolds. We can therefore conclude that the effect of zinc addition on the bioactive glass inhibited the osteostimulative properties of the material by slowing down its degradation profile. Additional studies are required to verify the possibility of 3-D scaffolds as local delivery systems of zinc and other materials with tailored composition**.**

Acknowledgements
I would like to thank Ms. Miia Juntunen and Ms. Minna Salomäki for their excellent technical assistance. Special thanks to Professor Lauri Pelliniemi, MD, PhD from Laboratory of Electron Microscopy, University of Turku for the assistance with SEM imaging. This research was supported by the competitive research grants from the Pirkanmaa Hospital District, the Finnish Funding Agency for Technology and Innovation (TEKES), the Finnish Cultural Foundation and the City of Tampere.

References

[1] Ikeuchi M, Ito A, Dohi Y, Ohgushi H, Shimaoka H, Yonemasu K, Tateishi T. Osteogenic differentiation of cultured rat and human bone marrow cells on the surface of zinc-releasing calcium phosphate ceramics. J Biomed Mater Res A 2003; 67: 1115-22.

[2] Ito A, Ojima K, Naito H, Ichinose N, Tateishi T. Preparation, solubility, and cytocompatibility of zinc-releasing calcium phosphate ceramics. J Biomed Mater Res 2000; 50: 178-83.

[3] Yamaguchi M, Oishi H, Suketa Y. Stimulatory effect of zinc on bone formation in tissue culture. Biochem Pharmacol 1987; 36: 4007-12.

[4] Ovesen J, Moller-Madsen B, Thomsen JS, Danscher G, Mosekilde L. The positive effects of zinc on skeletal strength in growing rats. Bone 2001; 29: 565-70.

[5] Popp JR, Love BJ, Goldstein AS. Effect of soluble zinc on differentiation of osteoprogenitor cells. J Biomed Mater Res A 2007; 81: 766-9.

[6] Wang T, Zhang JC, Chen Y, Xiao PG, Yang MS. Effect of zinc ion on the osteogenic and adipogenic differentiation of mouse primary bone marrow stromal cells and the adipocytic trans-differentiation of mouse primary osteoblasts. J Trace Elem Med Biol 2007; 21: 84-91.

[7] Ishikawa K, Miyamoto Y, Yuasa T, Ito A, Nagayama M, Suzuki K. Fabrication of Zn containing apatite cement and its initial evaluation using human osteoblastic cells. Biomaterials 2002; 23: 423-8.

[8] Kawamura H, Ito A, Miyakawa S, Layrolle P, Ojima K, Ichinose N, Tateishi T. Stimulatory effect of zinc-releasing calcium phosphate implant on bone formation in rabbit femora. J Biomed Mater Res 2000; 50: 184-90.

[9] Kawamura H, Ito A, Muramatsu T, Miyakawa S, Ochiai N, Tateishi T. Long-term implantation of zinc-releasing calcium phosphate ceramics in rabbit femora. J Biomed Mater Res A 2003; 65: 468-74.

[10] Aina V, Perardi A, Bergandi L, Malavasi G, Menabue L, Morterra C, Ghigo D. Cytotoxicity of zinc-containing bioactive glasses in contact with human osteoblasts. Chem Biol Interact 2007; 167: 207-18.

[11] Du RL, Chang J, Ni SY, Zhai WY, Wang JY. Characterization and in vitro bioactivity of zinc-containing bioactive glass and glass-ceramics. J Biomater Appl 2006; 20: 341-60.

[12] Kamitakahara M, Ohtsuki C, Inada H, Tanihara M, Miyazaki T. Effect of ZnO addition on bioactive CaO-SiO2-P2O5-CaF2 glass-ceramics containing apatite and wollastonite. Acta Biomater 2006; 2: 467-71.

[13] Lusvardi G, Malavasi G, Menabue L, Menziani MC, Pedone A, Segre U, Aina V, Perardi A, Morterra C, Boccafoschi F, Gatti S, Bosetti M, Cannas M. Properties of zinc releasing surfaces for clinical applications. J Biomater Appl 2008; 22: 505-26.

[14] Aho AJ, Suominen E, Alanen A, Yli-Urpo A, Knuuti J, Aho HJ. Remodeling of the tibia after grafting of a large cavity with particulate bioactive glass-hydroxylapatite--case report on treatment of fibrous dysplasia with 13 years' follow-up. Acta Orthop Scand 2003; 74: 766-70.

[15] Anderegg CR, Alexander DC, Freidman M. A bioactive glass particulate in the treatment of molar furcation invasions. J Periodontol 1999; 70: 384-7.

[16] Elshahat A, Shermak MA, Inoue N, Chao EY, Manson P. The use of Novabone and Norian in cranioplasty: a comparative study. J Craniofac Surg 2004; 15: 483-9.
[17] Lovelace TB, Mellonig JT, Meffert RM, Jones AA, Nummikoski PV, Cochran DL. Clinical evaluation of bioactive glass in the treatment of periodontal osseous defects in humans. J Periodontol 1998; 69: 1027-35.
[18] Merwin GE. Bioglass middle ear prosthesis: preliminary report. Ann Otol Rhinol Laryngol 1986; 95: 78-82.
[19] Peltola M, Kinnunen I, Aitasalo K. Reconstruction of orbital wall defects with bioactive glass plates. J Oral Maxillofac Surg 2008; 66: 639-46.
[20] Hench LL, Splinter RJ, Allen WC. Bonding Mechanism at the interface of ceramic prosthetic materials. J Biomed Mater Res Symposium 1971; 2: 117-41.
[21] Kokubo T, Ito S, Huang ZT, Hayashi T, Sakka S, Kitsugi T, Yamamuro T. Ca,P-rich layer formed on high-strength bioactive glass-ceramic A-W. J Biomed Mater Res 1990; 24: 331-43.
[22] Ducheyne P, Qiu Q. Bioactive ceramics: the effect of surface reactivity on bone formation and bone cell function. Biomaterials 1999; 20: 2287-303.
[23] Du RL, Chang J. The influence of Zn on the deposition of HA on sol-gel derived bioactive glass. Biomed Mater Eng 2006; 16: 229-36.
[24] Jaroch DB, Clupper DC. Modulation of zinc release from bioactive sol-gel derived SiO(2)-CaO-ZnO glasses and ceramics. J Biomed Mater Res A 2007; 82: 575-88.
[25] Zuk PA, Zhu M, Ashjian P, De Ugarte DA, Huang JI, Mizuno H, Alfonso ZC, Fraser JK, Benhaim P, Hedrick MH. Human adipose tissue is a source of multipotent stem cells. Mol Biol Cell 2002; 13: 4279-95.
[26] Zuk PA, Zhu M, Mizuno H, Huang J, Futrell JW, Katz AJ, Benhaim P, Lorenz HP, Hedrick MH. Multilineage cells from human adipose tissue: implications for cell-based therapies. Tissue Eng 2001; 7: 211-28.
[27] Lendeckel S, Jodicke A, Christophis P, Heidinger K, Wolff J, Fraser JK, Hedrick MH, Berthold L, Howaldt HP. Autologous stem cells (adipose) and fibrin glue used to treat widespread traumatic calvarial defects: case report. J Craniomaxillofac Surg 2004; 32: 370-3.
[28] Mesimäki K, Lindroos B, Törnwall J, Lindqvist C, Kontio R, Miettinen S, Suuronen R. Novel Maxillary Reconstruction with Ectopic Bone Formation by GMP Adipose Stem Cells. Tissue Engineering part A Submitted.
[29] Strem BM, Hicok KC, Zhu M, Wulur I, Alfonso Z, Schreiber RE, Fraser JK, Hedrick MH. Multipotential differentiation of adipose tissue-derived stem cells. Keio J Med 2005; 54: 132-41.
[30] Malavasi G, Lusvardi G, Pedone A, Menziani MC, Dappiaggi M, Gualtieri A, Menabue L. Crystallization kinetics of bioactive glasses in the ZnO-Na2O-CaO-SiO2 system. J Phys Chem A 2007; 111: 8401-8.
[31] Haimi S, Moimas L, Pirhonen E, Lindroos B, Huhtala H, Räty S, Kuokkanen H, Sándor GK. Calcium phosphate surface treatment of bioactive glass causes a delay in early osteogenic differentiation of adipose stem cells J Biomed Mater Res Part A In press.
[32] Moimas L, Markkula K, Schmid C, Pirhonen E, 2004. Three-dimensional Porous Bioactive Glass Fibre Scaffolds, FluidDynamic and Geometrical Characterization. In 9th Ceramics, Cells and Tissues - Materials for Tissue

Engineering, Chemistry and Microstructure: The Role for Ceramics. Consiglio Nazionale Delle Ricerche, Faenza, Italy.

[33] Moimas L, Biasotto M, Di Lenarda R, Schmid C, 2006. In situ Tissue Engineering, effect of a porous bioactive glass scaffold on bone healing: in vivo rabbit study. In 10th Ceramics, Cells and Tissues - Materials for Tissue Engineering, Chemistry and Microstructure: The Role for Ceramics. Consiglio Nazionale Delle Ricerche, Faenza, Italy.

[34] Kokubo T, Kushitani H, Sakka S, Kitsugi T, Yamamuro T. Solutions able to reproduce in vivo surface-structure changes in bioactive glass-ceramic A-W. J Biomed Mater Res 1990; 24: 721-34.

[35] Lindroos B, Maenpaa K, Ylikomi T, Oja H, Suuronen R, Miettinen S. Characterisation of human dental stem cells and buccal mucosa fibroblasts. Biochem Biophys Res Commun 2008; 368: 329-35.

[36] Gimble J, Guilak F. Adipose-derived adult stem cells: isolation, characterization, and differentiation potential. Cytotherapy 2003; 5: 362-9.

[37] Gonzalez P, Serra J, Liste S, Chiussi S, Leon B, Perez-Amor M. Raman spectroscopic study of bioactive silica based glasses. Journal of Non-Crystalline Solids 2003 320: 92-9

[38] Yamamoto A, Honma R, Sumita M. Cytotoxicity evaluation of 43 metal salts using murine fibroblasts and osteoblastic cells. J Biomed Mater Res 1998; 39: 331-40.

[39] Välimäki VV, Yrjans JJ, Vuorio EI, Aro HT. Molecular biological evaluation of bioactive glass microspheres and adjunct bone morphogenetic protein 2 gene transfer in the enhancement of new bone formation. Tissue Eng 2005; 11: 387-94.

[40] Xynos ID, Hukkanen MV, Batten JJ, Buttery LD, Hench LL, Polak JM. Bioglass 45S5 stimulates osteoblast turnover and enhances bone formation In vitro: implications and applications for bone tissue engineering. Calcif Tissue Int 2000; 67: 321-9.

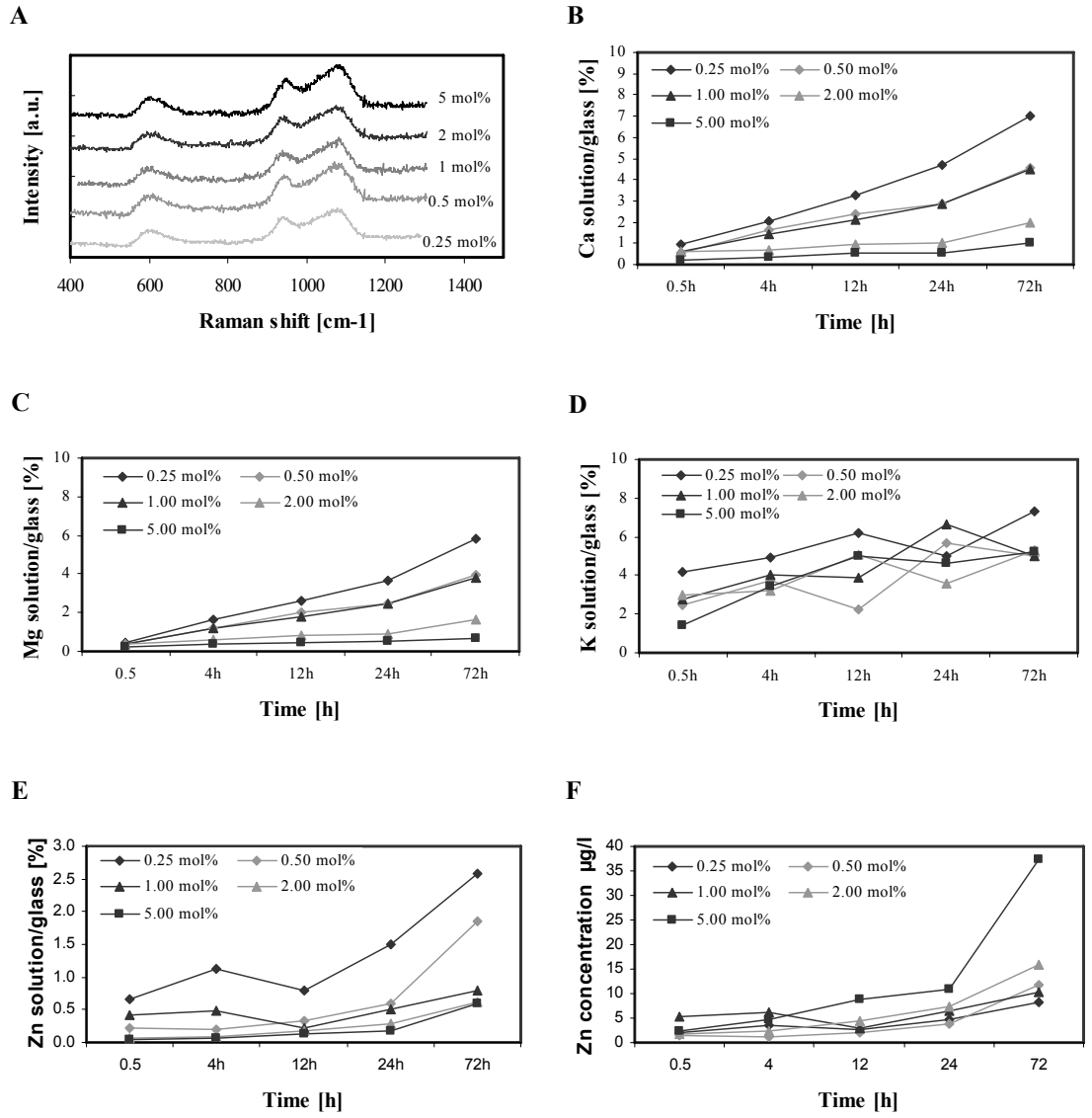

Fig. 1. (A) Effect of ZnO addition on bioactive glass structure: Raman spectra. (B) Effect of ZnO on calcium release. (C) Effect of ZnO on magnesium release. (D) Effect of ZnO on potassium release. (E) Effect of ZnO on zinc release. (F) Total amount of zinc released in the solution.

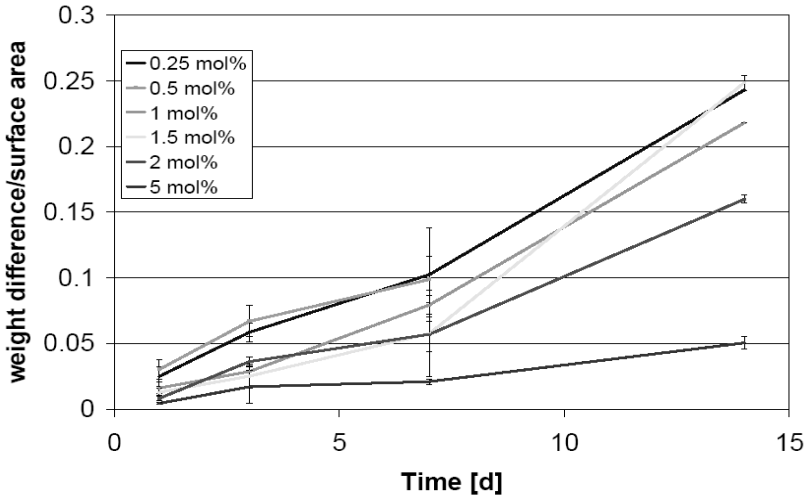

Fig. 2. (A) The weight variation of the fibres immersed in SBF.

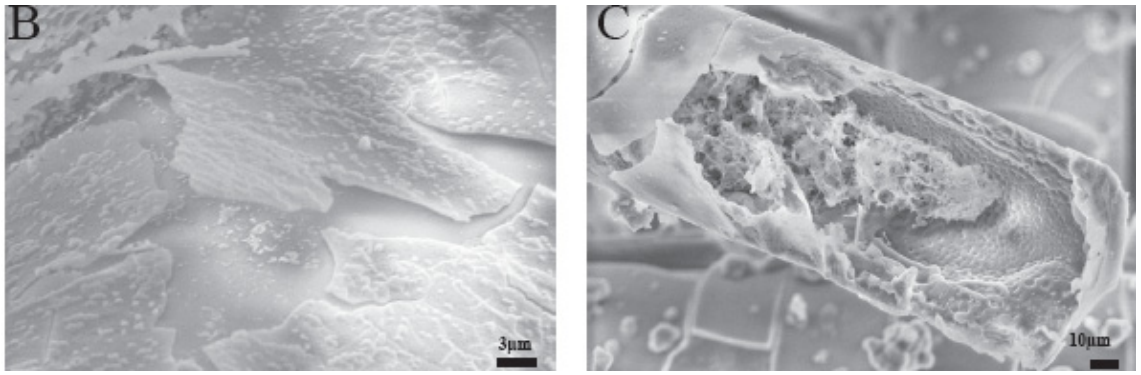

Fig. 2. (B) Thin calcium phosphate layer over fibre containing 5 mol% ZnO after immersion in SBF for 14 days. (C) Thick calcium phosphate outer layer on a significantly degraded fibre containing 0.5 mol% ZnO after immersion in SBF for 14 days.

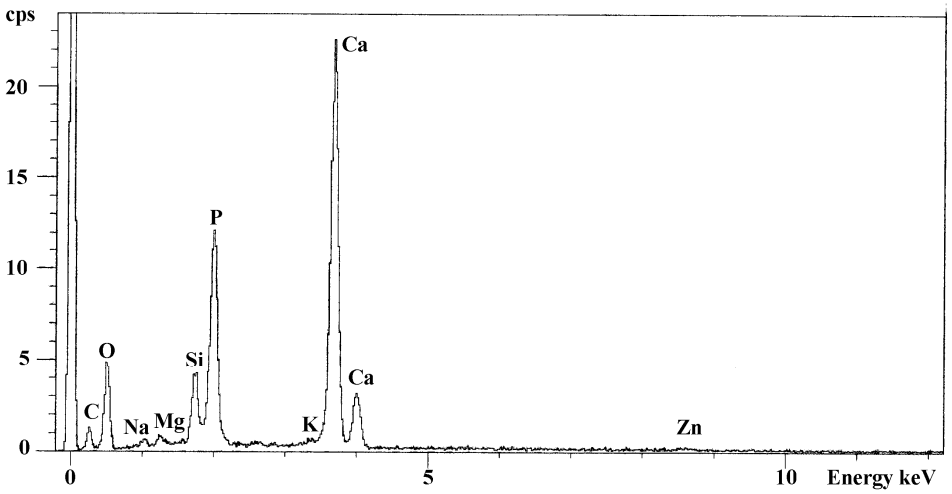

Fig. 2. (D) Elemental analysis of the calcium phosphate layer on a degraded fibre after 14 days of immersion in SBF.

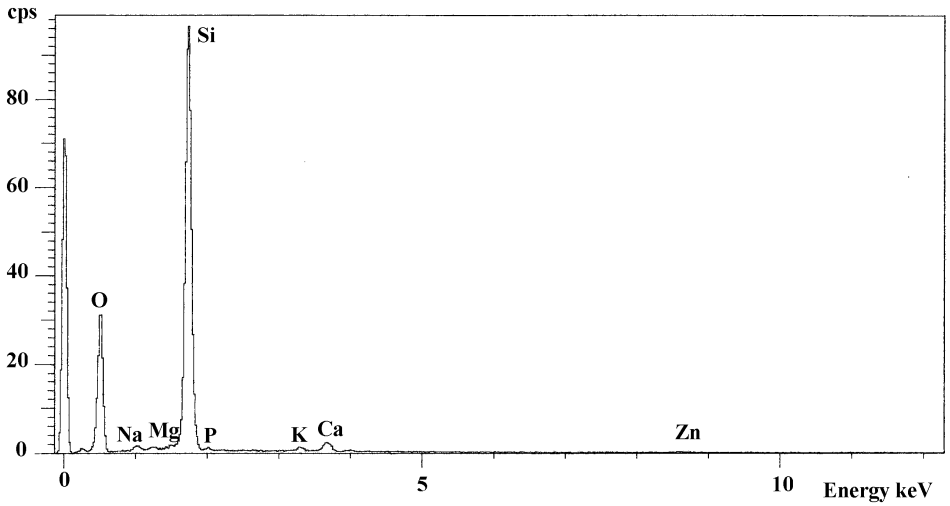

Fig. 2. (E) Elemental analysis of the glass fibre core after 14 days of immersion in SBF, strongly alkaline and alkaline earths ions depleted silica rich material.

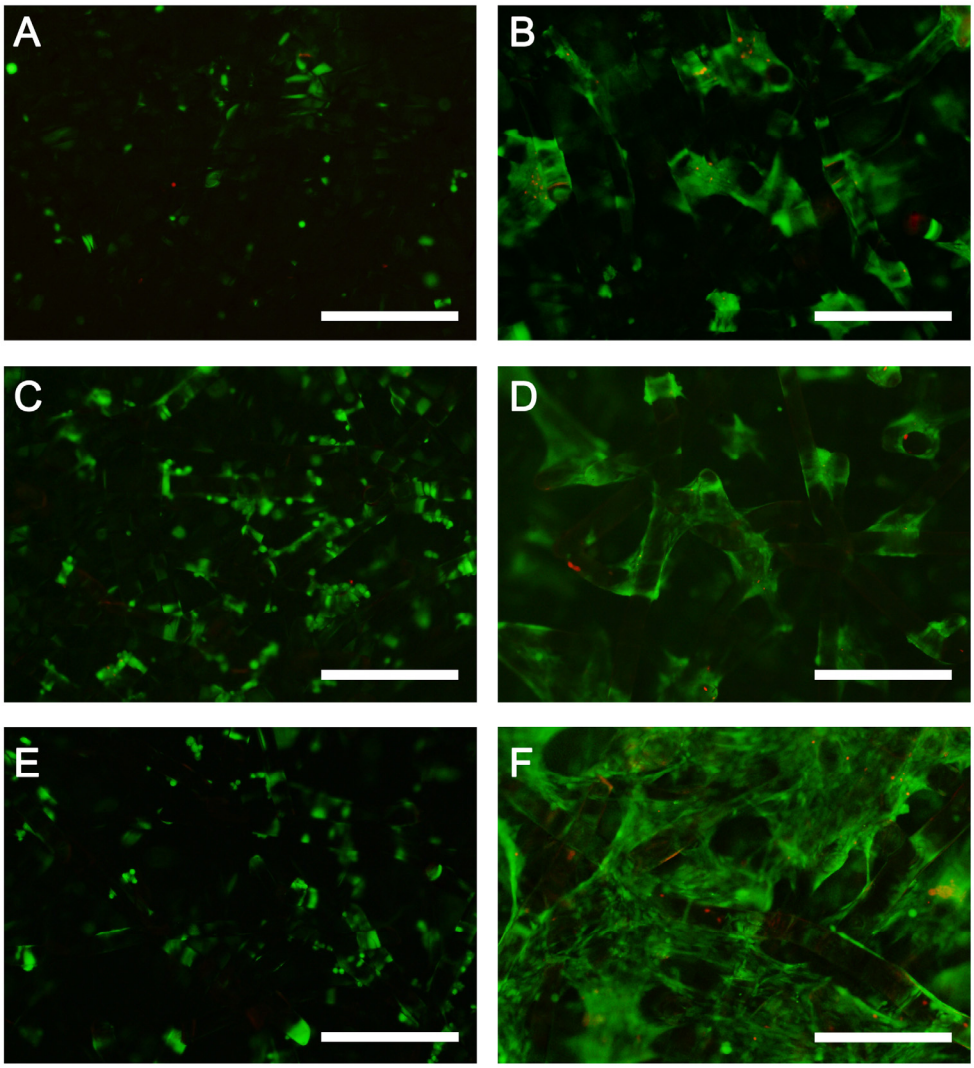

Fig. 3. Viable (green fluorescence) and dead (red fluorescence) hASCs attached to bioactive glass scaffolds. 0.25 mol% zinc scaffold (A, B); 1.0 mol% zinc scaffold (C, D); and 0 mol% zinc scaffold (E, F). Three hour time point (A, C, E); two week time point (B, D, F). Scale 500 µm.

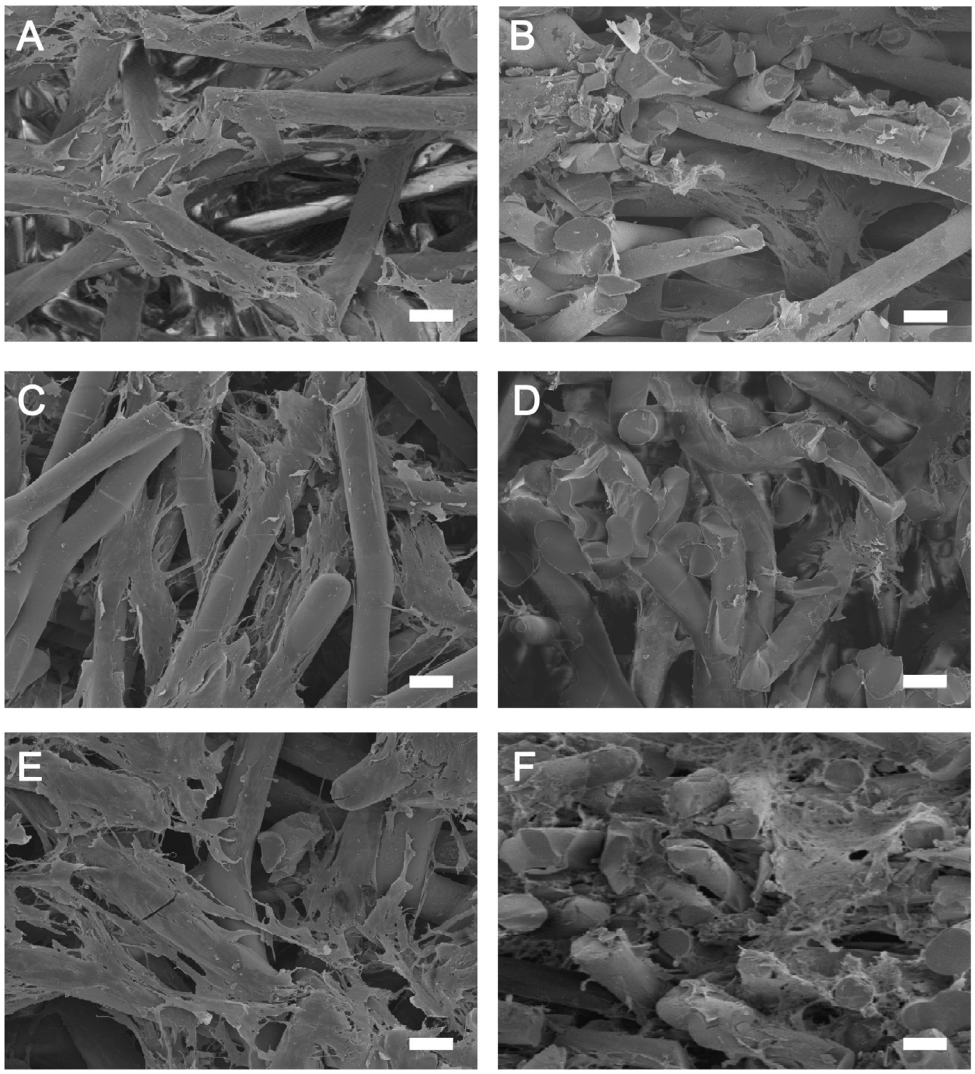

Fig. 4. Scanning electron micrographs of confluent cultures of hASCs grown on bioactive glass scaffolds at 2 weeks. 0.25 mol% zinc scaffold (A, B); 1.0 mol% zinc scaffold (C, D); and 0 mol% zinc scaffold (E, F). hASCs attached to the surface of the scaffold (A, C, E); hASCs attached in the middle of the scaffold (B, D, F). Scale 100 μm.

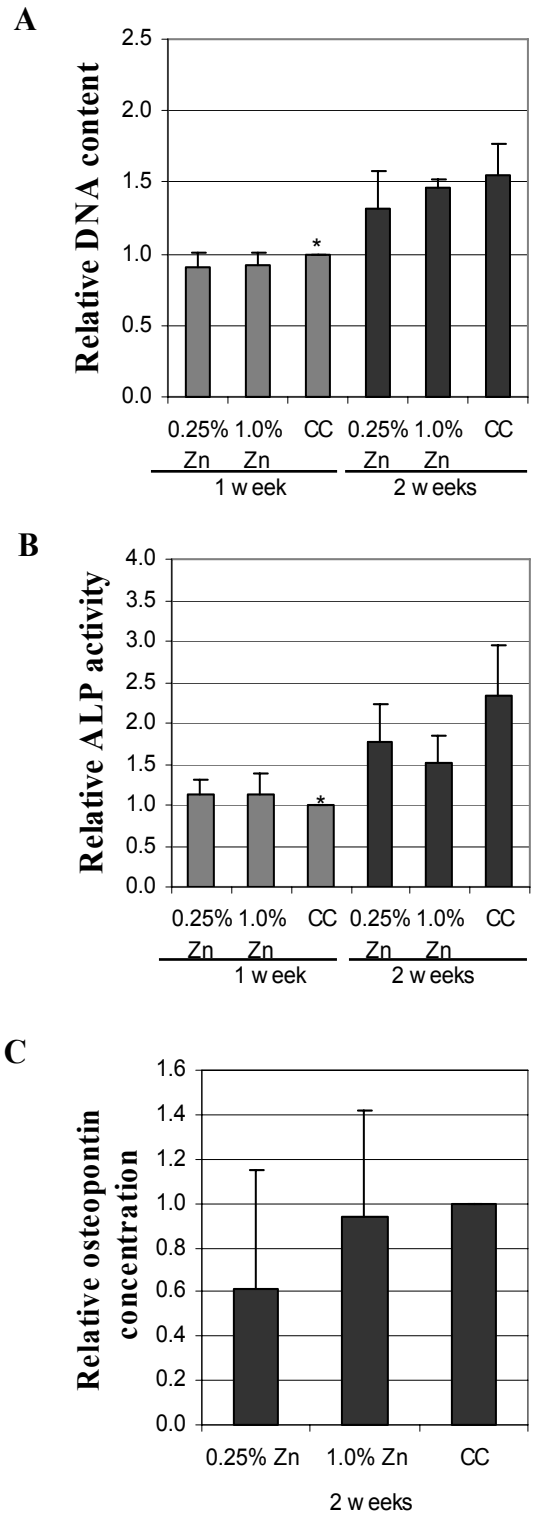

Fig. 5. Relative DNA content (A), ALP activity (B), and osteopontin concentration (C) of hASCs cultured for 1 and 2 weeks on bioactive glass scaffolds with or without zinc addition. Results are expressed as mean + SD. (A) *$p<0.05$ with respect to the 2-week DNA sample control composition scaffolds (n=4). (B) *$p<0.05$ with respect to the 2-week ALP sample of control composition scaffolds (n=4). (C) No significant differences were found (n=3).

This is a preprint of an article accepted for publication in Tissue Engineering Part A, copyright by Tissue Engineering

Growth and osteogenic differentiation of adipose stem cells on PLA/bioactive glass and PLA/β-TCP scaffolds

S. Haimi[a,*] MSc, N. Suuriniemi [a,*] MSc, A.M. Haaparanta[b] MSc, V. Ellä[b] MSc, B. Lindroos[a] MSc, H. Huhtala[c] MSc, S. Räty[d] MD, H. Kuokkanen[e] MD, PhD, G. K. Sándor[a] MD, DDS, PhD, M. Kellomäki[b] Dr Tech, S. Miettinen[a,*] MSc, R. Suuronen[a,b,f,*] MD, DDS, PhD

Corresponding author: Suvi Haimi

[a]Regea Institute for Regenerative Medicine, University of Tampere, Tampere, Finland
[b]Department of Biomedical Engineering, Tampere University of Technology, Tampere, Finland
[c]Tampere School of Public Health, University of Tampere, Tampere, Finland
[d]Department of Gastroenterology and Alimentary Tract Surgery, Tampere University Hospital, Tampere, Finland
[e]Department of Plastic Surgery of Tampere University Hospital, Tampere, Finland
[f]Department of Eye, Ear and Oral Diseases, Tampere University Hospital, Tampere, Finland

*Equal contribution

This is a preprint of an article accepted for publication in Tissue Engineering Part A, copyright by Tissue Engineering

Abstract

The aim of this study was to compare the effects of novel 3-dimensional composite scaffolds consisting of a bioactive phase (bioactive glass or β-tricalcium phosphate β-TCP 10 and 20wt%) incorporated within a polylactic acid (PLA) matrix on human adipose stem cells (ASC) viability, distribution, proliferation, and osteogenic differentiation. The viability and distribution of ASCs on the bioactive composite scaffolds was evaluated using Live/Dead fluorescence staining, environmental scanning electron microscopy (E-SEM), and SEM. There were no differences between the two concentrations of bioactive glass and β-TCP in PLA scaffolds on proliferation and osteogenic differentiation of ASCs. After 2 weeks in culture, DNA content and alkaline phosphatase (ALP) activity of ASCs cultured on PLA/β-TCP composite scaffolds were higher relative to other scaffold types. Interestingly, the cell number was significantly lower but the relative ALP/DNA ratio of ASCs was significantly higher in PLA/bioactive glass scaffolds than in other three scaffold types. In summary, these results indicate that the PLA/β-TCP composite scaffolds significantly enhance ASC proliferation and total ALP activity compared to other scaffold types. This supports the potential future use of PLA/β-TCP composites as effective scaffolds for tissue engineering and as bone replacement materials.

This is a preprint of an article accepted for publication in Tissue Engineering Part A, copyright by Tissue Engineering

Introduction

One approach for bone tissue engineering involves harvesting of autologous stem cells from the patient, which are at first cultured on a scaffold *in vitro*, and then implanted with the scaffold in the defect of the patient, where optimally the bone should regenerate at the rate at which the scaffold resorbs.[1-3]

Mesenchymal stem cells (MSCs) have recently received widespread attention in the field of tissue engineering. MSCs can be derived from different types of tissues but generally bone marrow-derived MSCs or adipose stem cells (ASCs) are used in bone tissue applications. ASCs can differentiate into osteoblastic cells, among other mesenchymal lineages *in vitro,* when treated with appropriate inducing factors.[4,5] ASCs are an ideal cell source for bone tissue engineering applications, because they are abundant, their procurement causes minimal morbidity, and their expansion is rapid *in vitro.*[6-8]

Poly lactic acid (PLA) polymers have been widely investigated as tissue engineering scaffolds due to their excellent mechanical properties and degradation profile even though they are not generally considered osteoconductive.[9-11] Composite scaffolds which include bioceramic or bioactive glass phases is one solution to improve the bioactivity. Bioactive glass is a well known bone substitute material in clinical use as it is remarkably biocompatible, biodegradable, osteoconductive, and provokes no significant inflammatory response.[12-15] On the surfaces of the bioactive glasses a layer of calcium phosphate is formed in the presence of body fluids. *In vivo* and *in vitro* studies have demonstrated that the development of this bioactive layer stimulates the adjacent tissues to form new bone (*i.e.* osteoinduction) in the absence of any osteogenic supplements.[13,16-18] Another well known bone substitute material is β-tricalcium phosphate (β-TCP) which has been studied extensively and used clinically as bone substitute material because of its similar molecular composition to human bone.[19-21] Among the bioceramics, β-TCP has excellent osteoconductivity, bioactivity and an ability to form a strong bone–calcium phosphate interface.[22] However, clinical applications of β-TCP and bioactive glass are limited due to their brittleness and low mechanical strength.[23,24] Our hypothesis was that the incorporation of bioactive glass or β-TCP into a biodegradable PLA will result in an osteoconductive composite scaffold that supports both cell proliferation as well as differentiation into osteoblasts in a mechanically stable construct.

Even though there are many studies on different bioactive glass and β-TCP/ biodegradable polymer composites,[25-29] only the effect of the concentration of bioactive glass or β-TCP in the composite on cell activity has been evaluated. However, no systematic comparison between PLA/β-TCP and PLA/bioactive glass composite scaffolds has been done. In the present study, we investigated and compared the effects of two novel biomaterial composite scaffolds; PLA/β-TCP and PLA/bioactive glass, upon human ASC morphology, proliferation and osteogenic differentiation.

Materials and methods

Material fabrication

Poly(L/D, L-lactide) (PLA) 70/30 (PURAC biochem bv, Gronichem, Netherlands) with inherent viscosity of ~ 3.1 dl/g was used as a matrix polymer. β-TCP ("Beta Whitlockite", Plasma Biotal Limited, Tideswell, UK) and bioactive glass, (BaG0127; 5%

Na_2O, 7.5% K_2O, 3% MgO, 25% CaO and 59.5% SiO_2, Åbo Akademi, Turku, Finland) were used as the filler materials. The particle size distribution of porous β-TCP granules was 75-106 μm and the bioactive glass was ground down to 75-125 μm.
The PLA solution of concentration of 2.0 wt% was prepared by dissolution of PLA in 1,4-Dioxane (Sigma-Aldrich, Helsinki, Finland). Either filler was added into the PLA solution. The PLA-filler ratios used are shown in Table 1. The solutions were frozen at -30 ˚C prior to freeze-drying. The solution was placed into custom-made Teflon moulds (Ø15 mm and height 3 mm) and frozen at -30 ˚C for 24 h prior to 24 h freeze-drying. As a control, plain PLA scaffolds were prepared with the same technique as composite scaffolds. After freeze-drying all of the samples were held in room temperature under vacuum for minimum of 48 hours before sterilization with gamma irradiation at 25 kGy.

Scaffold characterisation
The typical porous structure of the scaffolds is shown in the SEM micrographs in Figure 1. Two different functional surfaces were formed during the freeze-drying of the scaffolds. The denser top surface of the scaffolds (Fig. 1A), also referred as the skin layer, was formed on all scaffold types when the frozen solvent sublimated from the top surface during the freeze-drying process. The structures of the bioactive glass and β-TCP composite scaffolds were similar, therefore only the β-TCP SEM images are shown here. The β-TCP and bioactive glass granules were dispersed into the porous bottom surface, during manufacturing (Fig. 1B-D). However, some granules can be seen in the middle of the scaffold (Fig. 1B). The granule distribution on the porous surface and the difference between 10 and 20wt% of filler material is shown in Figures 1C and D. The interconnectivity of the pores is shown in Figure 2.

ASC isolation and culture
The study was conducted in accordance with the Ethics Committee of the Pirkanmaa Hospital District, Tampere, Finland. The ASCs were isolated from adipose tissue samples collected at operations and from liposuctions obtained from 6 donors (mean age=44±7). The adipose tissue samples were received from the Department of Plastic Surgery and from the Department of Gastroenterology and Alimentary Tract Surgery, Tampere University Hospital. The adipose tissue was digested with collagenase type I (1.5 mg/mL; Invitrogen, Paisley, UK). ASCs were expanded in T-75 polystyrene flasks (Nunc, Roskilde, Denmark) in maintenance medium consisting of DMEM/F-12 1:1 (Invitrogen), 10% FBS (Invitrogen), 1% L-glutamine (GlutaMAX I; Invitrogen) and 1% antibiotics/antimycotic (100 U/mL penicillin, 0.1 mg/mL streptomycin, and 0.25 μg/mL amphotericin B; Invitrogen). Cells from passages 4-7 were used for all experiments.

Flow cytometric surface marker expression analysis
After primary culture in T-75 flasks, the ASCs were harvested and analyzed by a fluorescence activated cell sorter (FACSAria; BD Biosciences, Erembodegem, Belgium). Monoclonal antibodies (MAb) against CD9-PE, CD10-PE-Cy7, CD13-PE, CD29-APC, CD49d-PE, CD90-APC, CD106-PE-Cy5, and CD166-PE (BD Biosciences); CD45-FITC (Miltenyi Biotech, Bergisch Gladbach, Germany); CD31-FITC, CD34-APC and CD44-FITC (Immunotools GmbH, Friesoythe, Germany); and CD105-PE (R&D Systems Inc, Minneapolis, MN, USA) were used. MAb against STRO-1 (R&D Systems Inc) and

Human Fibroblast Surface Protein (hFSP; Sigma-Aldrich, St. Louis, MO, USA) were conjugated with IgM-PE (CalTag Laboratories, Burlingame, CA, USA). A total of 10,000 cells per sample were used, and positive expression was defined as a level of fluorescence which was 99 % of the corresponding unstained cell sample.

Cell seeding and culture of ASC-seeded composite scaffolds

In each experiment, 3 to 4 patient samples were pooled together to yield enough cells for one experiment. Each scaffold was pre-treated with maintenance medium for 48 h at 37 ºC. The porous surfaces of the scaffolds were seeded with 350 000 cells in a 0.175 ml drop. The cells were allowed to attach to the scaffolds for 3 h at 37 ºC in 5% CO_2 before additional media was added. The cell-seeded scaffolds were cultured in maintenance medium until analyses.

Cell attachment and growth

Cell attachment and viability were studied using Live/Dead staining. Briefly, ASC-biomaterial constructs were incubated for 45 min at room temperature with a mixture of 5 µM CellTracker™ green (5-chloromethylfluorescein diacetate [CMFDA]; Molecular Probes, Eugene, OR, USA) and 2.5 µM Ethidium Homodimer-1 (EH-1; Molecular Probes). The viable cells (green fluorescence) and necrotic cells (red fluorescence) were examined using a fluorescence microscope.

Cell morphology evaluation

After the cells were cultured for 2 weeks, the scaffolds were fixed in 5% glutaraldehyde (Sigma-Aldrich) in 0.1 M phosphate buffer, pH 7.4, for 48 h. After PBS rinsing, the samples were dehydrated through a series of increasing concentrations of ethanol (70%, 96% and 100%). After the final dehydration step in absolute ethanol the samples were transferred to liquid carbon dioxide and dried in a critical point dryer. A gold–palladium coating was sputtered on the specimens for SEM observations. Two parallel scaffolds of each type were observed by SEM (Jeol JSM-5500, Sundbyberg, Sweden).
Additionally, Philips XL30 E-SEM-TMP environmental scanning electron microscope (E-SEM) (BioMater Centre, University of Kuopio, Finland) was used to evaluate the microstructure and morphology of the biomaterial scaffolds seeded with ASCs. The E-SEM images were taken using beam intensity at 8.0-12.0 kV and the gaseous secondary electron detectors at 1.0-4.0 Torr.

Cell proliferation and quantitative analysis of ALP activity

The DNA content of ASC-biomaterial constructs was measured using a CyQUANT® Cell proliferation assay kit (Molecular Probes, Invitrogen) as described earlier. [30] The quantitative ALP measurement was performed according to the Sigma ALP procedure as described earlier. [30]

Statistical analysis

Statistical analysis of the results was performed with SPSS, version 13. The effect of scaffold material and time of culture (1 week vs. 2 weeks) were studied using a paired Student's *t*-test. The effects between β-TCP and bioactive glass composite material on the DNA content and ALP activity were compared using a one-way ANOVA, after checking

for normal distribution and homogeneity of variance. Post hoc tests were performed to detect significant differences between groups. Data was reported as mean ± standard deviation and $p < 0.05$ was considered significant. The experiments were repeated three times.

Results

Flow cytometric surface marker expression analysis of ASCs

The FACS analysis demonstrated that the ASCs express the surface markers CD9, CD29, CD34, CD49d, CD105, CD166, CD44, CD10, CD13, CD90, STRO-1 and hFSP. The ASCs were negative for the haematopoietic markers CD31 and CD45 and for the vascular cell adhesion molecule CD106.

Cell attachment and growth on scaffolds

By 2 weeks, the number of viable cells had increased compared to the 3 hour time point (data not shown) observed by Live/Dead staining. At the 3 hour time point the cells were attached only on the region close to surface *i.e.* cell seeding area. No difference was observed in different scaffold types at 3 hours. The spreading of the cells inside the scaffolds had changed during 2 week culturing period. Generally, in each scaffold type the cells had migrated from the porous bottom surface towards the inner parts of the scaffolds, which confirmed the interconnectivity of the pores, but only a few cells were found on the dense top surface. The cell density at the region close to the porous surface was higher compared to the core of each scaffold type. At the region close to the surface, cells had formed cluster structures between the pores in all other scaffold types but not in PLA/20β-TCP, where the cells had spread more evenly (Fig. 3). There was no difference between different scaffold types on cell number or the cell viability in visual inspection.

Cell morphology

After 2-week cell culture period, SEM and E-SEM imaging were used to examine the cell morphology and spreading on the cell-biomaterial interface (Fig. 4). The cell morphology was unaffected by β-TCP or bioactive glass component in the scaffolds. During the 2-week culture period, ASCs started to colonise the scaffolds without forming a homogenous monolayer. Images with higher magnification (Fig. 4C) show ASCs stretching and forming projections on the porous surface of the scaffolds. The β-TCP and bioactive glass granules were clearly distinguished on the porous surface of the scaffolds and the ASCs were forming bridges between the granules on the PLA/β-TCP and PLA/bioactive glass composite scaffolds (Fig. 4A). ASCs were also detected inside the pores in different scaffolds. In each scaffold type the majority of ASCs were spread at the region close to the porous surface, which supports the observations made in Live/Dead staining.

Cell proliferation

The number of cells present on the scaffolds was assessed by measuring the total DNA content (Fig. 5). After 2 weeks in culture, the cell number was significantly higher in both PLA/β-TCP scaffolds than in other three scaffold types. Conversely, DNA content of ASC cultured on PLA/bioactive glass scaffolds was significantly lower compared to the

other scaffold types. There was no significant difference detected between the two concentrations of both β-TCP and bioactive glass (*i.e.* 10 wt% *versus* 20 wt%).

ASC differentiation

The effects of the 5 different scaffold types on the early differentiation of ASCs into osteogenic pathway were evaluated by quantitative measurement of ALP activity. At 2 weeks the relative ALP activity of ASCs cultured on PLA/10 β-TCP scaffolds was the same magnitude as ASCs cultured on PLA/20 β-TCP scaffolds but it was significantly higher compared to the other scaffold types (PLA, p=0.017, bioactive glass 10 wt%, p=0.023 and bioactive glass 20 wt%, p=0.022 Fig. 6). At 2 weeks the relative ALP activity of ASCs cultured on PLA/bioactive glass and PLA scaffold was comparable, but it is due to the lower cell number in PLA/bioactive glass scaffolds than in PLA scaffolds. These results indicate that relative ALP/DNA ratio was higher on PLA/bioactive glass scaffolds than in PLA and PLA/β-TCP scaffolds.

The effect of culturing period on ASCs proliferation and differentiation

We studied the effect of culturing period on ASCs proliferation and we found no increase of relative DNA content when the cells were cultured on bioactive glass composites for 2 weeks compared to 1 week (data not shown). In contrast, the DNA content of ASCs cultured on PLA/β-TCP composites and PLA scaffolds was increased at 2 weeks; however, no significant difference between 1 and 2 weeks was detected.

ASCs cultured on PLA and bioactive glass composite scaffolds produced two times higher levels of ALP activity at 2 weeks than at 1 week (data not shown). A significant increase at 2-week time point was only seen when ASCs were cultured on PLA/20 β-TCP scaffolds, although ALP activity of ASCs cultured on PLA/10 β-TCP scaffolds was also three times higher at 2 weeks than at 1 week.

Discussion

To our knowledge, this is the first reported study which compares the *in vitro* effects of PLA/β-TCP and PLA/bioactive glass composite scaffolds on ASC attachment, proliferation, and osteogenic differentiation. We also studied the effect of culturing period on proliferation and ALP activity of ASC cultured on different scaffold types in two time points.

The identity of ASCs was confirmed using FACS analysis. The FACS analysis results were consistent with previous results for MSCs.[31] A culture system using ASCs was chosen because these cells have the ability to differentiate into osteoblasts, similar to bone marrow-derived MSCs. A second advantage of using ASCs is that, unlike bone marrow MSCs, their use is not limited by a low harvest number of cells.[6,32]

Live/Dead staining and SEM imaging showed that the cell density at the region close to the surface was higher compared to the core of each scaffold type, which is attributed to the heterogenic structure of the composite scaffolds. The bioactive glass and β-TCP particles were clustered on the porous side of the composite scaffold, which made this region of the scaffold more hydrophilic. It is not surprising that the hydrophilic nature of this region enhanced the cell attachment and growth compared to other more hydrophobic parts of the scaffold. These results are also in agreement with previously published *in vitro* experiments, which have confirmed the positive effect of increasing concentration

of bioactive glass particles on poly(DL-lactide) (PDLLA) scaffolds to promote osteoblast and osteoblast-like cell adhesion and growth.[28,33] In PLA scaffolds the cells spread also to the region close to the porous surface, which may be explained by the overall hydrophobicity of the scaffold.

Our SEM results show that the cell morphology was unaffected by β-TCP or bioactive glass component in the scaffold material. This result differs from the findings of Tsigkou *et al*.[17] where the authors found that human fetal osteoblasts were less spread and elongated on PDLLA and PDLLA-bioactive glass 5 wt% composite films, whereas cells on PDLLA-bioactive glass 40 wt% composite films were elongated but with multiple protrusions spreading over the bioactive glass particles.

Bioactive glass has been studied intensively for over three decades in the bone regeneration applications. Specific bioactive glass compositions have been shown to promote proliferation and differentiation of human osteoblasts and rat MSCs into osteogenic lineages.[34-36] These publications have shown that bioactive glasses are superior scaffold materials in inducing osteogenic differentiation, although contradictory results also exist. Reilly *et al.* has recently shown that the positive effects of bioactive glass on bone growth in human patients are not mediated by accelerated differentiation of MSCs.[37] In addition, a poly(lactide-*co*-glycolide) (PLGA) scaffold coated with bioactive glass had no effect on ALP activity or osteocalcin production of human MSCs compared with uncoated scaffolds.[38] Our findings suggest that bioactive glass particles do not induce total ALP activity of ASCs more than PLA alone, although the relative ALP activity of a single cell *i.e.* ALP/DNA ratio on PLA/bioactive glass scaffolds was higher than in other scaffolds. This result is in contrast to Mayr-Wohlfart *et al*., who demonstrated that osteoblast-like cells grown on α-TCP have significantly higher ALP/DNA ratio compared to bioactive glass.[39]

It has been shown that adding increasing percentages of β-TCP to a lactic acid polymer matrix stimulates the proliferation and differentiation of human MSCs and osteogenous cells.[27,40] While it is difficult to compare our results with those of others who have used different composites, our results are similar to previous work which showed that proliferation and total ALP activity of ASCs was significantly higher in PLA/β-TCP scaffolds compared to PLA scaffolds.

In the present study, no significant differences between the effects of the two concentrations of bioactive glass and β-TCP were found on ASC attachment, proliferation and differentiation. This may be explained by the heterogeneous structure of the composite scaffold. If the filler particles would have been homogeneously arranged on the scaffold, the difference between the filler concentration may have been more evident.

Interestingly, the results of the effect of the culturing period on ASC proliferation showed that the cell number was at the same level on PLA/bioactive composite scaffolds, while the cell number was increased in three other scaffold types (in PLA/10 β-TCP significantly) at 2 weeks compared to 1 week. The relative ALP activity of ASCs, however, increased with time in all scaffold types.

This study demonstrated that of the studied scaffolds, PLA/bioactive glass scaffolds supported proliferation of ASCs the weakest, albeit ASCs exhibited the strongest differentiation capacity when cultured on PLA/bioactive glass scaffolds. An ideal scaffold for bone tissue engineering should, however, promote both cell proliferation and osteogenic

differentiation. Our results show that PLA/β-TCP composite scaffolds significantly enhance ASC proliferation and total ALP activity compared to PLA alone or composite forms of PLA/bioactive glass scaffolds. We conclude that PLA/β-TCP composite scaffolds demonstrate significant potential in future hard tissue engineering.

Acknowledgements

I would like to thank Ms. Miia Juntunen and Ms. Minna Salomäki for excellent technical assistance. Special thanks for Mr. Tuomas Huttunen for graphic processing and consultation. And also Arto Koistinen in the BioMater Centre, University of Kuopio, for the outstanding technical assistance and guidance of the E-SEM equipment. Thanks also to Professor Lauri Pelliniemi from Laboratory of Electron Microscopy, University of Turku. This research was supported by the competitive research funding of the Pirkanmaa Hospital District, the Finnish Funding Agency for Technology and Innovation (TEKES), the Finnish Cultural Foundation and the City of Tampere.

This is a preprint of an article accepted for publication in Tissue Engineering Part A, copyright by Tissue Engineering

References

1. Jones, J.R., Tsigkou, O., Coates, E.E., Stevens, M.M., Polak, J.M., Hench, L.L. Extracellular matrix formation and mineralization on a phosphate-free porous bioactive glass scaffold using primary human osteoblast (HOB) cells. Biomaterials **28**(9), 1653-1663, 2007.
2. Ohgushi, H., Caplan, A.I. Stem cell technology and bioceramics: from cell to gene engineering. J Biomed Mater Res **48**(6), 913-927, 1999.
3. Takezawa, T. A strategy for the development of tissue engineering scaffolds that regulate cell behavior. Biomaterials **24**(13), 2267-2275, 2003.
4. Zuk, P.A., Zhu, M., Ashjian, P., De Ugarte, D.A., Huang, J.I., Mizuno, H., et al. Human adipose tissue is a source of multipotent stem cells. Mol Biol Cell **13**(12), 4279-4295, 2002.
5. Zuk, P.A., Zhu, M., Mizuno, H., Huang, J., Futrell, J.W., Katz, A.J., et al. Multilineage cells from human adipose tissue: implications for cell-based therapies. Tissue Eng **7**(2), 211-228, 2001.
6. Hattori, H., Sato, M., Masuoka, K., Ishihara, M., Kikuchi, T., Matsui, T., et al. Osteogenic potential of human adipose tissue-derived stromal cells as an alternative stem cell source. Cells Tissues Organs **178**(1), 2-12, 2004.
7. Slater, B., Kwan, M., Wan, D., Longaker, M. From adiposity to bone. International Congress Series **1302**, 79-88, 2007.
8. Strem, B.M., Hedrick, M.H. The growing importance of fat in regenerative medicine. Trends Biotechnol **23**(2), 64-66, 2005.
9. Navarro, M., Ginebra, M.P., Planell, J.A., Zeppetelli, S., Ambrosio, L. Development and cell response of a new biodegradable composite scaffold for guided bone regeneration. J Mater Sci Mater Med **15**(4), 419-422, 2004.
10. Ren, J., Ren, T., Zhao, P., Huang, Y., Pan, K. Repair of mandibular defects using MSCs-seeded biodegradable polyester porous scaffolds. J Biomater Sci Polym Ed **18**(5), 505-517, 2007.
11. Wang, S., Cui, W., Bei, J. Bulk and surface modifications of polylactide. Anal Bioanal Chem **381**(3), 547-556, 2005.
12. Hench, L.L., Andersson, O. *Bioactive glasses*. In: Hench LL, Wilson J, editors. In An Introduction to Bioceramics., Singapore: World Scientific; 1993, p. 41-62.
13. Hench, L.L., Paschall, H.A. Direct chemical bond of bioactive glass-ceramic materials to bone and muscle. J Biomed Mater Res **7**(3), 25-42, 1973.
14. Jarcho, M. Calcium phosphate ceramics as hard tissue prosthetics. Clin Orthop Relat Res **157**, 259-278, 1981.
15. Kitsugi, T., Yamamuro, T., Nakamura, T., Kotani, S., Kokubo, T., Takeuchi, H. Four calcium phosphate ceramics as bone substitutes for non-weight-bearing. Biomaterials **14**(3), 216-224, 1993.
16. Hench, L.L., Paschall, H.A. Histochemical responses at a biomaterial's interface. J Biomed Mater Res **8**(3), 49-64, 1974.
17. Tsigkou, O., Hench, L.L., Boccaccini, A.R., Polak, J.M., Stevens, M.M. Enhanced differentiation and mineralization of human fetal osteoblasts on PDLLA containing Bioglass composite films in the absence of osteogenic supplements. J Biomed Mater Res A **80**(4), 837-851, 2007.

This is a preprint of an article accepted for publication in Tissue Engineering Part A, copyright by Tissue Engineering

18. Vrouwenvelder, W.C., Groot, C.G., de Groot, K. Histological and biochemical evaluation of osteoblasts cultured on bioactive glass, hydroxylapatite, titanium alloy, and stainless steel. J Biomed Mater Res **27**(4), 465-475, 1993.
19. Dorozhkin, S.V., Epple, M. Biological and medical significance of calcium phosphates. Angew Chem Int Ed Engl **41**(17), 3130-3146, 2002.
20. Hench, L.L., Wilson, J. Surface-active biomaterials. Science **226**(4675), 630-636, 1984.
21. Sun, H., Wu, C., Dai, K., Chang, J., Tang, T. Proliferation and osteoblastic differentiation of human bone marrow-derived stromal cells on akermanite-bioactive ceramics. Biomaterials **27**(33), 5651-5657, 2006.
22. LeGeros, R.Z. Properties of osteoconductive biomaterials: calcium phosphates. Clin Orthop Relat Res **395**, 81-98, 2002.
23. Hench, L.L. The story of Bioglass. J Mater Sci Mater Med **17**(11), 967-978, 2006.
24. Wang, M. Developing bioactive composite materials for tissue replacement. Biomaterials **24**(13), 2133-2151, 2003.
25. Kim, S.S., Sun Park, M., Jeon, O., Yong Choi, C., Kim, B.S. Poly(lactide-co-glycolide)/hydroxyapatite composite scaffolds for bone tissue engineering. Biomaterials **27**(8), 1399-1409, 2006.
26. Niemeyer, P., Krause, U., Fellenberg, J., Kasten, P., Seckinger, A., Ho, A.D., et al. Evaluation of mineralized collagen and alpha-tricalcium phosphate as scaffolds for tissue engineering of bone using human mesenchymal stem cells. Cells Tissues Organs **177**(2), 68-78, 2004.
27. Takahashi, Y., Yamamoto, M., Tabata, Y. Osteogenic differentiation of mesenchymal stem cells in biodegradable sponges composed of gelatin and beta-tricalcium phosphate. Biomaterials **26**(17), 3587-3596, 2005.
28. Verrier, S., Blaker, J.J., Maquet, V., Hench, L.L., Boccaccini, A.R. PDLLA/Bioglass composites for soft-tissue and hard-tissue engineering: an in vitro cell biology assessment. Biomaterials **25**(15), 3013-3021, 2004.
29. Yang, X.B., Webb, D., Blaker, J., Boccaccini, A.R., Maquet, V., Cooper, C., et al. Evaluation of human bone marrow stromal cell growth on biodegradable polymer/bioglass composites. Biochem Biophys Res Commun **342**(4), 1098-1107, 2006.
30. Lindroos, B., Maenpaa, K., Ylikomi, T., Oja, H., Suuronen, R., Miettinen, S. Characterisation of human dental stem cells and buccal mucosa fibroblasts. Biochem Biophys Res Commun **368**(2), 329-335, 2008.
31. Gronthos, S., Franklin, D.M., Leddy, H.A., Robey, P.G., Storms, R.W., Gimble, J.M. Surface protein characterization of human adipose tissue-derived stromal cells. J Cell Physiol **189**(1), 54-63, 2001.
32. Strem, B.M., Hicok, K.C., Zhu, M., Wulur, I., Alfonso, Z., Schreiber, R.E., et al. Multipotential differentiation of adipose tissue-derived stem cells. Keio J Med **54**(3), 132-141, 2005.
33. Boccaccini, A.R., Notingher, I., Maquet, V., Jerome, R. Bioresorbable and bioactive composite materials based on polylactide foams filled with and coated by Bioglass particles for tissue engineering applications. J Mater Sci Mater Med **14**(5), 443-450, 2003.
34. Bosetti, M., Cannas, M. The effect of bioactive glasses on bone marrow stromal cells differentiation. Biomaterials **26**(18), 3873-3879, 2005.

This is a preprint of an article accepted for publication in Tissue Engineering Part A, copyright by Tissue Engineering

35. Bosetti, M., Zanardi, L., Hench, L., Cannas, M. Type I collagen production by osteoblast-like cells cultured in contact with different bioactive glasses. J Biomed Mater Res A **64**(1), 189-195, 2003.
36. Xynos, I.D., Hukkanen, M.V., Batten, J.J., Buttery, L.D., Hench, L.L., Polak, J.M. Bioglass 45S5 stimulates osteoblast turnover and enhances bone formation In vitro: implications and applications for bone tissue engineering. Calcif Tissue Int **67**(4), 321-329, 2000.
37. Reilly, G.C., Radin, S., Chen, A.T., Ducheyne, P. Differential alkaline phosphatase responses of rat and human bone marrow derived mesenchymal stem cells to 45S5 bioactive glass. Biomaterials **28**(28), 4091-4097, 2007.
38. Leach, J.K., Kaigler, D., Wang, Z., Krebsbach, P.H., Mooney, D.J. Coating of VEGF-releasing scaffolds with bioactive glass for angiogenesis and bone regeneration. Biomaterials **27**(17), 3249-3255, 2006.
39. Mayr-Wohlfart, U., Fiedler, J., Gunther, K.P., Puhl, W., Kessler, S. Proliferation and differentiation rates of a human osteoblast-like cell line (SaOS-2) in contact with different bone substitute materials. J Biomed Mater Res **57**(1), 132-139, 2001.
40. Aunoble, S., Clement, D., Frayssinet, P., Harmand, M.F., Le Huec, J.C. Biological performance of a new beta-TCP/PLLA composite material for applications in spine surgery: in vitro and in vivo studies. J Biomed Mater Res A **78**(2), 416-422, 2006.

This is a preprint of an article accepted for publication in Tissue Engineering Part A, copyright by Tissue Engineering

Table 1. A. PLA/β-TCP composite scaffolds, B. PLA/Bioactive glass composite scaffolds.

A.	**PLA [wt%]**	**β-TCP [wt%]**
PLA	**100**	**0**
PLA/10 β-TCP	**90**	**10**
PLA/20 β-TCP	**80**	**20**

B.	**PLA [wt%]**	**Bioactive glass [wt%]**
PLA	**100**	**0**
PLA/10 Bioactive glass	**90**	**10**
PLA/20 Bioactive glass	**80**	**20**

This is a preprint of an article accepted for publication in Tissue Engineering Part A, copyright by Tissue Engineering

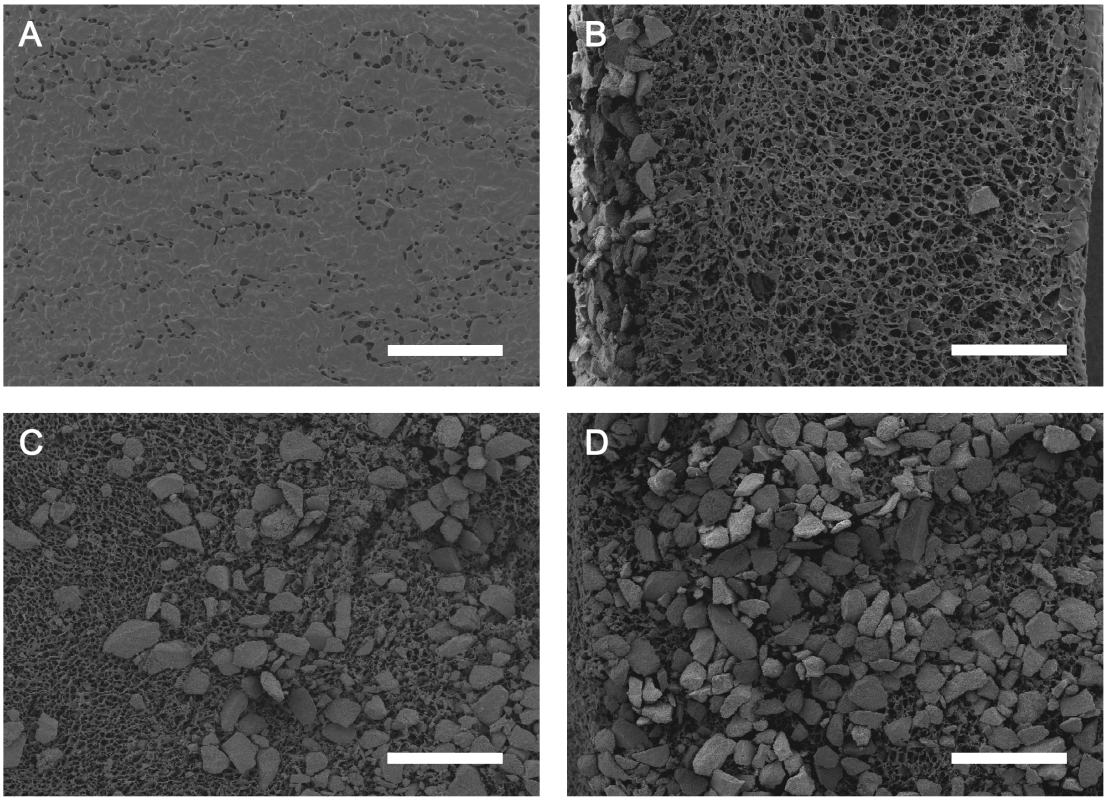

Figure 1. SEM images of A) dense top surface of PLA scaffold B) cross section of PLA/20 β-TCP scaffold, C) porous bottom surface of PLA/10 β-TCP scaffold, D) porous bottom surface of PLA/20 β-TCP scaffold. Scale 500 μm.

This is a preprint of an article accepted for publication in Tissue Engineering Part A, copyright by Tissue Engineering

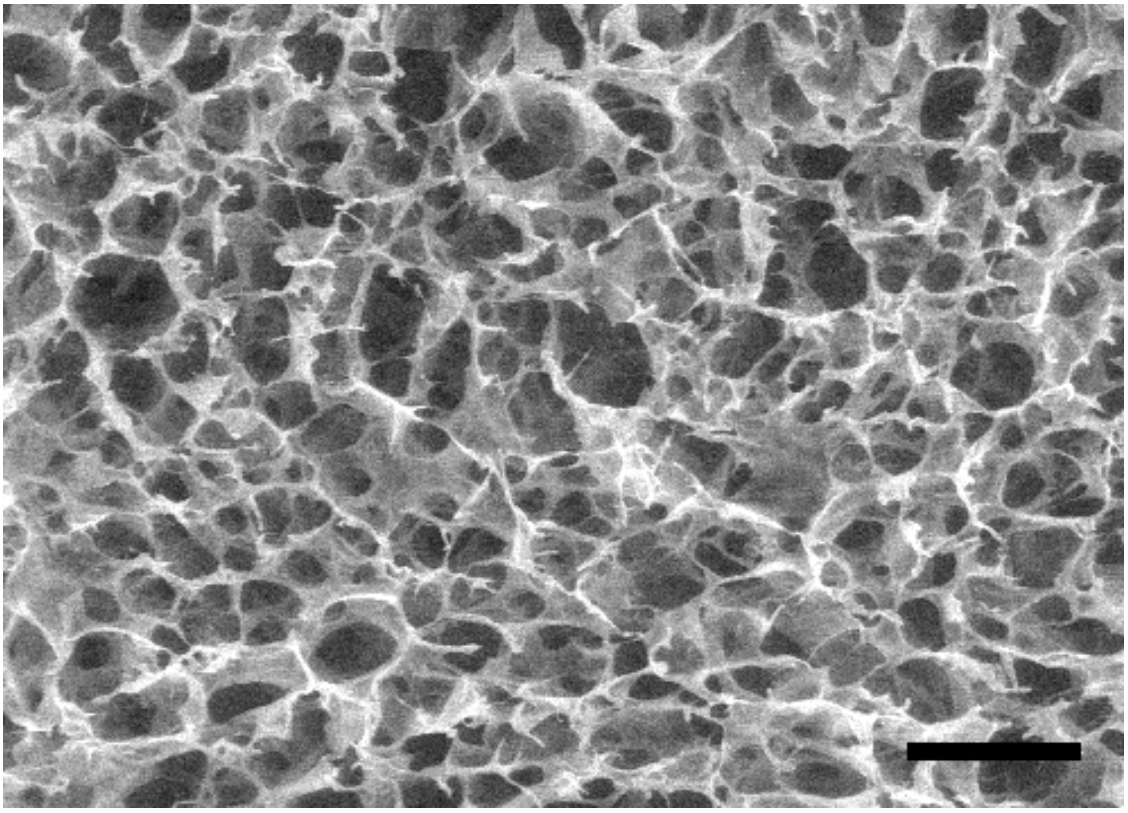

Figure 2. E-SEM image of porous bottom surface of PLA scaffold. Scale 100 μm.

This is a preprint of an article accepted for publication in Tissue Engineering Part A, copyright by Tissue Engineering

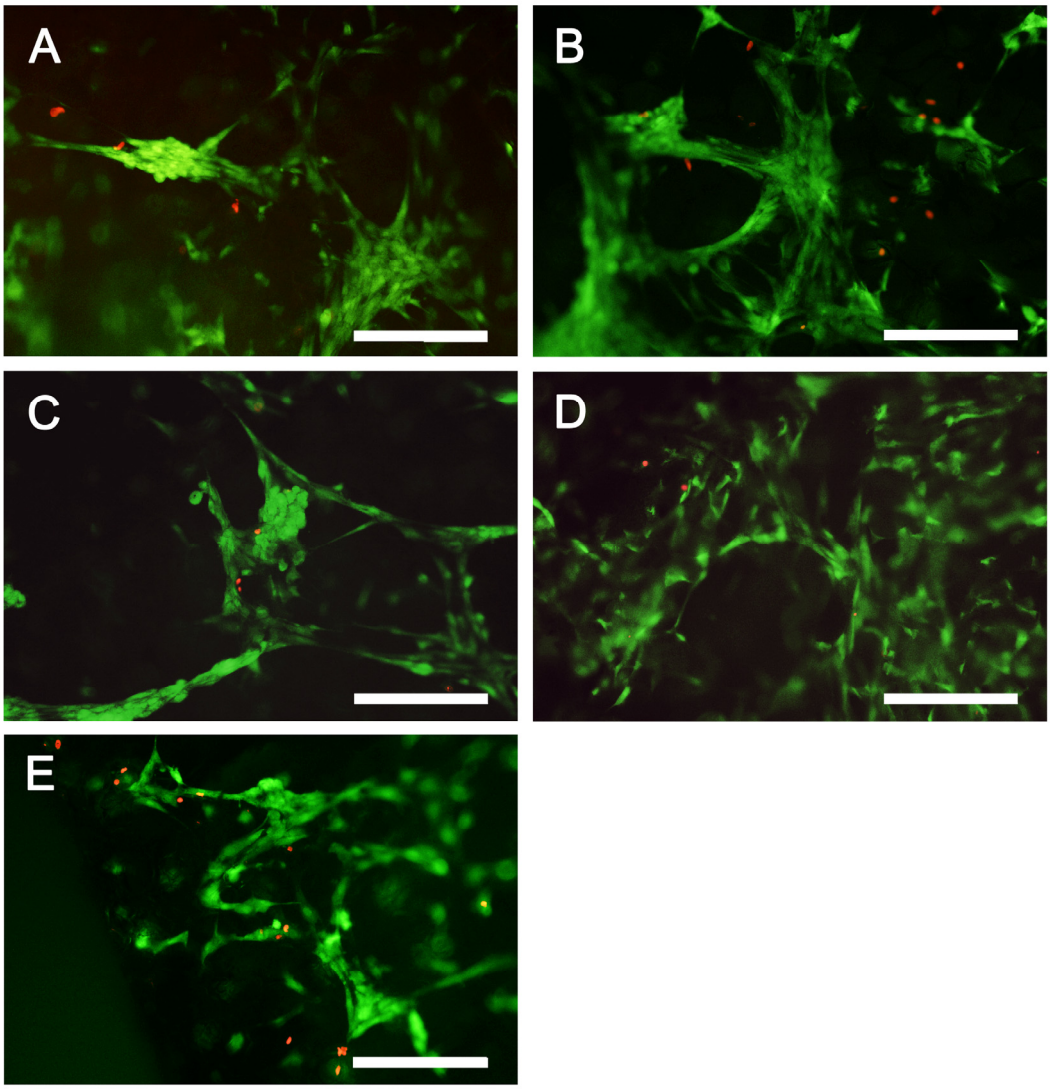

Figure 3. Representative images of viable (green fluorescence) and dead (red fluorescence) ASCs attached to A) PLA/ 10bioactive glass scaffold, B) PLA/20bioactive glass scaffold, C) PLA/10 β-TCP scaffold, D) PLA/20 β-TCP scaffold, and E) PLA scaffold after 2 weeks in culture. Scale 200 μm.

This is a preprint of an article accepted for publication in Tissue Engineering Part A, copyright by Tissue Engineering

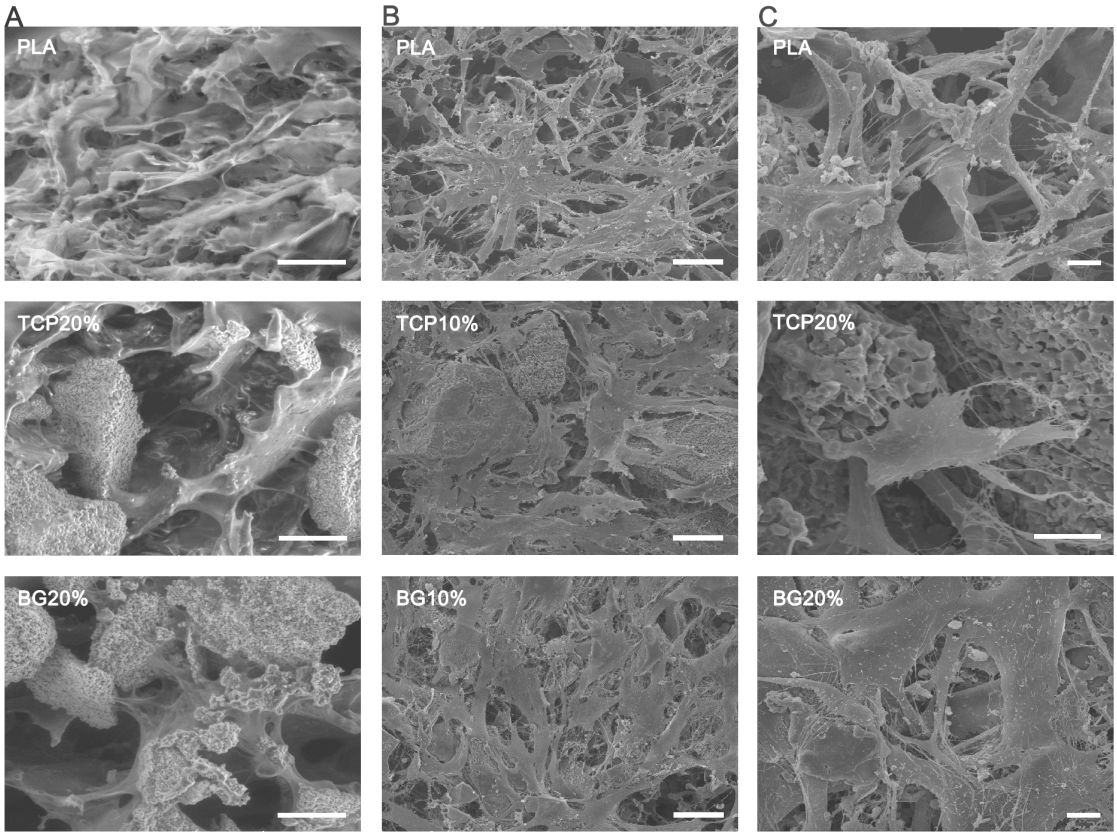

Figure 4. E-SEM images of A) ASCs on the PLA, PLA/20 β-TCP (TCP) and PLA/20 bioactive glass (BG) (scale 50 μm). B) SEM micrographs of ASCs on the PLA, PLA/10β-TCP and PLA/10bioactive glass (scale 50 μm). C) SEM micrographs of ASCs on the PLA, PLA/20β-TCP and PLA/20bioactive glass (scale 10 μm).

This is a preprint of an article accepted for publication in Tissue Engineering Part A, copyright by Tissue Engineering

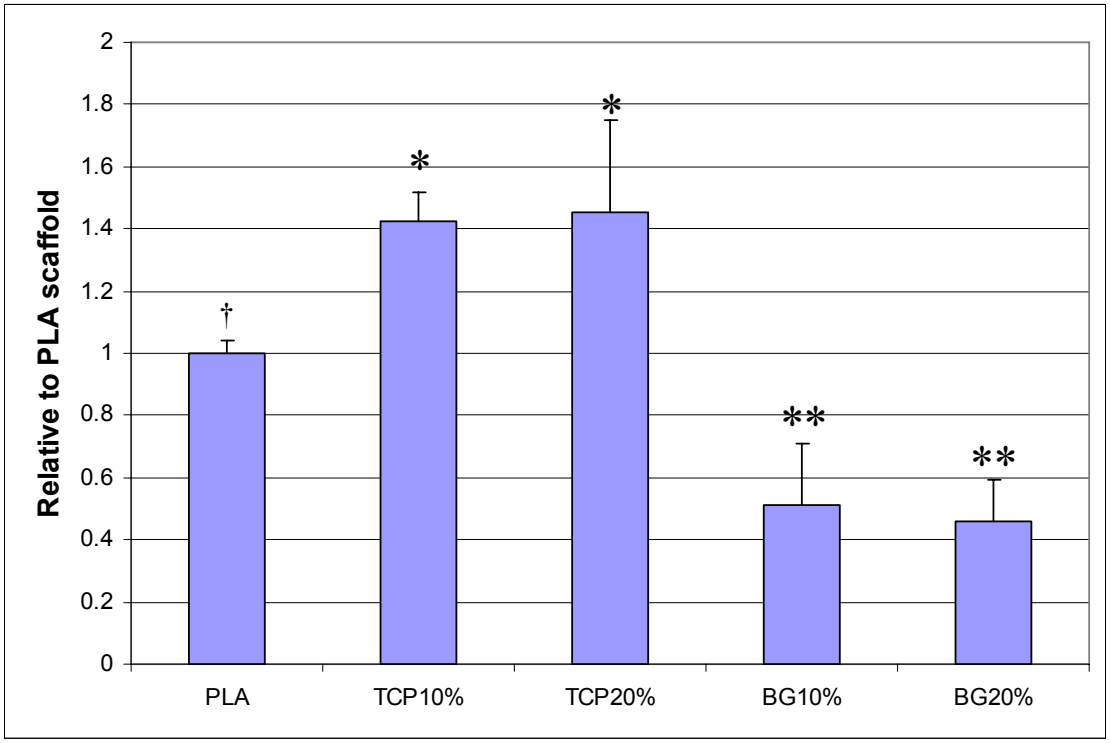

Figure 5. Relative DNA content of ASCs cultured for 2 weeks on PLA, PLA/β-TCP (TCP) and PLA/Bioactive glass (BG) scaffolds. Results are expressed as mean +S.D. relative DNA content in 3 experiments (n=4). *p<0.05 with respect to PLA, bioactive glass 10 and 20 wt%, **p<0.05 with respect to PLA, β-TCP 10 and 20 wt%, †p<0.05 with respect to β-TCP 10 and 20wt%, and bioactive glass 10 and 20 wt%.

This is a preprint of an article accepted for publication in Tissue Engineering Part A, copyright by Tissue Engineering

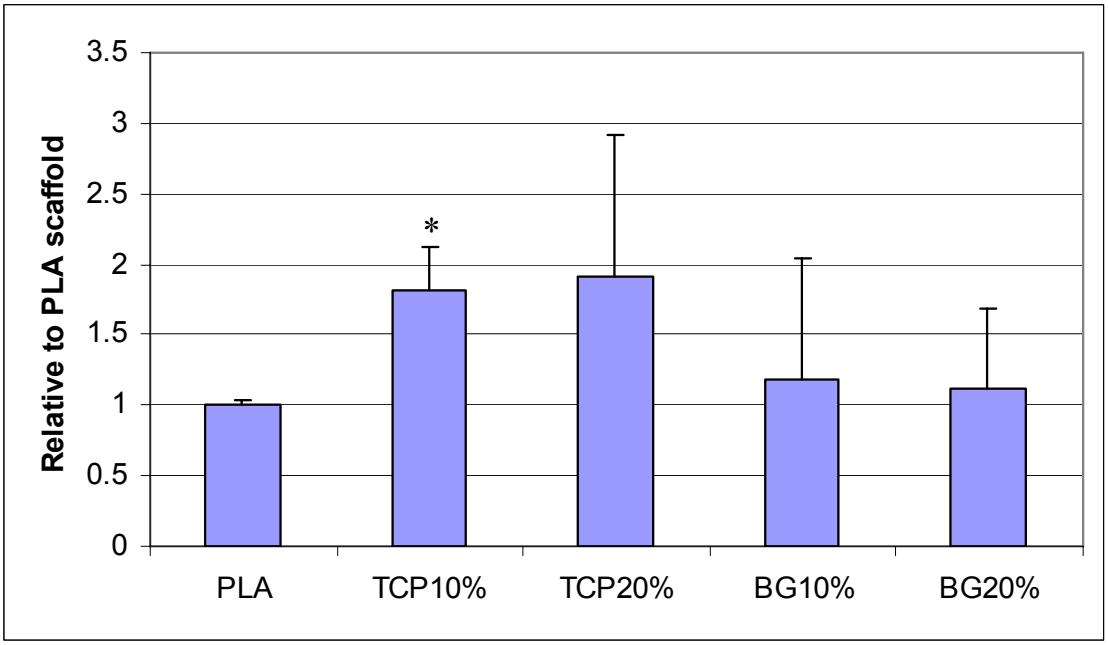

Figure 6. Relative ALP activity of ASCs cultured for 2 weeks on PLA, PLA/β-TCP (TCP) and PLA/Bioactive glass (BG) scaffolds. Results are expressed as mean +S.D. relative ALP activity in 3 experiments (n=4). *p<0.05 with respect to PLA, bioactive glass 10 and 20 wt%.